University of Windsor
Scholarship at UWindsor

Electronic Theses and Dissertations | Theses, Dissertations, and Major Papers

1-1-2002

Analysis of concrete beams prestressed and post-tensioned with carbon fiber reinforced polymer (CFRP) bars.

Mohamad Fathy Abd El Aziz
University of Windsor

Follow this and additional works at: https://scholar.uwindsor.ca/etd

Recommended Citation

Abd El Aziz, Mohamad Fathy, "Analysis of concrete beams prestressed and post-tensioned with carbon fiber reinforced polymer (CFRP) bars." (2002). *Electronic Theses and Dissertations*. 6939.
https://scholar.uwindsor.ca/etd/6939

This online database contains the full-text of PhD dissertations and Masters' theses of University of Windsor students from 1954 forward. These documents are made available for personal study and research purposes only, in accordance with the Canadian Copyright Act and the Creative Commons license—CC BY-NC-ND (Attribution, Non-Commercial, No Derivative Works). Under this license, works must always be attributed to the copyright holder (original author), cannot be used for any commercial purposes, and may not be altered. Any other use would require the permission of the copyright holder. Students may inquire about withdrawing their dissertation and/or thesis from this database. For additional inquiries, please contact the repository administrator via email (scholarship@uwindsor.ca) or by telephone at 519-253-3000ext. 3208.

NOTE TO USERS

The diskette is not included in this original manuscript. It is available for consultation at the author's graduate school library.

This reproduction is the best copy available.

UMI®

Reproduced with permission of the copyright owner. Further reproduction prohibited without permission.

Reproduced with permission of the copyright owner. Further reproduction prohibited without permission.

ANALYSIS OF CONCRETE BEAMS PRESTRESSED AND POST-TENSIONED WITH CARBON FIBER REINFORCED POLYMER (CFRP) BARS

By

MOHAMAD FATHY ABD EL AZIZ

A Thesis
Submitted to the Faculty of Graduate Studies and Research
through the department of Civil and Environmental Engineering
in partial fulfillment of the requirements for the degree of Master of Applied Science at the University of Windsor

Windsor, Ontario, Canada
2002

Reproduced with permission of the copyright owner. Further reproduction prohibited without permission.

Library and Archives Canada

Published Heritage Branch

395 Wellington Street
Ottawa ON K1A 0N4
Canada

Bibliothèque et Archives Canada

Direction du Patrimoine de l'édition

395, rue Wellington
Ottawa ON K1A 0N4
Canada

Your file Votre référence
ISBN: 978-0-494-17041-0
Our file Notre référence
ISBN: 978-0-494-17041-0

NOTICE:
The author has granted a non-exclusive license allowing Library and Archives Canada to reproduce, publish, archive, preserve, conserve, communicate to the public by telecommunication or on the Internet, loan, distribute and sell theses worldwide, for commercial or non-commercial purposes, in microform, paper, electronic and/or any other formats.

The author retains copyright ownership and moral rights in this thesis. Neither the thesis nor substantial extracts from it may be printed or otherwise reproduced without the author's permission.

AVIS:
L'auteur a accordé une licence non exclusive permettant à la Bibliothèque et Archives Canada de reproduire, publier, archiver, sauvegarder, conserver, transmettre au public par télécommunication ou par l'Internet, prêter, distribuer et vendre des thèses partout dans le monde, à des fins commerciales ou autres, sur support microforme, papier, électronique et/ou autres formats.

L'auteur conserve la propriété du droit d'auteur et des droits moraux qui protège cette thèse. Ni la thèse ni des extraits substantiels de celle-ci ne doivent être imprimés ou autrement reproduits sans son autorisation.

In compliance with the Canadian Privacy Act some supporting forms may have been removed from this thesis.

While these forms may be included in the document page count, their removal does not represent any loss of content from the thesis.

Conformément à la loi canadienne sur la protection de la vie privée, quelques formulaires secondaires ont été enlevés de cette thèse.

Bien que ces formulaires aient inclus dans la pagination, il n'y aura aucun contenu manquant.

Canada

Reproduced with permission of the copyright owner. Further reproduction prohibited without permission.

Mohamad Fathy Abd El Aziz
© 2002
All Rights Reserved

Reproduced with permission of the copyright owner. Further reproduction prohibited without permission.

ABSTRACT

Bars made of composite fiber reinforced polymers (FRP) are becoming more popular in prestressing concrete structures. Using FRP bars is an approach to avoid corrosion problems, which are encountered in concrete structures reinforced with conventional steel, especially when built in hostile environments. It also takes advantage of the high strength of the fibers. The variations in the properties between FRP and steel reinforcements lead to significant differences in the behaviour between beams prestressed with FRP and those prestressed with steel. Consequently, there is a need for a modified method of analysis and a modified code of practice that takes into consideration the different behaviour and the new properties of FRP.

A full-scale test was undertaken at the Construction Technology Laboratories for a double-tee beam prestressed internally and externally with carbon fibers. An analysis has been conducted to evaluate the behaviour and the ultimate strength of the beam by using the classical analytical equations to examine their correlation with the structural test results. The stresses and deflections obtained from the analysis showed good comparison with the test results.

An iterative design procedure is also proposed to estimate the ultimate load carrying capacity of the beam taking into consideration the variation of the stress that occurs in the unbonded tendons during the different stages of loading. A computer program was developed to cover the iterative procedure of the analysis and predicts the ultimate load carrying capacity. The analytical process for evaluating the ultimate moment is based on the deflected shape of the double-tee beam. To calculate the

Reproduced with permission of the copyright owner. Further reproduction prohibited without permission.

deflection the effective moment of inertia has to be evaluated using new equations suggested by Salem Faza and the ACI. A Load deflection curve was constructed and compared to the actual load deflection curve obtained from the structural test data.

Herein, it may be also noted that while both the FRP bars and the concrete are classified as brittle materials, the analysis show a relatively ductile behaviour of the structural system of combined pretensioned and post-tensioned FRP/concrete.

Reproduced with permission of the copyright owner. Further reproduction prohibited without permission.

ACKNOWLEDGEMENTS

First of all, my sincere thanks and gratitude are due to God who helped and blessed me during the days of my study and research.

The author wishes to express his sincere thanks and appreciation to his advisor Dr. George Abdel Sayed for his constant support, encouragement, inspiration and valuable supervision. Deep thanks are due to his co-advisors Dr. Murty K.S. Madugula and Dr. Nabil Grace for their guidance and advice.

Finally, from the bottom of my heart, I would like to extend extra special thanks for my loving parents for their love, care and encouragement.

Reproduced with permission of the copyright owner. Further reproduction prohibited without permission.

TABLE OF CONTENTS

ABSTRACT.....iv

ACKNOWLEDGEMENTS.....vi

TABLE OF CONTENTS.....vi

LIST OF TABLES.....xi

LIST OF FIGURES.....xiii

NOTATION.....xv

CHAPTER 1. INTRODUCTION.....1

1.1 General.....1

1.2 Objectives and Research Significance.....1

CHAPTER 2. LITERATURE REVIEW.....3

2.1 General.....3

2.2 Fiber Reinforced Polymers.....3

2.2.1 Carbon Fiber.....4

2.2.2 Glass Fiber.....5

2.2.3 Aramid Fiber.....6

2.3 FRP Reinforced and/or Prestressed Structures.....8

2.3.1 Double-Tee CFRP/GFRP Bridge System.....8

2.3.2 Externally Prestressed Concrete Beams with Multiple Deviators.....9

2.3.3 Failure Mechanisms and their Effect on the Ductility and the Ultimate Carrying Capacity of Beams Prestressed with Carbon Fibers.....10

2.3.4 Effect of Externally Draped CFRP Tendons.....11

Reproduced with permission of the copyright owner. Further reproduction prohibited without permission.

2.3.5 Efficiency of Beams Pre-Tensioned with CFRP.....11

2.3.6 Ductility of Prestressed Bridges.....12

2.3.7 Behaviour of Prestressed Concrete Beams Strengthened by External FRP Post-Tensioned Tendons.....12

2.3.8 The Taylor Bridge, Headingley, Manitoba, Canada.....13

2.4 Full Scale Test of DT-Beam Prestressed Internally and Externally Using FRP bars.....14

2.4.1 Fabrication.....14

2.4.2 Structural Test.....15

2.4.3 Some Test Data.....17

2.4.3.1 Strain Gauge Readings and Deflections for Phase A: Application of Internal Prestressing.....17

2.4.3.2 Strain Gauge Readings and Deflections for Phase B: Sixty Percent for External Post – Tensioning.....17

2.4.3.3 Strain Gauge Readings and Deflections for Phase C: Casting-Topping.....18

2.4.3.4 Strain Gauge Readings and Deflections for Phase D: Full Post-Tensioning.....18

CHAPTER 3.ANALYSIS OF PRESTRESSED DOUBLE-TEE BEAM.....19

3.1 General.....19

3.2 Calculation of Losses.....19

3.2.1 Elastic Shortening.....20

3.2.2 Calculation of Creep.....21

Reproduced with permission of the copyright owner. Further reproduction prohibited without permission.

3.3 Phase A: Application of Internal Prestressing.....22

3.3.1 Elastic Shortening for Pre-Tensioned Tendons.....23

3.3.2 Calculation of Stresses.....24

3.3.3 Calculations for Deflection.....27

3.3.3.1 Calculations for Deflection at Mid Span.....27

3.3.3.2 Calculations for Deflection at Quarter Span.....28

3.4 Phase B: Sixty Percent of External Post-Tensioning.....30

3.4.1 Elastic Shortening of Pre-Tensioned Tendons due to Sixty Percent of External Post-Tensioning.....30

3.4.2 Calculation of Stresses.....31

3.4.3 Calculations for Deflection.....36

3.4.3.1 Calculations for Deflection at Mid Span.....36

3.4.3.2 Calculations for Deflection at Quarter Span.....39

3.5 Phase C: Casting-Topping.....42

3.5.1 Calculation of Stresses.....42

3.5.2 Calculations for Deflection.....47

3.5.2.1 Calculations for Deflection at Mid Span.....48

3.5.2.2 Calculations for Deflection at Quarter Span.....49

3.6 Phase D: Full Post-Tensioning.....51

3.6.1 Elastic Shortening of Pre-Tensioned Tendons due to Full Post-Tensioning.....51

3.6.2 Calculation of Stresses.....52

Reproduced with permission of the copyright owner. Further reproduction prohibited without permission.

3.6.3 Calculations for Deflection.....57

3.6.3.1 Calculations for Deflection at Mid Span.....57

3.6.3.2 Calculations for Deflection at Quarter Span.....59

3.7 Calculating the Cracking Moment, Mcr.....61

3.8 Effective Rigidity of The Double-Tee Beam.....61

3.9 Calculating the Ultimate Moment.....63

CHAPTER 4.COMPARISON AND DISCUSSION.....68

4.1 General.....68

4.2 Phase A: Application of Internal Prestressing.....70

4.3 Phase B: Sixty Percent of External Post-Tensioning.....73

4.4 Phase C: Casting-Topping.....78

4.5 Phase D: Full Post-Tensioning.....82

4.6 The Cracking Moment.....88

4.7 The Ultimate Moment.....88

CHAPTER 5.CONCLUSIONS AND RECOMMENDATION.....99

5.1 Conclusions.....99

5.2 Recommendation.....100

APPENDIX A. Analysis Computations.....101

APPENDIX B. The Ultimate Moment Computer Program.....124

APPENDIX C. Output Data From the Computer Program.....129

REFERENCES.....148

VITA AUCTORIS.....151

Reproduced with permission of the copyright owner. Further reproduction prohibited without permission.

LIST OF TABLES

Table 2-1: Different Types of Carbon Fibers.....6

Table 2-2: Typical Properties of Glass Fiber.....7

Table 2-3: Typical Properties of Aramid Fiber.....7

Table 3-1: Stresses at Mid and Quarter Span for Phase A.....27

Table 3-2: Deflections at Mid and Quarter Span for Phase A.....29

Table 3-3: Stresses at Mid and Quarter Span for Phase B.....36

Table 3-4: Deflections at Mid and Quarter Span for Phase B.....41

Table 3-5: Stresses at Mid and Quarter Span for Phase C.....47

Table 3-6: Deflections at Mid and Quarter Span for Phase C.....50

Table 3-7: Stresses at Mid and Quarter Span for Phase D.....57

Table 3-8: Deflections at Mid and Quarter Span for Phase D.....60

Table 3-9: Summary of Results and the Ultimate Moment Based on the Deflection Calculated Using the ACI Equation.....66

Table 3-10: Summary of results and the Ultimate Moment Based on the Deflection Calculated Using Faza Equation.....67

Table 4-1: Stresses Obtained from the Analysis and the Stresses Obtained from Strain Measurement for Phase A.....70

Table 4-2: Deflections Obtained from the Analysis and from the Lab Measurement for Phase A.....72

Table 4-3: Stresses Obtained from the Analysis and the Stresses Obtained from Strain Measurement for Phase B.....77

Reproduced with permission of the copyright owner. Further reproduction prohibited without permission.

Table 4-4: Deflections Obtained from the Analysis and from the Lab Measurement for Phase B.....77

Table 4-5: Stresses Obtained from the Analysis and the Stresses Obtained from Strain Measurement for Phase C.....81

Table 4-6: Deflections Obtained from the Analysis and from the Lab Measurement for Phase C.....81

Table 4-7: Stresses Obtained from the Analysis and the Stresses Obtained from Strain Measurement for Phase D.....87

Table 4-8: Deflections Obtained from the Analysis and from the Lab Measurement for Phase D.....87

Table 4-9: Increase in the Post-Tensioning Force Based on the Deflection Calculated from the ACI Equation.....92

Table 4-10: Increase in the Post-Tensioning Force Based on the Deflection Calculated from Faza Equation.....93

Table 4-11: Comparison between Stresses and Strains for the Top Concrete, Pretensioned Tendons and Post-Tensioned Tendons Based on the Deflection Calculated According to the ACI Equation.....94

Table 4-12: Comparison Between Stresses and Strains for the Top Concrete, Pretensioned Tendons and Post-Tensioned Tendons Based on the Deflection Calculated According to Faza equation.....95

Reproduced with permission of the copyright owner. Further reproduction prohibited without permission.

LIST OF FIGURES

Figure 2-1: Stress-Strain Behaviour for Different Types of ACM and Steel.....5

Figure 2-2: Structural Test Setup. (Final report submitted by Construction Technology Laboratories).....16

Figure 3-1: Dimensions of the Beam in Phase A.....25

Figure 3-2: Distribution of Stresses at Mid Span for Phase A.....26

Figure 3-3: Distribution of Stresses at Quarter Span for Phase A.....26

Figure 3-4: Dimensions of the Beam in Phase B.....33

Figure 3-5: Distribution of Stresses at Mid Span for Phase B.....34

Figure 3-6: Distribution of Stresses at Quarter Span for Phase B.....35

Figure 3-7: Dimensions of the Beam in Phase C.....44

Figure 3-8: Distribution of Stresses at Mid Span for Phase C.....45

Figure 3-9: Distribution of Stresses at Quarter Span for Phase C.....46

Figure 3-10: Dimensions of The Beam in Phase D.....54

Figure 3-11: Distribution of Stresses at Mid Span for Phase D.....55

Figure 3-12: Distribution of Stresses at Quarter Span for Phase D.....56

Figure 3-13: Flow Chart for the Computer Program.....65

Figure 4-1: Deflections at Mid Span Obtained from the Lab for the Different Prestressing Phases.....69

Figure 4-2: Stresses Obtained from the Analysis vs. Stresses Obtained from Strain Reading at Mid Span for Phase A.....71

Reproduced with permission of the copyright owner. Further reproduction prohibited without permission.

Figure 4-3: Stresses Obtained from the Analysis vs. Stresses obtained from the Strain Reading at Quarter Span for Phase A.....71

Figure 4-4: Effect of Creep on the Stresses at Mid Span for Phase B.....75

Figure 4-5: Effect of Creep on the Stresses at Quarter Span for Phase B.....76

Figure 4-6: Effect of Creep on the Stresses at the Mid Span for Phase C.....79

Figure 4-7: Effect of Creep on the Stresses at Quarter Span for Phase C.....80

Figure 4-8: Increase of Coefficient of Creep vs. Time.....82

Figure 4-9: Stresses Obtained from the Analysis vs. Stresses Obtained from the Strain Reading before Introducing the Creep Effect at Mid Span D.....83

Figure 4-10: Stresses Obtained from the Analysis vs. Stresses Obtained from the Strain Reading after Introducing the Creep Effect at Mid Span D.....84

Figure 4-11: Stresses Obtained from the Analysis vs. Stresses Obtained from the Strain Reading before Introducing the Creep Effect at Quarter Span for Phase D.....85

Figure 4-12: Stresses Obtained from the Analysis vs. Stresses Obtained from the Strain Reading after Introducing the Creep Effect at Quarter Span for Phase D.....86

Figure 4-13: Stress-Strain Curve of Concrete.....91

Figure 4-14: Comparison Between Load-Deflection Curve obtained from the Lab and Load Deflection Curves obtained from the Analysis.....96

Figure 4 –15: Comparison Between the Top Concrete Strain obtained from the Lab and the Concrete Strain obtained from the Analysis.....97

Figure 4-16: Post-Tensioning Force Measured from the Lab vs. Post-Tensioning Force Obtained From the Analysis.....98

Reproduced with permission of the copyright owner. Further reproduction prohibited without permission.

NOTATION

A = area of DT-beam cross section

A_C = area of DT-beam composite section

A_T = area of carbon fibers

C_t = coefficient of creep

C_u = ultimate creep coefficient

E_T = modulus of elasticity of carbon fibers

E_{ci} = modulus of elasticity for young concrete

E_C = modulus of elasticity for mature concrete

e_1 = eccentricity of pretensioned tendons at mid span

e_2 = eccentricity of post-tensioned tendons at mid span

e_3 = eccentricity of pretensioned tendons at quarter span

e_4 = eccentricity of post – tensioned tendons at quarter span

f_C = stress of concrete at level of tendon

F_o = force in the pretensioned tendons before losses

F_n = force in the pretensioned tendons after losses

I_g = moment of inertia for the total gross section

I_C = moment of inertia for the composite section

I_{cr} = cracking moment of inertia

I_e = effective moment of inertia

Reproduced with permission of the copyright owner. Further reproduction prohibited without permission.

I_m = modified moment of inertia

M_a = applied moment on the beam

M_C = cantilever moment

M_{cr} = cracking bending moment

M_D = dead load moment due to own-weight of the double-tee beam

M_S = dead load moment due to the top composite slab

M_T = moment due to the eccentricity of the pretensioned tendons at the end

P_1 = sixty percent of post-tensioning force

P_2 = total force of post-tensioning

Q_{cr} = correction factor

W_D = dead load due to the self weight of the double-tee beam

Y_t = distance from the c.g. of the section to the extreme top fiber of the beam

Y_b = distance from the c.g. of the section to the extreme bottom fiber of the beam

θ_1 = first draping angle for the post-tensioned tendons

θ_2 = second draping angle for post-tensioned tendons

ϕ = draping angle of the pretensioned tendons

Reproduced with permission of the copyright owner. Further reproduction prohibited without permission.

CHAPTER ONE

INTRODUCTION

1.1 General

Advanced composite materials (ACM) are receiving special attention form engineers. They have high specific strength (strength to weight ratio), excellent fatigue resistance and low relaxation. Because of these characteristics, advanced composite materials are promising materials that provide solutions for structures built in hostile environments. ACM are produced in the form of fiber-reinforced polymers (FRP). The main groups of FRP are Carbon Fiber Reinforced Polymer (CFRP), Glass Fiber Reinforced Polymer (GFRP) and Aramid Fiber Reinforced Polymer (AFRP).

Experimental concrete bridges prestressed with FRP-tendons and constructed in different parts of the world are needed in order to demonstrate the actual behaviour and the successful use of these materials in bridges. A test was conducted up to failure of a full-scale bridge and its results became available to the author. This test provides valuable information on the actual behaviour of a composite FRP/concrete structure in which a combined pretensioned and post-tensioned system is used.

1.2 Objectives and Research Significance

Using FRP in prestressing, either pre-tensioning or post-tensioning, is faced with a major obstacle, which is the lack of solid guidelines for analysis that may lead us to

Reproduced with permission of the copyright owner. Further reproduction prohibited without permission.

evaluate the performance of such systems. As a consequence, there is an urgent need to find out if the classical analytical methods lead to reliable results, which have a good agreement with the experimental data. The objective of the analysis presented here is to investigate the classical analytical equations and the correlation of their results to the actual behaviour from available experimental data for a full size tested beam.

Reproduced with permission of the copyright owner. Further reproduction prohibited without permission.

CHAPTER TWO

LITERATURE REVIEW

2.1 General

This chapter provides a brief review for Fiber Reinforced Polymer (FRP), their different types, general characteristics and published research related to bridges prestressed with carbon fibers.

2.2 Fiber Reinforced Polymers

Fiber Reinforced Polymers (FRP) are composed of fibers embedded in a polymeric matrix. They exhibit several properties suitable for use as structural reinforcing and prestressing elements. The matrix of a polymer or resin has two main functions. It enables the load to be transferred between fibers and it protects the fibers from the environmental effects. The most common resins used in composites are the unsaturated polyesters, epoxies, and vinyl esters.

The unsaturated polyesters are produced by the condensation polymerization of dicarboxylic acids and dihydric alcohols. The main advantage in the unsaturated polyester is the affordable cost. Other advantages include ease in handling, processing, and fabrication. Some types are high corrosion resistant and fire retardants. Although epoxies can be expensive, it may be worth the cost when high performance is required. The acrylic esters are dissolved in a styrene monomer to produce vinyl ester resins, which

Reproduced with permission of the copyright owner. Further reproduction prohibited without permission.

are cured with organic peroxides. A composite product containing a vinyl ester resin can withstand high toughness demand and offer excellent corrosion resistance. The vinyl ester has higher physical properties than polyesters and costs less than epoxies.

The fiber is the important constituent in composites. A great deal of research and development has been done with the fibers on the effects in the types, volume fraction, and orientations. The fiber generally occupies 30%-70% of the volume in the composites. Fiber reinforced polymers are produced in the form of bars in order to be used for reinforcement and prestressing, the most common types of fibers are carbon, glass and aramid fibers.

2.2.1 Carbon Fiber

Carbon fiber is the strongest and most durable fiber material, it can be made from three types of polymer precursors: Polyacrylonitrile (PAN) fiber, Rayon fiber, and Pitch. The tensile stress-strain curve is linear to the point of rupture (Figure 2-1) and different varieties of carbon fibers can be produced as shown in Table 2-1. However, Rayon and Pitch precursors are used to produce low modulus carbon fibers and PAN precursors are made into higher modulus carbon fibers.

The double-tee (DT) beam was internally prestressed using Leadline carbon fiber bars, which are characterized by their high strength, corrosion-free and non-magnetic properties. Carbon fiber composite cables (CFCC) were used for the external post-tensioning. CFCC cables are of PAN type. The CFCC cables have their fibers twisted to allow better redistribution of the stresses through the cross section.

Reproduced with permission of the copyright owner. Further reproduction prohibited without permission.

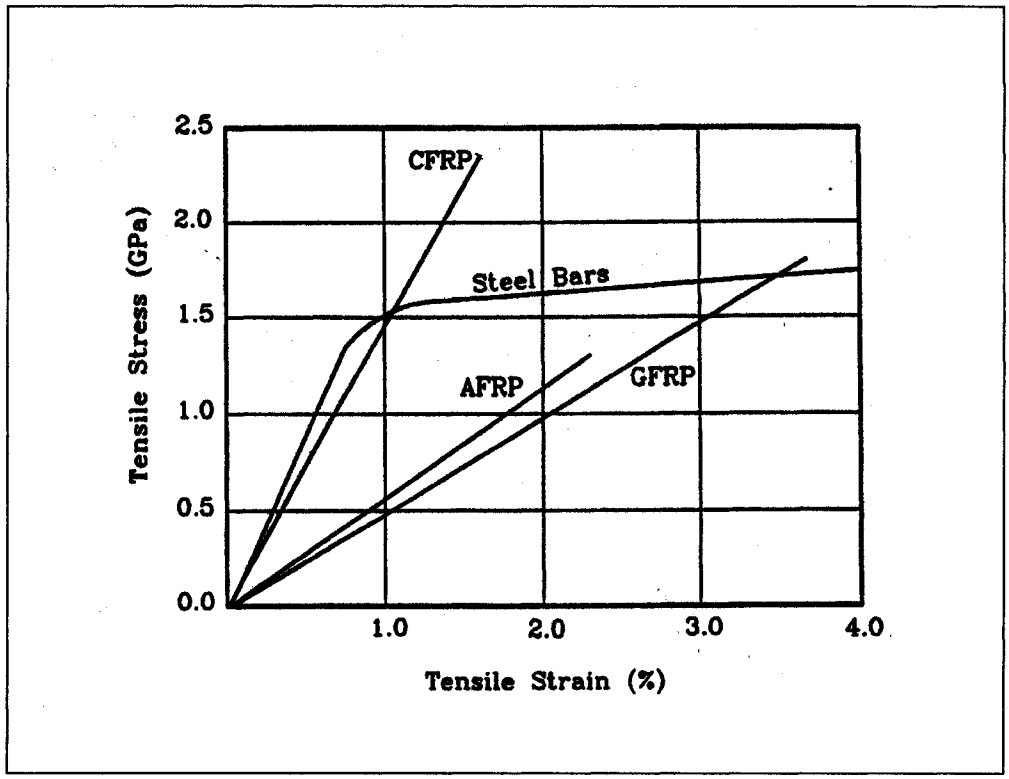

Figure 2-1: Stress-Strain Behaviour for Different Types of ACM and Steel

2.2.2 Glass Fiber

Glass fibers are divided into three classes: E-glass, S-glass and C-glass. Of the three fibers, the E-glass is the most common material used in structures. It is produced from lime-alumina-borosilicate, which can be easily obtained from abundance of raw materials like sand. The major disadvantages of glass fibers are their poor resistance to alkaline and their creep under sustained load. Table 2-2 shows the typical properties for E and S glass fibers.

Reproduced with permission of the copyright owner. Further reproduction prohibited without permission.

2.2.3. Aramid Fiber

The Aramid Fibers have high strength but very poor fatigue and creep resistance. Although there are several grades of Aramid Fiber, the two most common ones used in structural applications are Kevlar 29 and Kevlar 49. The stress-strain relationship for Kevlar 29 is linear to a value of 83 GPa but the curve becomes slightly concave upward to a value of 100 GPa at rupture. For Kevlar 49 the curve is linear to a value of 124 GPa at rupture. Table 2-3 shows the typical properties for aramid fibers.

Table 2-1: Different types of carbon fibers

Typical Properties	High Strength	High Modulus	Ultra-High Modulus
Density (g/cm^3)	1.80	1.90	2.00-2.10
Young's Modulus (GPa)	230	370	520-620
Tensile Strength (GPa)	2.48	1.79	1.03-1.31
Elongation at rupture (%)	1.10	0.50	0.20

(ZWEBEN, C. Introduction to Mechanical Behaviour and Properties of Composites Materials; DCDE, Volume 1; 1989.)

Reproduced with permission of the copyright owner. Further reproduction prohibited without permission.

Table 2-2: Typical properties of glass fibers

Typical Properties	E-Glass	S-Glass
Density (g/cm^3)	2.60	2.50
Young's Modulus (GPa)	72	87
Tensile Strength (GPa)	1.72	2.53
Elongation at rupture (%)	2.40	2.90

(ZWEBEN, C. Introduction to Mechanical Behaviour and Properties of Composites Materials; DCDE, Volume 1; 1989.)

Table 2-3: Typical properties of aramid fibers

Typical Properties	Kevlar 29	Kevlar 49
Density (g/cm3)	1.44	1.44
Young's Modulus (GPa)	83	124
Tensile Strength (GPa)	2.27	2.27
Elongation at rupture (%)	2.80	1.80

(ZWEBEN, C.; Introduction to Mechanical Behaviour and Properties of Composites Materials; DCDE, Volume 1; 1989.)

Reproduced with permission of the copyright owner. Further reproduction prohibited without permission.

2.3 FRP Reinforced and/or Prestressed Structures

The deterioration of superstructures of bridges is a serious issue as this deterioration leads to a reduction in the carrying capacity of these bridges and eventually they become structurally or functionally deficient. These deteriorated superstructures must be replaced with a new system that adequately serve the future traffic needs while offering superior corrosion-free solution when compared with conventional bridge systems.

Far reaching research has been conducted to examine the behaviour of FRP bars and their use in concrete structures. Also bridges prestressed with CFRP have been examined to determine their strength, ductility and serviceability. The following summarizes the work published about the characteristics and performance of these bridges.

2.3.1 Double-Tee CFRP/GFRP Bridge System

Grace and Abdel Sayed developed a system by employing a double-tee (DT) girder cross-section prestressed internally and externally with carbon fiber reinforced polymer (Grace and Abdel Sayed 1996). An experimental program was undertaken to examine the behaviour of this bridge system during different phases of construction. Four bridge models were constructed, instrumented and tested under static, dynamic, fatigue and ultimate loadings. The response to internal prestressing, additional deck slab and external prestressing is recorded. Test results show that the proposed precast prestressed DT bridge system is very promising and offers significant reduction in construction costs and time since the formwork and on-site shoring are eliminated. Furthermore, the use and

Reproduced with permission of the copyright owner. Further reproduction prohibited without permission.

proper implementation of composite reinforcing bars and prestressing strands in the design and construction of this new bridge concept should result in corrosion-free and crack-free bridges. The use of the DT bridge system is expected to lead to substantial savings in highway maintenance cost.

2.3.2 Externally Prestressed Concrete Beams with Multiple Deviators

Srinivasa and Mathew (1996) outlined a procedure for the analysis of externally prestressed concrete beams to determine the tendon stress at different load conditions and the effect of multiple deviators on the behaviour of the system. When externally unbonded tendons are compared with internal bonded tendons, the tendon stress calculation is more involved in the shift of the tendon eccentricity and the possible friction resistance at deviator points. Normally, friction resistance between tendon and deviator depends on the coefficient of friction. Also, as an extreme case, a tendon can be fully bonded to the deviator or it can be fully unbonded if there is no friction. Based on the experimental investigation, which was undertaken to verify the analysis procedure presented in the paper, Srinivasa reported that frictional resistance has influence on deflection, stress in tendon and cracking at service load. Furthermore, depending on the forces developed in the tendons segments, a tendon that is not slipping at the service stage might slip at a deviation point when approaching the ultimate load. Thus, if frictional resistance at deviators is neglected, deflection and cracking may be overestimated at the service stage, whereas if fully fixity is assumed for the tendons ultimate load carrying capacity may be overestimated. The load carrying capacity of

Reproduced with permission of the copyright owner. Further reproduction prohibited without permission.

structures designed with only two deviators at one third points, that otherwise would have been reduced due to cable eccentricity, could be superior by an additional deviator at the mid span. Also, providing deviators at reasonably closed intervals will reduce the eccentricity variation of cables along the span and the likelihood of resonance of cables due to moving loads (in bridges). At the same time, too many deviators may complicate the construction procedure.

2.3.3 Failure Mechanisms and their Effect on the Ductility and the Ultimate load Carrying Capacity of Beams Prestressed with CFRP bars.

The ductility and the ultimate strength of beams prestressed with CFRP is highly dependant on the failure mechanism of the system. Tommaso et al., (CSCE 1996), investigated the ductility by using double-flanged T sections prestressed with FRP tendons and untensioned longitudinal bars and stirrups made of either FRP or steel bars. The ductility is estimated using load displacement as well as moment curvature responses obtained from the models. For the prediction of the mode of failure and for the computation of the ductility, a mathematical model has been developed which predicts the moment curvature responses for beams under any combination of loads, nevertheless the model does not account for any bond slip. Each load carrying capacity was analyzed by changing the height of the beam, the initial prestressing and the reinforcing index, in order to guarantee the same ultimate moment. In doing so, common basis for comparison were found to point out ductility implications due to the use of Carbon fiber in lieu of steel. Results confirm, although in many cases a failure mechanism of tendon rupture

Reproduced with permission of the copyright owner. Further reproduction prohibited without permission.

ensures the highest load carrying capacity it implies a lower ductility if compared with a failure mechanism dictating concrete crushing.

2.3.4 Effect of Externally Draped CFRP Tendons

Grace and Abdel Sayed (1998) presented a paper on the effect of externally draped CFRP tendons on the strength of bridges. Four prestressed concrete bridge models were constructed and tested under different loading conditions. Several factors were investigated as the deviator angle, deviator diameter, presence of the cushioning material between the deviator and the tendon and the twisting angle taking place during post-tensioning process. Based on the test results, it was concluded that the strength of the CFRP tendons is adversely affected by the magnitude of the draping angle. Reducing the draping angle, increasing the deviator diameter and cushioning the tendon at the deviator minimize the reduction in the tendon breaking force. Furthermore, it was found that externally draped tendons allow for larger deflection under ultimate load.

2.3.5 Efficiency of Beams Pre-Tensioned with CFRP

Abdelrahman, et al., (1995) modeled four girders from twenty-six girders of The Central Street Beddington Trail Bridge in Calgary to probe the effectiveness of pre-tensioning beams with FRP bars. Four 1/3 scale prestressed concrete T-Beams pre-tensioned by FRP bars were constructed and tested under static and dynamic loading to investigate the flexural behaviour at various limit states including fatigue behaviour. Test

Reproduced with permission of the copyright owner. Further reproduction prohibited without permission.

results showed that failure occurred by the rupture of the tendons at a higher load than the anticipated values. This could be attributed to the under estimation of the ultimate strength of the tendons, which is normally controlled by the type of the anchorage assembly. This indicates that the pre-tensioned system is a reasonable system to utilize the high strength of the FRP. Regarding the cyclic loading, the beams survived two million cycles with a seventy- percent of the cracking load without measurable effect on beam stiffness.

2.3.6 Ductility of Prestressed Bridges

Ductility has become a serious concern since researchers started to use carbon fibers in prestressing elements. A paper by Grace and Abdel Sayed (1998) studied the behaviour of the superstructure of the Bridge Street Bridge to determine the adequacy of the superstructure of the bridge system. Four 1/3 – scale bridge models where constructed and tested. The test results indicated that a combination of externally draped tendons and longitudinally bonded and transversely bonded tendons lead to a substantial increase in the ductility of prestressed concrete structures.

2.3.7 Behaviour of Prestressed Concrete Beams Strengthened by External FRP Post-Tensioned Tendons

To understand the behaviour and the applicability of using carbon fiber reinforced plastic (FRP) tendon as an external post-tensioning for strengthening and retrofitting of

Reproduced with permission of the copyright owner. Further reproduction prohibited without permission.

existing damaged beams, Jerret and Ahmad (1996) discuss the results of flexural tests for prestressed concrete beams strengthened with external CFRP tendons and also the results of related analytical model. The specimens tested in this research were a series of concrete beams prestressed with steel strands and strengthened with external CFRP post-tensioning. Test results show that the beams failed by crushing of concrete, however the testing of one of the beams stopped at about 98 % of its expected failure load due to the failure of one of the FRP anchorages. The Ultimate strength of the CFRP post – tensioned beams was approximately 146 % and 215 % of the strength of the control beam. The predictions of the analytical model are in reasonable agreement with the experimental results, yet, the predictions overestimated the ultimate strength by 7.80 % to 9.50 % while mid span deflections were overestimated by 15 % to 21%

2.3.8 The Taylor Bridge, Headingley, Manitoba, Canada

The simply supported superstructure of the Taylor Bridge consists of forty precast prestressed concrete I-Girders with a cast in place reinforced concrete deck. Four of the girders were prestressed using both straight and draped CFRP tendons. Two of the girders use CFRP reinforcements to fully replace conventional steel reinforcement. A testing program was conducted to determine the behaviour of the CFRP prestressed model and its characteristics. It was concluded that the flexural resistance of the CFRP prestressed girders is approximately one and half times greater when compared to the girders pre-tensioned using conventional steel prestressing tendons. Moreover, the transfer length for the CFRP tendons is shorter and required spiral reinforcement to be used to prevent

Reproduced with permission of the copyright owner. Further reproduction prohibited without permission.

tensile bursting at the ends. This also required half of the tendons to be debonded over a short length to ease the transfer of the prestressing stresses to the girders.

2.4 Full Scale Test of DT-Beam Prestressed Internally and Externally Using FRP bars

2.4.1 Fabrication

The DT beam was fabricated by Prestress Systems Inc (PSI) in Windsor, it was cast using a single pan form having the two stems, top flange and transverse diaphragms. Each stem has thirty Leadline CFRP tendons for the internal prestressing. Each CFRP tendon was individually pretensioned to 87 kN. Regarding the pretensioning procedure, the jacking force was applied to each tendon and was measured using a load cell and anchored. Once the force was applied, the stressing assembly was moved to the next tendon and the same procedure continued until all the sixty Leadline CFRP tendons were pretensioned. After prestressing all the tendons, the concrete was cast and the force in the pretensioned tendons was released after two days from the concrete cast.

The DT beam has four external cables for post-tensioning, these cables were installed after the beam was removed from the forms, all four cables were instrumented with load cells at one end. Post-tensioning was applied to the four CFCC tendons in two separate stages. The initial post-tensioning consisted of 60 % of the total post-tensioning force and the final stage consisted of the remaining 40 %.

After fabrication the beam was shipped to Construction Technology Laboratories (CTL). Thereafter, the reinforcement for the top slab was placed and 75 mm concrete

Reproduced with permission of the copyright owner. Further reproduction prohibited without permission.

topping was cast over the top flange of the DT beam. The remaining 40 % of the post – tensioned force was applied after the hardening of the top slab.

2.4.2 Structural Test

The setup for the flexural test is shown in Figure 2-2, the beam was loaded along two lines creating constant moment region symmetrical about mid span of the beam. For each line, two bearing points were used to apply the load on the beam, which are coincident with the beam webs. The loads applied to the beam were monitored using load cells and the displacement at the mid and quarter span was recorded using displacement transducers at each location. The strain distribution over the section was also recorded at mid and quarter span using strain gauges embedded in the concrete (CTL report). Some of the recorded test results are presented in chapter four in comparison with the analytical results.

Reproduced with permission of the copyright owner. Further reproduction prohibited without permission.

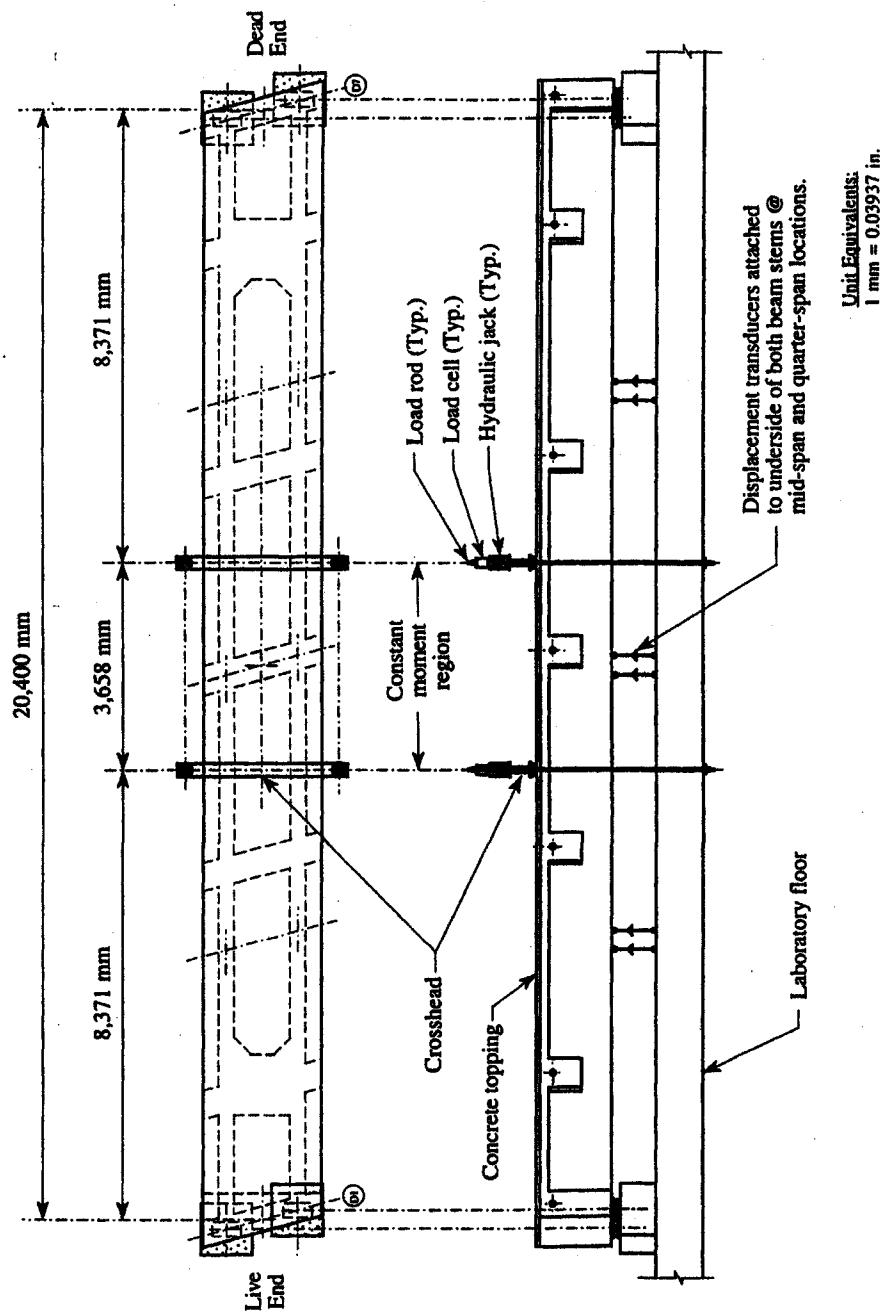

Figure 2-2: Structural test setup.
(Final report submitted by Construction Technology Laboratories.)

Reproduced with permission of the copyright owner. Further reproduction prohibited without permission.

2.4.3 Some Test Data

2.4.3.1 Strain Gauge Readings and Deflections for Phase A: Application of Internal Prestressing

		Mid span	Quarter span (Live end)	Quarter span (Dead end)
Strains ($\mu\varepsilon$)	Top	90	122	50
	Bottom	464	433	448
Stresses Calculated From Strains (MPa)	Top	1.98	2.68	1.10
	Bottom	10.21	9.53	9.85
Deflection Measured in Lab (mm)		13.2	9.80	11.40

2.4.3.2 Strain Gauge Readings and deflections for Phase B: Sixty Percent for External Post - Tensioning

		Mid span	Quarter span (Live end)	Quarter span (Dead end)
Strains ($\mu\varepsilon$)	Top	107	134	59
	Bottom	718	517	587
Stresses Calculated From Strains (MPa)	Top	3.42	4.29	1.89
	Bottom	23	16.54	18.80
Deflection Measured in Lab (mm)		20.1	13.90	15.60

Reproduced with permission of the copyright owner. Further reproduction prohibited without permission.

2.4.3.3 Strain Gauge Readings and deflections for Phase C: Casting Topping

		Mid span	Quarter span (Live end)	Quarter span (Dead end)
Strains ($\mu\varepsilon$)	**Top**	221	256	233
	Bottom	594	485	507
Stresses Calculated From Strains (MPa)	**Top**	7.07	8.20	7.45
	Bottom	19	15.52	16.23
Deflection Measured in Lab (mm)		11.6	7.70	9.60

2.4.3.4 Strain Gauge Readings and deflections for Phase D: Full Post - Tensioning

		Mid span	Quarter span (Live end)	Quarter span (Dead end)
Strains ($\mu\varepsilon$)	**Top**	241	345	198
	Bottom	656	502	601
Stresses Calculated From Strains (MPa)	**Top**	7.71	11.07	6.34
	Bottom	21	16.06	19.23
Deflection Measured in Lab (mm)		14.3	9.5	11.20

Reproduced with permission of the copyright owner. Further reproduction prohibited without permission.

CHAPTER THREE

ANALYSIS OF PRESTRESSED DOUBLE-TEE BEAM

3.1 General

An approach for the analysis for the prestressed and post-tensioned Double-Tee beam is presented in this chapter. It investigates the behaviour of the beam at different construction and loading phases, using classical and successive approach, to predict the strength and the serviceability of the beam. The results of the analysis are later compared with full-scale experimental data (Chapter Four) to evaluate and verify the structural assumptions.

3.2 Losses Calculations

The analysis of the prestressed DT-beam takes into consideration the effective force in the prestressed tendon at each phase of loading with the appropriate material properties at that time. The main losses, which are calculated within this analysis, are the elastic shortening and the creep of concrete.

Reproduced with permission of the copyright owner. Further reproduction prohibited without permission.

3.2.1 Elastic Shortening

As the prestress is transferred to the DT-beam, the member shortens and the prestressed tendons shorten with it. Hence there is loss of prestress in the tendon.

The following procedure is used to calculate the elastic shortening at any stage of loading:

a) The stress in concrete at level of tendon is calculated by the formula,

$$f_C = \frac{F}{A} + \frac{F \times e^2}{I_g} - \frac{M_D \times e}{I_g} \qquad (3.1\ a)$$

where,

F = the prestressing force (internal or external) transferred to the beam for the designated stage of loading.

e = the eccentricity of the tendons (internal or external).

M_D = bending moment due to the own weight

A = cross section area of the beam.

Ig = the gross moment of inertia which is effective since no cracks has taken place at this phase of loading.

b) The loss of stress in the tendons is calculated by multiplying the stress of concrete at level of tendon by the modular ratio = $\frac{E_T}{E_C}$

i.e. Loss of stress = $\frac{E_T}{E_C} \times f_C$ (3.1 b)

Reproduced with permission of the copyright owner. Further reproduction prohibited without permission.

where,

E_T = the modulus of elasticity for the tendons.

E_C = the modulus of elasticity for the concrete.

c) The loss in the pretensiong force = Loss of stress × A_T (3.1 c)

where,

A_T = the total cross section area for the pretensioned tendons.

d) Total pre-tensioned force after losses,

$F_1 = F -$ Loss of force (3.1 d)

3.2.2 Calculation of Creep

Several independent and interacting factors related to the material properties, curing, environmental conditions and loading conditions influence the magnitude of the creep strains. The major factors related to the composition of the mix that influence creep are the type and the amount of cement, water cement ratio, aggregate type and content. Herein, creep increases with the increase in the w/c ratio, cement content and air entrainment. The ambient relative humidity and temperature are also significant factors related to the environment that influence creep, a decrease in the relative humidity and an increase in the temperature increases the creep strain. All these factors are taken into account in the calculation of creep throughout the different stages of loading, as by knowing the time of loading, composition of the concrete mix and the surrounding

Reproduced with permission of the copyright owner. Further reproduction prohibited without permission.

environmental condition the creep coefficient was estimated to a good extent. A commonly accepted procedure to determine a creep coefficient C_t is outlined by the recommendations of the ACI Committee 209. By calculating the creep coefficient, the creep strain can be evaluated since the creep coefficient is defined as the ratio of creep strain to the initial elastic strain.

The creep coefficient at time t can be estimated by the following expression,

$$C_t = \frac{t^{0.60}}{10 + t^{0.60}} \times C_u \times Q_{cr} \qquad \text{(ACI Committee 209, Report No. ACI 209R-82)} \qquad (3.1\ e)$$

In the preceding expression t is the time in days after loading and C_u is the ultimate creep coefficient, which varies between 1.30 and 4.15. In the absence of specific creep data the average value suggested in the analysis for C_u is 2.35. The introduction of the correction factor Q_{cr} is to modify the equation of the creep coefficient to account for non-standard conditions.

3.3 Phase A: Application of Internal Prestressing

The loads acting on the DT-beam at this phase are mainly the prestressing force from the pre-tensioned sixty CFRP tendons and the own-weight of the beam. Each CFRP tendon was individually pretensioned to a target load of (87 kN) which was transferred to the concrete after hardening. On the other hand, the own-weight of the beam was counteracting the upward deflection of the beam produced by the internal prestressing.

Reproduced with permission of the copyright owner. Further reproduction prohibited without permission.

3.3.1 Elastic Shortening for Pre-Tensioned Tendons

An initial force of (5220 kN) is transferred to the DT-beam at this phase by the internal prestressing, however, this force is reduced due to the elastic shortening and a new effective value for the force has to be calculated.

a) The stress of concrete at level of tendon is calculated by the formula,

$$f_C = \frac{F_o}{A} + \frac{F_o \times e_1^{\,2}}{I_g} - \frac{M_D \times e_1}{I_g} \qquad (3.2\ a)$$

where,

F_0 = 5220 kN, which is the initial pretensioned force between the bulkheads.

$$\text{b) Loss of stress} = \frac{E_T}{E_{CI}} \times f_C \qquad (3.2\ b)$$

The concrete was two days mature at this phase with an initial value for $E_{CI} = 22 \times 10^3$ MPa. (Final report submitted by Construction Technology Laboratories)

c) The loss in the pre-tensioning force = Loss of stress × A_T (3.2 c)

d) Total pre-tensioned force after losses,

$$F_1 = F_o - \textit{Loss of force} \qquad (3.2\ d)$$

Leading to F_1 = 5057 kN.

Reproduced with permission of the copyright owner. Further reproduction prohibited without permission.

3.3.2 Calculation of Stresses

The stresses are calculated at mid and quarter span using the final prestressing force after the elastic shortening of concrete and the moment due to the own-weight of the beam. In this phase the beam was under compression and uncracked. Reasonable predictions of its behaviour can be made by assuming that the material stress strain relationships are linearly elastic for concrete. Figure 3-1 shows the dimensions of the beam. Figure 3-2 and Figure 3-3 shows the distribution of the stresses at mid and quarter span.

$$f_2 = -\frac{F_1}{A} + \frac{F_1 \times e_1 \times Y_t}{I_g} - \frac{M_D \times Y_t}{I_g} \qquad (3.3\text{ a})$$

$$f_1 = -\frac{F_1}{A} - \frac{F_1 \times e_1 \times Y_b}{I_g} + \frac{M_D \times Y_b}{I_g} \qquad (3.3\text{ b})$$

where,

e_1 = the eccentricity of the pre-tensioned tendons relative to the section.

Y_t = distance from the c.g. of the section to the extreme top fiber of the beam.

Y_b = distance from the c.g. of the section to the extreme bottom fiber of the beam.

The effect of creep on the pretensioned force was not calculated in this phase, as the loading was sustained only for two days. As the beam experienced an upward deflection due to the pretensioning force it was resting on an effective support of length l_2 .The effective span was estimated by a trial and error to evaluate the span on which the own-weight of the beam will act to obtain approximately the corresponding value for the deflection measured in the lab.

Reproduced with permission of the copyright owner. Further reproduction prohibited without permission.

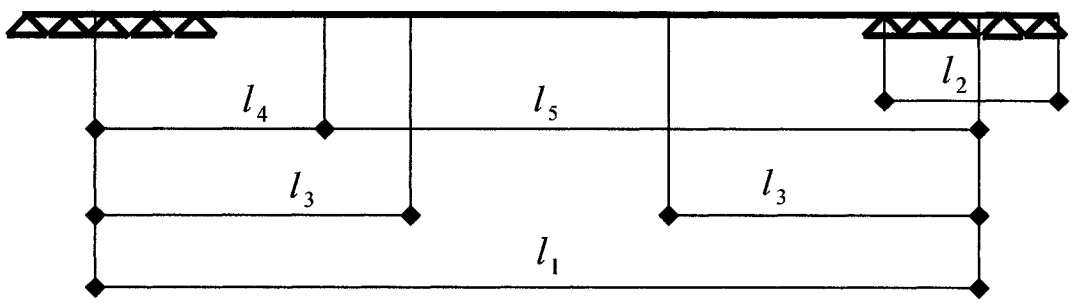

Where,

l_1 = Effective span of the DT-beam in the pretensioning phase.

l_2 = Length of the effective support

l_3 = Distance from the edge support to the point of application of the pre-tensioning force.

l_4 = Distance from the support to the quarter span

$l_5 = l_1 - l_4$

Figure 3-1: Dimensions of the beam in Phase A

Reproduced with permission of the copyright owner. Further reproduction prohibited without permission.

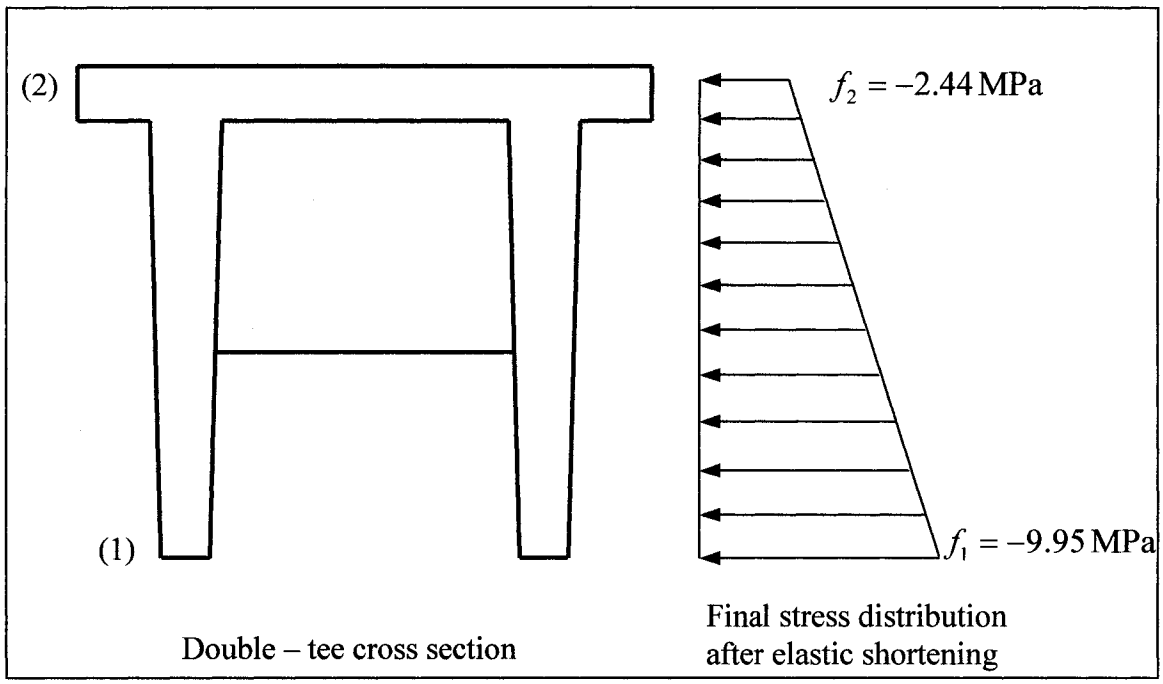

Figure 3-2: Distribution of Stresses at Mid Span for Phase A

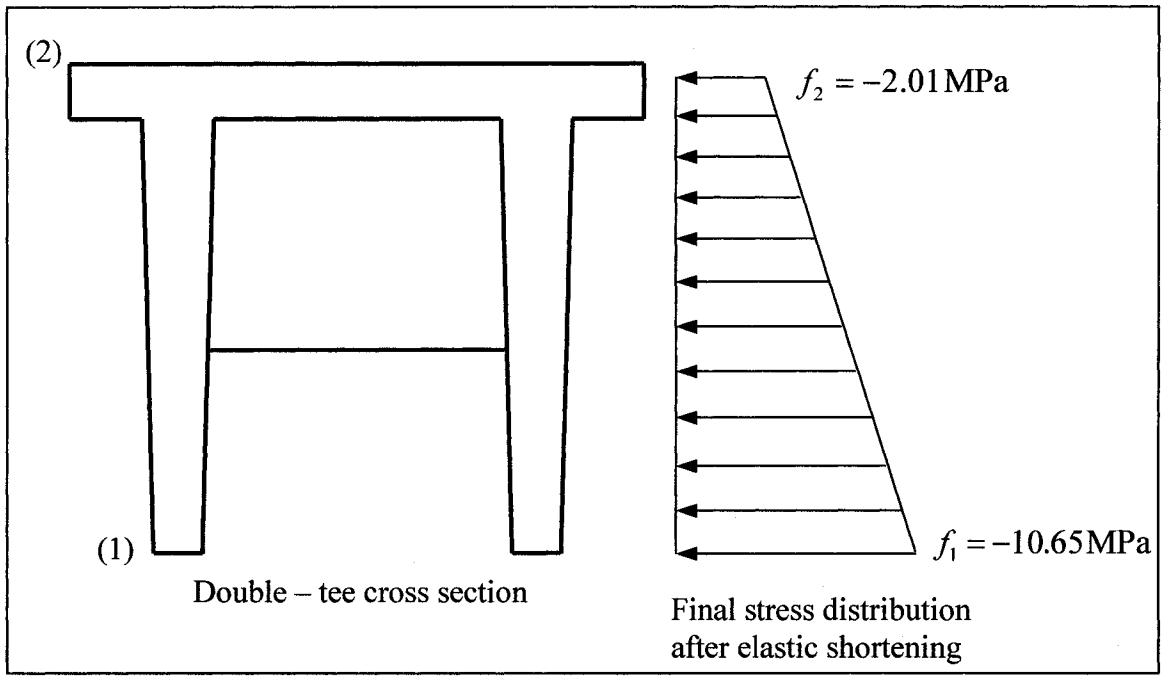

Figure 3-3: Distribution of Stresses at Quarter Span for Phase A

Reproduced with permission of the copyright owner. Further reproduction prohibited without permission.

Table 3-1: Stresses at Mid and Quarter Span for Phase A

Stresses (MPa)		Mid Span	Quarter Span
Final stresses after elastic shortening.	Top Stress (MPa)	-2.44	-2.01
	Bottom Stress (MPa)	-9.95	-10.65

3.3.3 Calculations for Deflection

The beam at this phase was under compression and uncracked, so reasonable predictions of its behaviour can be calculated assuming that the material stress strain relationships are linearly elastic for concrete. As the beam was uncracked the gross moment of inertia has been used in calculating the deflections for both mid and quarter spans.

3.3.3.1 Calculations for Deflection at Mid Span

Downward deflection due to own-weight, (Hibbeler 1999)

$$\delta_1 = \frac{5 \times W_D \times l_1^4}{384 \times E_{Ci} \times I_g} \qquad (3.4\ a)$$

Reproduced with permission of the copyright owner. Further reproduction prohibited without permission.

Upward deflection due to the pre-tensioning force, (CSCE, 2000)

$$\delta_2 = \frac{F_1 \times Sin\phi \times l_3}{24 \times E_{Ci} \times I_g}\left(3 \times l_1^{\,2} - 4 \times l_3^{\,2}\right) \qquad (3.4\text{ b})$$

Deflection due to eccentricity of the tendons at the end, (Hibbeler 1999)

$$\delta_3 = \frac{M_T \times l_1^{\,2}}{8 \times E_{Ci} \times I_g} \qquad (3.4\text{ c})$$

The total upward deflection,

$$\delta_t = -\delta_1 + \delta_2 + \delta_3 \qquad (3.4\text{ d})$$

3.3.3.2 Calculations for Deflection at Quarter Span

Downward deflection due to own-weight, (CSCE, 2000)

$$\delta_1 = \frac{W_D \times l_4}{24 \times E_{Ci} \times I_g}\left(l_4^{\,3} - 2 \times l_1 \times l_4^{\,2} + l_1^{\,3}\right) \qquad (3.5\text{ a})$$

Upward deflection due to the pre-tensioning force, (CSCE, 2000)

$$\delta_2 = \frac{F_1 \times Sin\phi \times l_4}{6 \times E_{Ci} \times I_g}\left(3 \times l_1 \times l_3 - 3 \times l_3^{\,2} - l_4^{\,2}\right) \qquad (3.5\text{ b})$$

Deflection due to eccentricity of the tendons at the end, (Hibbeler 1999)

Left moment,

Reproduced with permission of the copyright owner. Further reproduction prohibited without permission.

$$\delta_3 = \frac{M_T \times l_5}{6 \times E_{Ci} \times I_g \times l_1}\left(l_5^{\,2} - 3 \times l_1 \times l_5 + 2 \times l_1^{\,2}\right) \qquad (3.5\text{ c})$$

Right moment,

$$\delta_4 = \frac{M_T \times l_4}{6 \times E_{Ci} \times I_g \times l_1}\left(l_4^{\,2} - 3 \times l_1 \times l_4 + 2 \times l_1^{\,2}\right) \qquad (3.5\text{ d})$$

The total upward deflection,

$$\delta = -\delta_1 + \delta_2 + \delta_3 + \delta_4 \qquad (3.5\text{ e})$$

Table 3-2: Deflections at Mid and Quarter Span for Phase A

<table>
<tr><th>Deflection (mm)</th><th>Mid Span</th><th colspan="2">Quarter Span</th></tr>
<tr><td>Downward deflection due to the own-weight of the beam (mm)</td><td>-8.41</td><td colspan="2">-5.02</td></tr>
<tr><td>Deflection due to the upward pressure of the pretensioning force (mm)</td><td>4.68</td><td colspan="2">2.81</td></tr>
<tr><td rowspan="2">Upward deflection due to the eccentricity of the pretensioned tendons at the end (mm)</td><td rowspan="2">15.02</td><td>Effect of the eccentricity of the tendons from the left end</td><td>3.89</td></tr>
<tr><td>Effect of eccentricity of the tendons from the right end</td><td>5.82</td></tr>
<tr><td>Total upward deflection (mm)</td><td>11.29</td><td colspan="2">7.50</td></tr>
</table>

Reproduced with permission of the copyright owner. Further reproduction prohibited without permission.

3.4 Phase B: Sixty Percent of External Post – Tensioning

Herein, sixty percent of the post-tensioning force was applied in two steps: thirty percent of the required target load level was reached in the first phase by pulling the tendons from one side, and the remaining thirty percent was reached by pulling the tendons from the other side. During this phase the beam was supported on its two intermediate transverse diaphragms (D2 and D6) and no cracks were developed, thus, the gross moment of inertia is used in calculating the stresses and deflections.

3.4.1 Elastic Shortening of Pre-Tensioned Tendons at Sixty Percent of External Post-Tensioning

The stress of concrete at level of tendons is,

$$f_C = \frac{F_1}{A} + \frac{F_1 \times e_1^2}{I_g} + \frac{P_1}{A} + \frac{P_1 \times e_1^2}{I_g} - \frac{M_D \times e_1}{I_g} \qquad (3.6\text{ a})$$

where,

F_1 = 5057 kN

P_1 = sixty percent of post-tensioning force =1072 kN

$$\text{Loss of stress} = \frac{E_T}{E_C} \times f_C \qquad (3.6\text{ b})$$

The concrete was seven days mature in this stage reaching its full strength and it had a final value of $E_C = 32 \times 10^3$ MPa. (Final report submitted by Construction Technology Laboratories).

Reproduced with permission of the copyright owner. Further reproduction prohibited without permission.

The loss in the pre-tensioning force = Loss of stress × A_T (3.6 c)

Total pre-tensioned force after losses,

$F_2 = F_1 -$ Loss of force (3.6 d)

Leading to $F_2 = 4913$ kN.

3.4.2 Calculation of Stresses

The post-tensioned force applied in this phase shortened the beam causing more losses due to elastic shortening. The stresses are calculated at mid and quarter span using the effective prestressing force after the elastic shortening of concrete, the post-tensioned force and the own-weight of the beam using equations 3.7a and 3.7 b. Figure 3-4 shows the dimensions of the beam in this phase. Figure 3-5 and Figure 3-6 show the distribution of the stresses at mid span and quarter span.

$$f_2 = -\frac{F_2}{A} - \frac{P_1}{A} + \frac{F_2 \times e_1 \times Y_t}{I_g} + \frac{P_1 \times e_2 \times Y_t}{I_g} - \frac{M_D \times Y_t}{I_g} \quad (3.7\text{ a})$$

$$f_1 = -\frac{F_2}{A} - \frac{P_1}{A} - \frac{F_2 \times e_1 \times Y_b}{I_g} - \frac{P_1 \times e_2 \times Y_b}{I_g} + \frac{M_D \times Y_b}{I_g} \quad (3.7\text{ b})$$

The pretensioned force used in calculating the stresses has to be modified due to the effect of creep. The coefficient of creep has to be calculated, which defines the ratio of the creep strain to the initial strain in concrete.

Reproduced with permission of the copyright owner. Further reproduction prohibited without permission.

The coefficient of creep is calculated using the ACI formula,

$$C_{t1} = \frac{t_1^{0.60}}{10 + t_1^{0.60}} \times C_u \times Q_{cr}, \qquad (3.8\ a)$$

where,

t_1 = five days.

The creep strain is,

$$\varepsilon_{cr} = C_{ti} \times \varepsilon_i \qquad (3.8\ b)$$

The increase in the strain in concrete is accompanied by a reduction in the stress in the pretensioning force, which is calculated by the formula,

$$f_r = E_t \times \varepsilon_{cr} \qquad (3.8\ c)$$

where,

f_r is the reduction in stress in the pretensioning force in this stage

The pretensioned force after the creep loss is,

$$F_3 = F_2 - f_r \times A_T \qquad (3.8\ d)$$

where,

$F_2 = 4913$ kN

Leading to $F_3 = 4874$ kN

The stresses are calculated again at mid and quarter span with the new pretensioned force calculated after the effect of creep.

Reproduced with permission of the copyright owner. Further reproduction prohibited without permission.

$$f_2 = -\frac{F_3}{A} - \frac{P_1}{A} + \frac{F_3 \times e_1 \times Y_t}{I_g} + \frac{P_1 \times e_2 \times Y_t}{I_g} - \frac{M_D \times Y_t}{I_g} \quad (3.9\text{ a})$$

$$f_1 = -\frac{F_3}{A} - \frac{P_1}{A} - \frac{F_3 \times e_1 \times Y_b}{I_g} - \frac{P_1 \times e_2 \times Y_b}{I_g} + \frac{M_D \times Y_b}{I_g} \quad (3.9\text{ b})$$

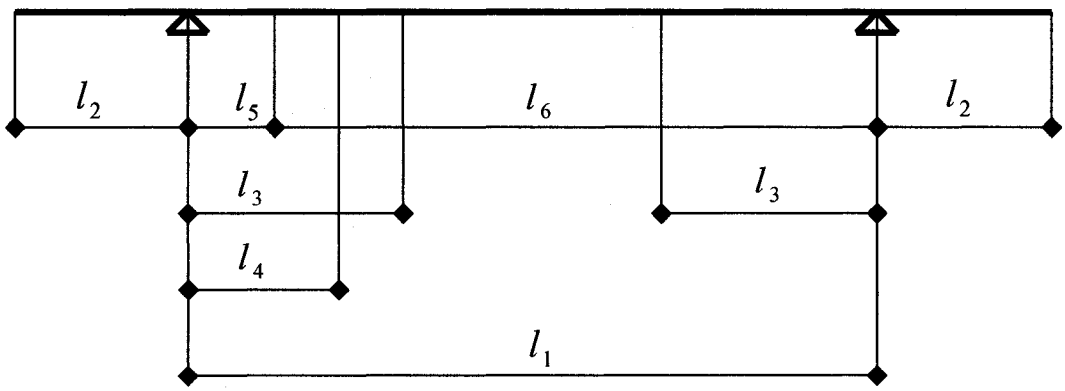

Where, l_1 = Span between internal diaphragms.(supports during this phase)

l_2 = Span of the cantilever.

l_3 = Distance from the internal diaphragm to the point of application of the pre-tensioning force.

l_4 = Distance from the internal diaphragm to the first deviator of the post-tensioning force.

l_5 = Distance from the internal diaphragm to the quarter span.

$l_6 = l_1 - l_5$

Figure 3-4: Dimensions of the Beam in Phase B

Reproduced with permission of the copyright owner. Further reproduction prohibited without permission.

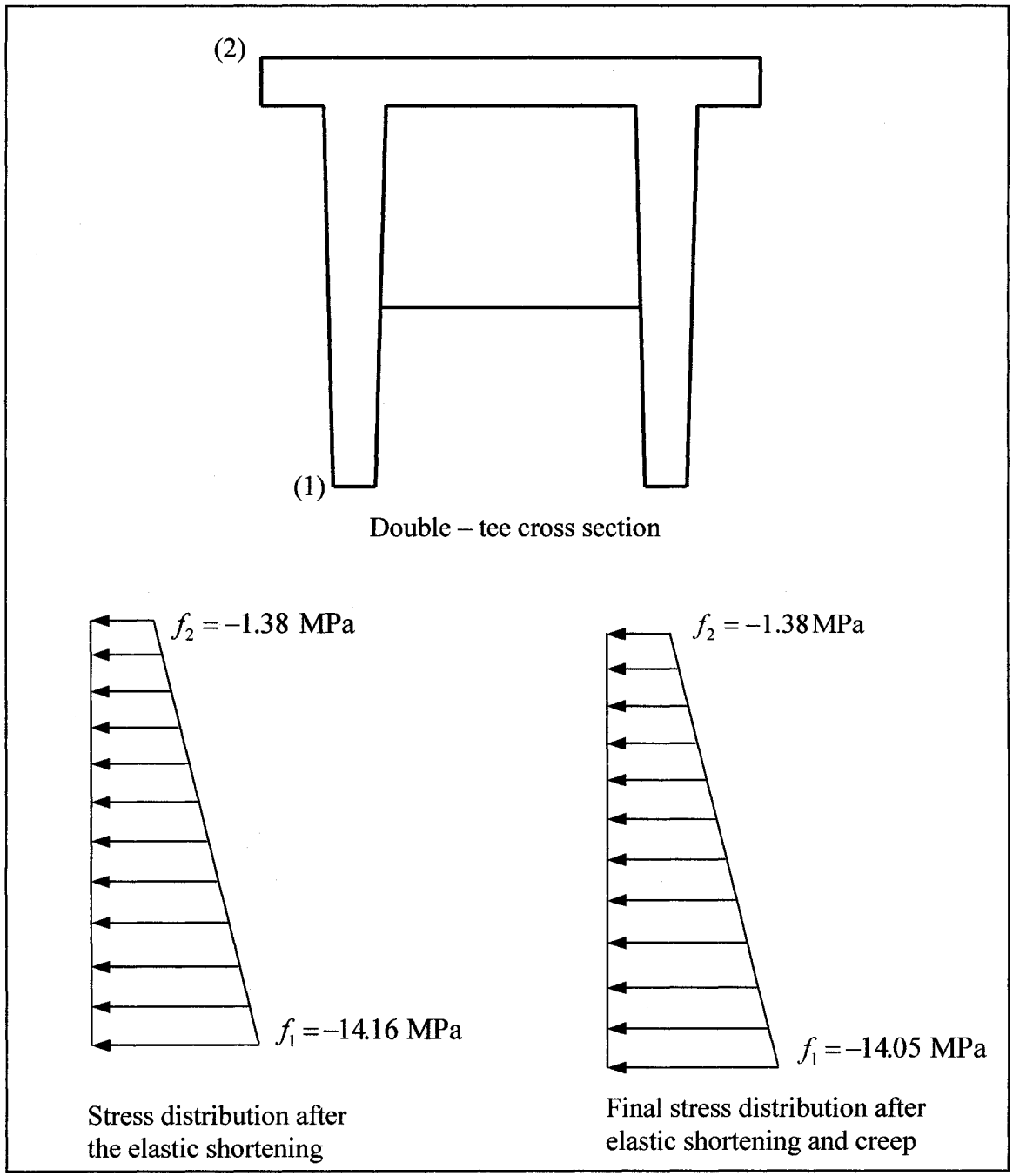

Figure 3-5: Distribution of Stresses at Mid Span for Phase B

Reproduced with permission of the copyright owner. Further reproduction prohibited without permission.

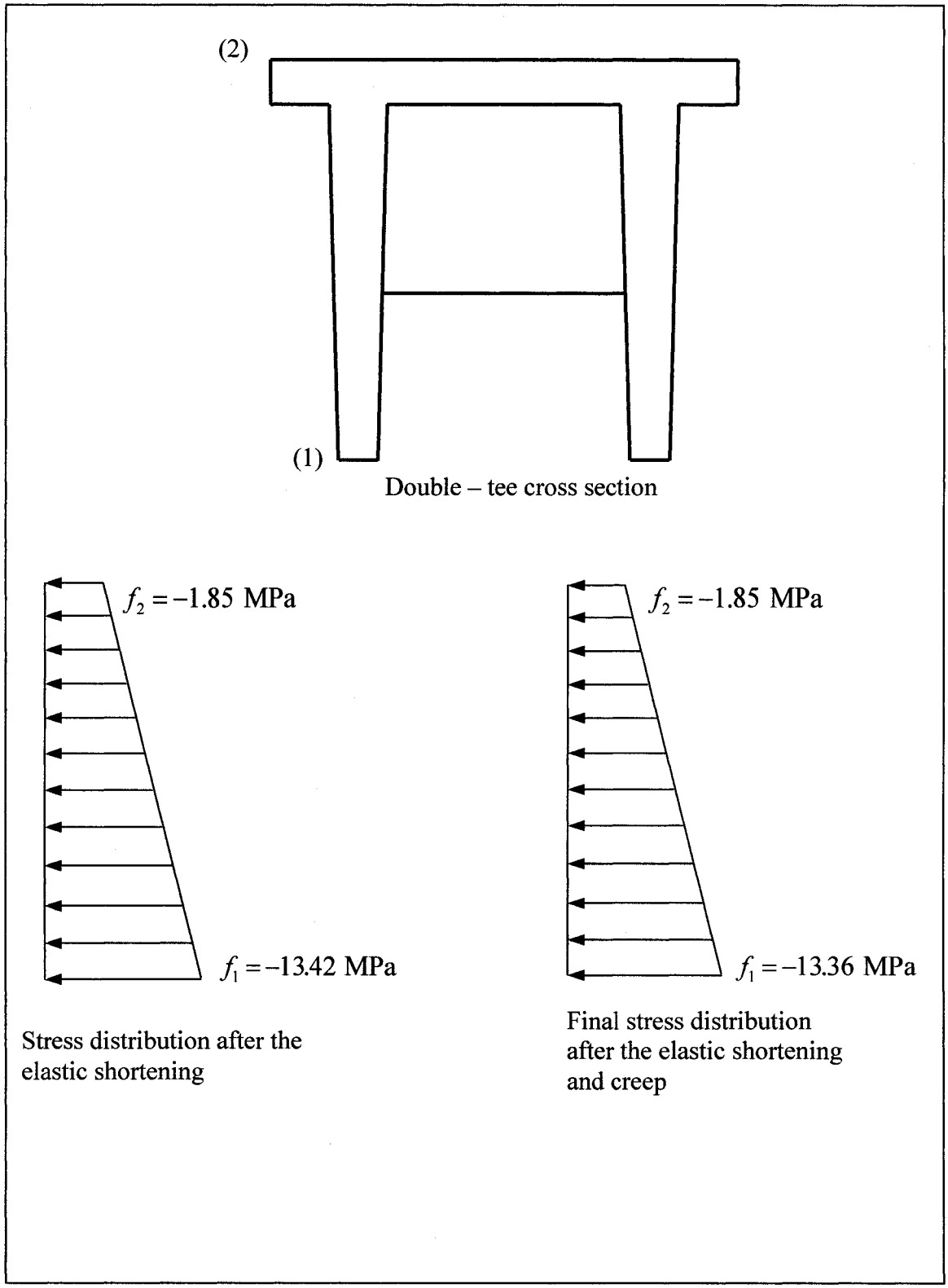

Figure 3-6: Distribution of Stresses at Quarter Span for Phase B

Reproduced with permission of the copyright owner. Further reproduction prohibited without permission.

Table 3-3: Stresses at Mid and Quarter Span for Phase B

Stresses (MPa)		Mid Span	Quarter Span
Stresses after elastic shortening.	Top Stress (MPa)	-1.382	-1.852
	Bottom Stress (MPa)	-14.164	-13.426
Final stresses after elastic shortening and creep	Top Stress (MPa)	-1.386	-1.850
	Bottom Stress (MPa)	-14.053	-13.368

3.4.3 Calculations for Deflection

The beam was uncracked in this phase so the gross moment of inertia is used in calculating the deflections for both mid and quarter spans.

3.4.3.1 Calculations for Deflection at Mid Span

Downward deflection due to own-weight, (Hibbeler 1999)

$$\delta_1 = \frac{5 \times W_D \times l_1^4}{384 \times E_C \times I_g} \qquad (3.10\ a)$$

Reproduced with permission of the copyright owner. Further reproduction prohibited without permission.

Upward deflection due to the effect of cantilevers, (Hibbeler 1999)

$$\delta_2 = \frac{M_C \times l_1^{\,2}}{8 \times E_C \times I_g} \qquad (3.10\text{ b})$$

Upward deflection due to the pre-tensioning force, (CSCE, 2000)

$$\delta_3 = \frac{F_3 \times Sin\phi \times l_3}{24 \times E_C \times I_g}\left(3 \times l_1^{\,2} - 4 \times l_3^{\,2}\right) \qquad (3.10\text{ c})$$

Deflection due to eccentricity of the tendons at the end, (Hibbeler 1999)

$$\delta_4 = \frac{M_T \times l_1^{\,2}}{8 \times E_C \times I_g} \qquad (3.10\text{ d})$$

Deflection due to external post-tensioning, (CSCE, 2000)

$$\delta_5 = \frac{2 \times P_1 \times Sin\theta_1 \times l_1^{\,3}}{48 \times E_C \times I_g} \qquad (3.10\text{ e})$$

$$\delta_6 = \frac{\left(P_1 \times Sin\theta_2 - P_1 \times Sin\theta_1\right) \times l_4}{24 \times E_C \times I_g}\left(3 \times l_1^{\,2} - 4 \times l_4^{\,2}\right) \qquad (3.10\text{ f})$$

The total upward deflection,

$$\delta = -\delta_1 + \delta_2 + \delta_3 + \delta_4 + \delta_5 + \delta_6 \qquad (3.10\text{ g})$$

The end of the cantilever, in this phase, was taken as a reference point for measuring the deflection for the mid and quarter spans. Owing to the effect of prestressing, the end of the cantilever experienced a downward deflection, this value should be added to the

Reproduced with permission of the copyright owner. Further reproduction prohibited without permission.

upward deflection at the mid and quarter span to get the relative deflection between the two points. The downward deflection at the end of the cantilever is calculated using the following procedure:

The slope at the support is calculated due to the pretensioning force, (Hibbeler 1999)

$$\alpha_1 = \frac{F_3 \times Sin\phi}{2 \times E_C \times I_g}(l_1 - l_3) \qquad (3.10\text{ h})$$

The slope at the support is calculated due to the post-tensioning force, (Hibbeler 1999)

$$\alpha_2 = \frac{P_1 \times Sin\theta_1 \times l_1^{\,2}}{16 \times E_C \times I_g} \qquad (3.10\text{ I})$$

$$\alpha_3 = \frac{(P_1 \times Sin\theta_2 - P_1 \times Sin\theta_1)}{2 \times E_C \times I_g}(l_1 - l_4) \qquad (3.10\text{ j})$$

The total slope at the support,

$$\alpha_T = \alpha_1 + \alpha_2 + \alpha_3 \qquad (3.10\text{ k})$$

The downward deflection at the end of the cantilever,

$$\delta_C = \alpha_T \times l_2 \qquad (3.10\text{ l})$$

The relative deflection between the mid span and the end of the cantilever

$$\delta_R = \delta_C + \delta \qquad (3.10\text{ m})$$

3.4.3.2 Calculations for Deflection at Quarter Span

Downward deflection due to own-weight, (CSCE, 2000)

$$\delta_1 = \frac{W_D \times l_5}{24 \times E_C \times I_g}\left(l_5^{\,3} - 2 \times l_1 \times l_5^{\,2} + l_1^{\,3}\right) \qquad (3.11\text{ a})$$

Reproduced with permission of the copyright owner. Further reproduction prohibited without permission.

Upward deflection due to the effect of cantilevers, (Hibbeler 1999)

Left cantilever moment,

$$\delta_2 = \frac{M_C \times l_6}{6 \times E_C \times I_g \times l_1}\left(l_6^{\,2} - 3 \times l_1 \times l_6 + 2 \times l_1^{\,2}\right) \qquad (3.11\ b)$$

Right cantilever moment,

$$\delta_3 = \frac{M_C \times l_5}{6 \times E_C \times I_g \times l_1}\left(l_5^{\,2} - 3 \times l_1 \times l_5 + 2 \times l_1^{\,2}\right) \qquad (3.11\ c)$$

Upward deflection due to the pressure of the pre-tensioning force, (CSCE, 2000)

$$\delta_4 = \frac{F_3 \times Sin\phi \times l_5}{6 \times E_C \times I_g}\left(3 \times l_1 \times l_3 - 3 \times l_3^{\,2} - l_5^{\,2}\right) \qquad (3.11\ d)$$

Deflection due to eccentricity of the tendons at the end, (Hibbeler 1999)

Left moment,

$$\delta_5 = \frac{M_T \times l_6}{6 \times E_C \times I_g \times l_1}\left(l_6^{\,2} - 3 \times l_1 \times l_6 + 2 \times l_1^{\,2}\right) \qquad (3.11\ e)$$

Right moment,

$$\delta_6 = \frac{M_T \times l_5}{6 \times E_C \times I_g \times l_1}\left(l_5^{\,2} - 3 \times l_1 \times l_5 + 2 \times l_1^{\,2}\right) \qquad (3.11\ f)$$

Deflection due to external post-tensioning (CSCE, 2000)

$$\delta_7 = \frac{2 \times P_1 \times Sin\theta \times l_5}{48 \times E_C \times I_g}\left(3 \times l_1 - 4 l_5^{\,2}\right) \qquad (3.11\ g)$$

Reproduced with permission of the copyright owner. Further reproduction prohibited without permission.

$$\delta_8 = \frac{(P_1 \times Sin\theta_2 - P_1 \times Sin\theta 1) \times l_5}{6 \times E_C \times I_g}\left(3 \times l_1 \times l_4 - 3 \times l_7^{\,2} - l_4^{\,2}\right) \quad (3.11\ h)$$

The total upward deflection,

$$\delta = -\delta_1 + \delta_2 + \delta_3 + \delta_4 + \delta_5 + \delta_6 + \delta_7 + \delta_8 \quad (3.11\ I)$$

The relative deflection is calculated between the quarter span and the end of the cantilever using the same procedure followed for the mid span.

The slope at the support is calculated due to the pretensioning force, (Hibbeler 1999)

$$\alpha_1 = \frac{F_3 \times Sin\phi}{2 \times E_C \times I_g}(l_1 - l_3) \quad (3.11\ j)$$

The slope at the support is calculated due to the post-tensioning force, (Hibbeler 1999)

$$\alpha_2 = \frac{P_1 \times Sin\theta_1 \times l_1^{\,2}}{16 \times E_C \times I_g} \quad (3.11\ k)$$

$$\alpha_3 = \frac{(P_1 \times Sin\theta_2 - P_1 \times Sin\theta_1)}{2 \times E_C \times I_g}(l_1 - l_4) \quad (3.11\ l)$$

The total slope at the support,

$$\alpha_T = \alpha_1 + \alpha_2 + \alpha_3 \quad (3.11\ m)$$

The downward deflection at the end of the cantilever,

$$\delta_C = \alpha_T \times l_2 \quad (3.11\ n)$$

The relative deflection between the mid span and the end of the cantilever

$$\delta_R = \delta_C + \delta \quad (3.11\ o)$$

Reproduced with permission of the copyright owner. Further reproduction prohibited without permission.

Table 3-4: Deflections at Mid and Quarter Span for Phase B

Deflection (mm)	Mid Span	Quarter Span	
Downward deflection due to the own-weight of the beam (mm)	-3.88	-2.02	
Upward deflection due to the effect of cantilevers (mm)	0.45	Deflection due to left cantilever	0.10
		Deflection due to right cantilever	0.16
Deflection due to the upward pressure of the pretensioning force (mm)	2.17	1.15	
Upward deflection due to the eccentricity of the pretensioned tendons at the end (mm)	8.59	Effect of the eccentricity of the tendons from the left end	1.91
		Effect of eccentricity of the tendons from the right end	2.99
Upward deflection due to external post - tensioning	2.87	1.47	
Total upward deflection (mm)	10.20	5.76	
Downward deflection of the cantilever	-2.48	-2.48	
Relative deflection (mm)	12.68	8.24	

Reproduced with permission of the copyright owner. Further reproduction prohibited without permission.

3.5 Phase C: Casting Topping

The beam was transported to Construction Technology Laboratories to be tested and in this phase it was resting at its external diaphragms. Concrete topping of seventy-five mm thick was cast over the top flange of the DT- beam and no additional external prestressing force was applied on the beam during this phase. Figure 3-7 shows the dimensions of the beam in this phase. Figure 3-8 and Figure 3-9 show the distribution of stresses for both mid and quarter span.

3.5.1 Calculation of Stresses

The top and bottom stresses before the introduction of the creep effect are,

$$f_2 = -\frac{F_3}{A} - \frac{P_1}{A} + \frac{F_3 \times e_1 \times Y_t}{I_g} + \frac{P_1 \times e_2 \times Y_t}{I_g} - \frac{M_D \times Y_t}{I_g} - \frac{M_S \times Y_t}{I_g} \qquad (3.12\text{ a})$$

$$f_1 = -\frac{F_3}{A} - \frac{P_1}{A} - \frac{F_3 \times e_1 \times Y_b}{I_g} - \frac{P_1 \times e_2 \times Y_b}{I_g} + \frac{M_D \times Y_b}{I_g} + \frac{M_S \times Y_b}{I_g} \qquad (3.12\text{ b})$$

where,

Ms = moment due to own-weight of the top slab

F_3 = 4874 kN

The coefficient of creep is calculated using the ACI formula,

$$C_{t2} = \frac{t_2^{0.60}}{10 + t_2^{0.60}} \times C_u \times Q_{cr}, \qquad (3.13\text{ a})$$

Reproduced with permission of the copyright owner. Further reproduction prohibited without permission.

where,

t_2 = nineteen days.

The increase in the creep strain is,

$$\varepsilon_{cr} = (C_{ti} - C_{t2}) \times \varepsilon_i \qquad (3.13\ b)$$

The increase in the strain in concrete is accompanied by a reduction in the stress in the pretensioning force, which is calculated by the formula,

$$f_{r2} = E_T \times \varepsilon_{cr} \qquad (3.13\ c)$$

Where,

f_r is the reduction in stress in the pretensioning force in this stage

The pretensioned force after the creep loss is,

$$F_4 = F_3 - f_{r2} \times A_T \qquad (3.13\ d)$$

Leading to F_4 = 4857 kN

The stresses at the mid and quarter span is calculated after the losses in the pretensioned force due to the effect of creep,

The top and bottom stresses after the introduction of the creep effect are,

$$f_2 = -\frac{F_4}{A} - \frac{P_1}{A} + \frac{F_4 \times e_1 \times Y_t}{I_g} + \frac{P_1 \times e_2 \times Y_t}{I_g} - \frac{M_D \times Y_t}{I_g} - \frac{M_S \times Y_t}{I_g} \qquad (3.14\ a)$$

$$f_1 = -\frac{F_4}{A} - \frac{P_1}{A} - \frac{F_4 \times e_1 \times Y_b}{I_g} - \frac{P_1 \times e_2 \times Y_b}{I_g} + \frac{M_D \times Y_b}{I_g} + \frac{M_S \times Y_b}{I_g} \qquad (3.14\ b)$$

Reproduced with permission of the copyright owner. Further reproduction prohibited without permission.

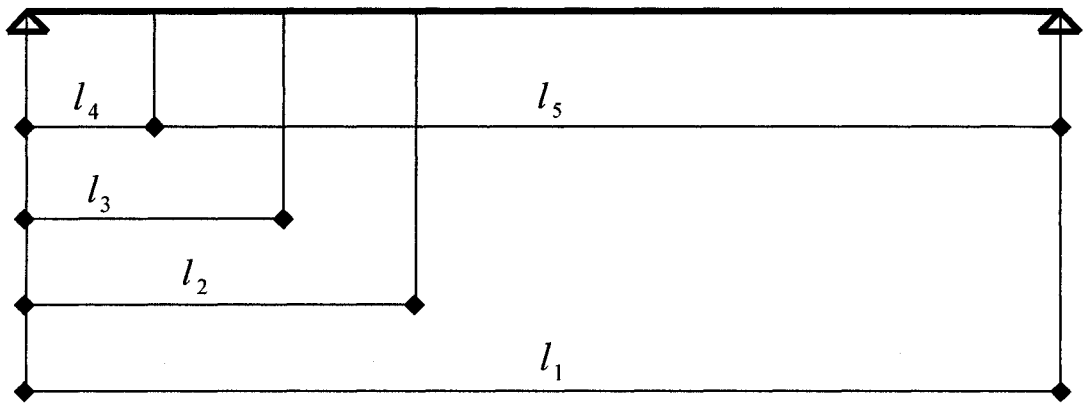

Where, l_1 = Span between external diaphragms (end supports).

l_2 = Distance from the end support to the point of application of the pre – tensioning force.

l_3 = Distance from the end support to the first deviator of the post – tensioning force.

l_4 = Distance from the end support to the quarter span.

$l_5 = l_1 - l_4$

Figure 3-7: Dimensions of the Beam in Phase C

Reproduced with permission of the copyright owner. Further reproduction prohibited without permission.

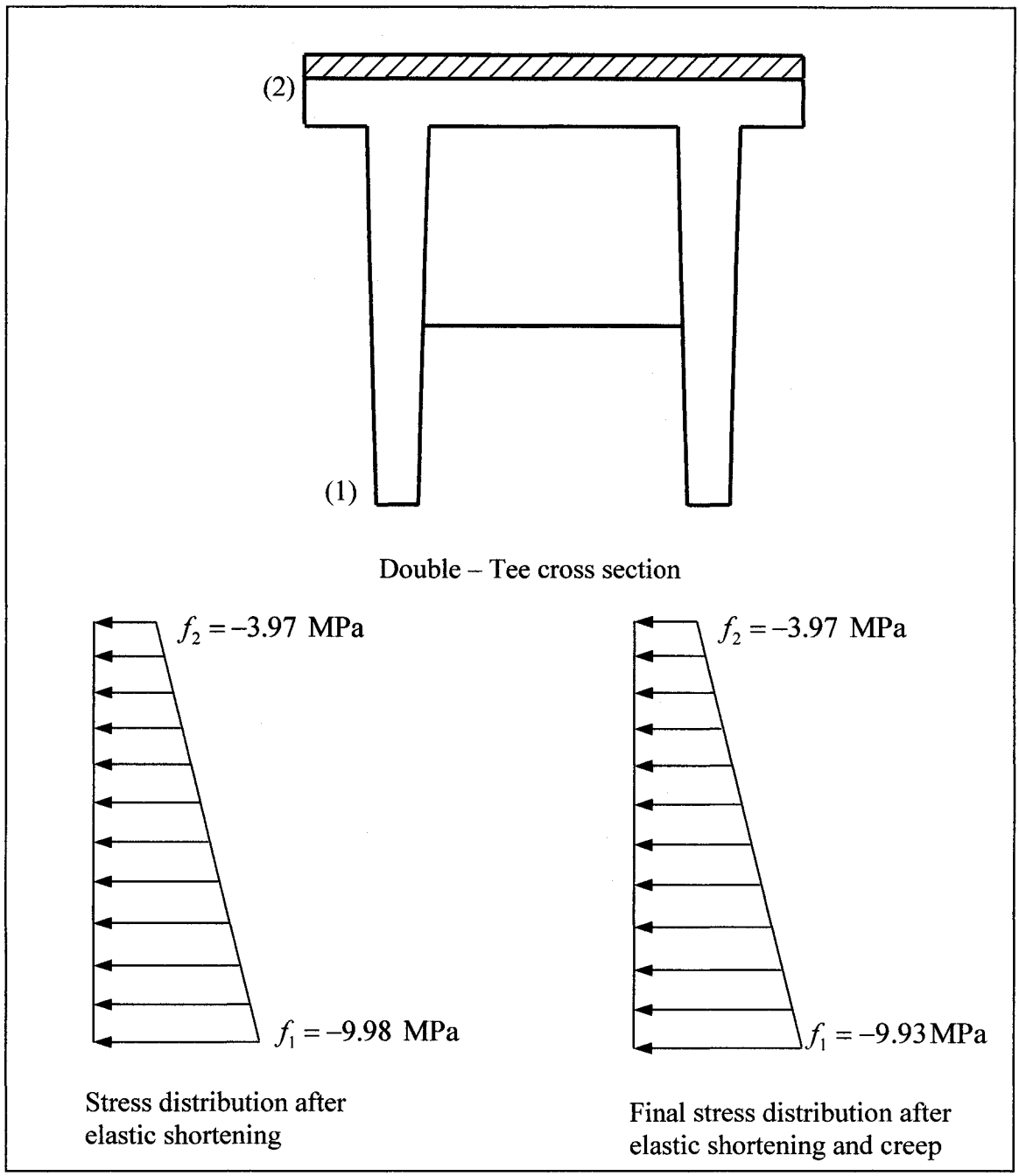

Figure 3-8: Distribution of Stresses at Mid Span for Phase C

Reproduced with permission of the copyright owner. Further reproduction prohibited without permission.

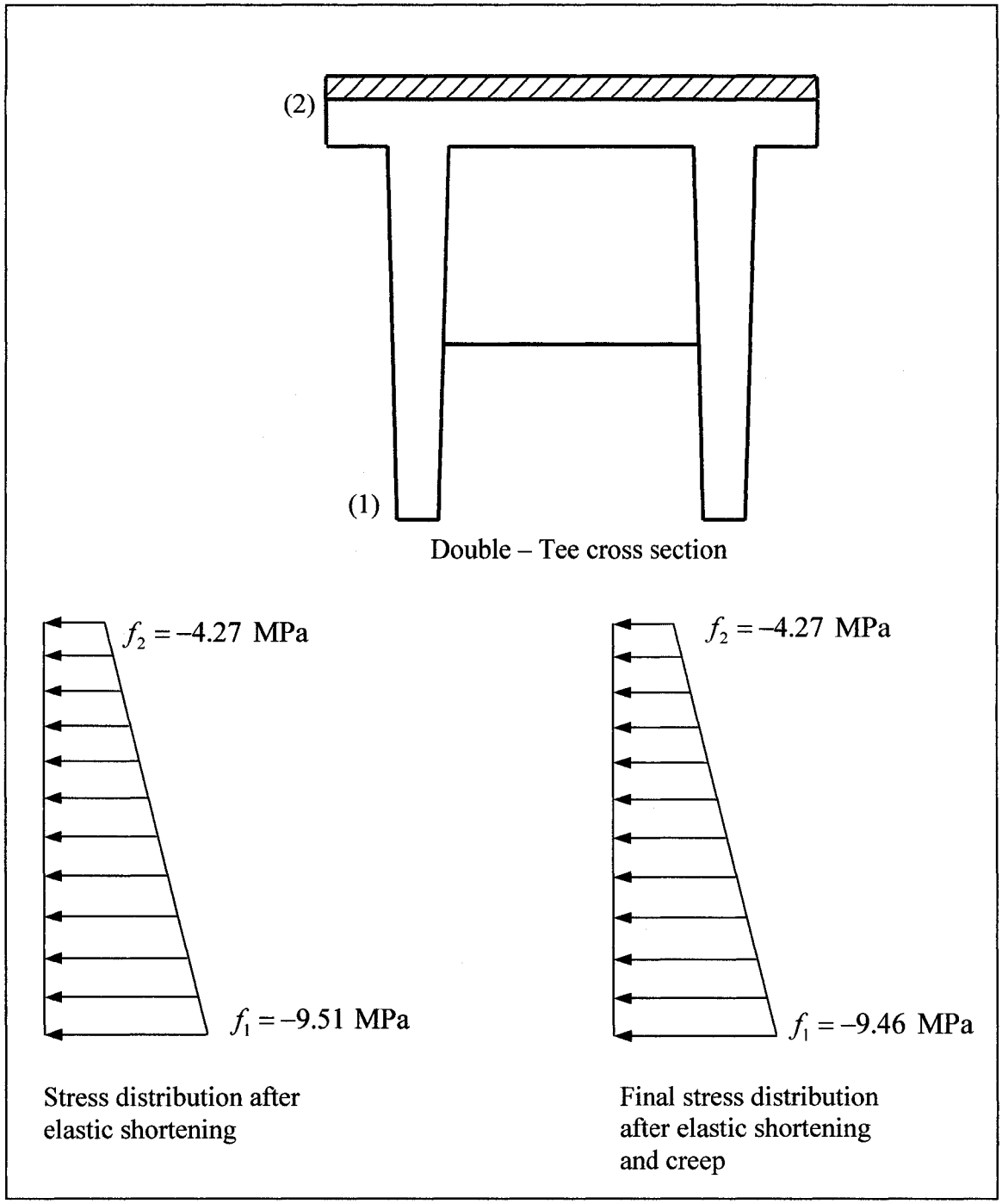

Figure 3-9: Distribution of Stresses at Quarter Span for Phase C

Reproduced with permission of the copyright owner. Further reproduction prohibited without permission.

Table 3-5: Stresses at Mid and Quarter Span for Phase C

Stresses (MPa)		Mid Span	Quarter Span
Stresses after elastic shortening.	Top Stress (MPa)	-3.97	-4.27
	Bottom Stress (MPa)	-9.98	-9.51
Final stresses after elastic shortening and creep	Top Stress (MPa)	-3.97	-4.27
	Bottom Stress (MPa)	-9.93	-9.46

3.5.2 Calculations for Deflection

The top slab added in this phase increased the dead load acting on the double –tee beam and that caused an increase in the compression stresses in the top fibers and a reduction in the compression stresses in the bottom fibers, however, no tension stresses were developed and the gross moment of inertia still can be used in calculating the deflections.

Reproduced with permission of the copyright owner. Further reproduction prohibited without permission.

3.5.2.1 Calculations for Deflection at Mid Span

Downward deflection due to own-weight, (Hibbeler 1999)

$$\delta_1 = \frac{5 \times W_D \times l_1^4}{384 \times E_C \times I_g} \quad (3.15\text{ a})$$

Deflection due to topping (Hibbeler 1999)

$$\delta_2 = \frac{5 \times W_S \times l_1^4}{384 \times E_C \times I_g} \quad (3.15\text{ b})$$

Upward deflection due to the pre-tensioning force, (CSCE, 2000)

$$\delta_3 = \frac{F_4 \times Sin\theta \times l_2}{24 \times E_C \times I_g}\left(3 \times l_1^2 - 4 \times l_2^2\right) \quad (3.15\text{ c})$$

Deflection due to eccentricity of the tendons at the end, (Hibbeler 1999)

$$\delta_4 = \frac{M_T \times l_1^2}{8 \times E_C \times I_g} \quad (3.15\text{ d})$$

Deflection due to external post-tensioning, (CSCE, 2000)

$$\delta_5 = \frac{2 \times P_1 \times Sin\theta \times l_1^3}{48 \times E_C \times I_g} \quad (3.15\text{ e})$$

$$\delta_6 = \frac{\left(P_1 \times Sin\theta_2 - P_1 \times Sin\theta_1\right) \times l_3}{24 \times E_C \times I_g}\left(3 \times l_1^2 - 4 \times l_3^2\right) \quad (3.15\text{ f})$$

Reproduced with permission of the copyright owner. Further reproduction prohibited without permission.

The total upward deflection,

$$\delta = -\delta_1 - \delta_2 + \delta_3 + \delta_4 + \delta_5 + \delta_6 \qquad (3.15\ g)$$

3.5.2.2 Calculations for Deflection at Quarter Span

Downward deflection due to own-weight, (CSCE, 2000)

$$\delta_1 = \frac{W_D \times l_4}{24 \times E_C \times I_g}\left(l_1^{\,3} - 2 \times l_1 \times l_4^{\,2} + l_4^{\,3}\right) \qquad (3.16\ a)$$

Deflection due to topping, (CSCE, 2000)

$$\delta_2 = \frac{W_S \times l_4}{24 \times E_C \times I_g}\left(l_1^{\,3} - 2 \times l_1 \times l_4^{\,2} + l_4^{\,3}\right) \qquad (3.16\ a)$$

Upward Deflection due to the pre-tensioning force, (CSCE, 2000)

$$\delta_3 = \frac{F_4 \times Sin\phi \times l_4}{6 \times E_C \times I_g}\left(3 \times l_1 \times l_2 - 3 \times l_2^{\,2} - l_4^{\,2}\right) \qquad (3.16\ c)$$

Deflection due to eccentricity of the tendons at the end, (Hibbeler 1999)

Left moment,

$$\delta_4 = \frac{M_T \times l_5}{6 \times E_C \times I_g \times l_1}\left(l_5^{\,2} - 3 \times l_1 \times l_5 + 2 \times l_1^{\,2}\right) \qquad (3.16\ d)$$

Right moment,

$$\delta_5 = \frac{M_D \times l_4}{6 \times E_C \times I_g \times l_1}\left(l_4^{\,2} - 3 \times l_1 \times l_4 + 2 \times l_1^{\,2}\right) \qquad (3.16\ e)$$

Reproduced with permission of the copyright owner. Further reproduction prohibited without permission.

Deflection due to external post – tensioning, (CSCE, 2000)

$$\delta_6 = \frac{2 \times P_1 \times Sin\theta \times l_4}{48 \times E_C \times I_g}\left(3 \times l_1^{\,2} - 4 \times l_4^{\,2}\right) \quad (3.16\text{ f})$$

$$\delta_7 = \frac{\left(P_1 \times Sin\theta_2 - P_1 \times Sin\theta_1\right) \times l_4}{6 \times E_C \times I_g}\left(3 \times l_1 \times l_3 - 3 \times l_3^{\,2} - l_4^{\,2}\right) \quad (3.16\text{ g})$$

The total upward deflection,

$$\delta_f = -\delta_1 - \delta_2 + \delta_3 + \delta_4 + \delta_5 + \delta_6 + \delta_7 \quad (3.16\text{ h})$$

Table 3-6: Deflections at Mid and Quarter Span for Phase C

Deflection (mm)	Mid Span	Quarter Span	
Downward deflection due to the Self – weight of the beam and topping (mm)	-13.46	-9.57	
Deflection due to the upward pressure of the pretensioning force (mm)	5.52	3.87	
Upward deflection due to the eccentricity of the pretensioned tendons at the end (mm)	12.47	Effect of the eccentricity of the tendons from the left end	3.89
		Effect of eccentricity of the tendons from the right end	5.45
Upward deflection due to external post - tensioning	6.9	4.83	
Total upward deflection (mm)	11.43	8.47	

Reproduced with permission of the copyright owner. Further reproduction prohibited without permission.

3.6 Phase D: Full Post-Tensioning

By this phase, the remaining forty percent of the post-tensioning force was effective and the beam is ready to be tested under live loading. The concrete topping was hardened and full composite action can be assumed. Figure 3-10 shows the dimensions of the beam. Figures 3-11 and 3-12 show the distribution of stresses for the mid and quarter span.

3.6.1 Elastic Shortening of Pre-Tensioned Tendons due to Full Post – Tensioning

The stress of concrete at level of tendons is,

$$f_C = \frac{F_4}{A} + \frac{F_4 \times e_1^{\,2}}{I_g} + \frac{P_2}{A} + \frac{P_2 \times e_1^2}{I_g} - \frac{M_D \times e_1}{I_g} \qquad (3.17\text{ a})$$

where,

$F_4 = 4857$ kN

P_2 = full post-tensioning force =1796 kN

$$\text{Loss of stress} = \frac{E_T}{E_C} \times f_C \qquad (3.17\text{ b})$$

The concrete was twenty-nine days mature in this stage reaching its full strength and it had a final value of $E_C = 32 \times 10^3$ MPa. (Final report submitted by construction Technology laboratories).

Reproduced with permission of the copyright owner. Further reproduction prohibited without permission.

The loss in the pre-tensioning force = Loss of stress × A_T (3.17 c)

Total pre-tensioned force after losses,

$F_5 = F_4 -$ Loss of force (3.17 d)

Leading to $F_5 = 4724$ kN

3.6.2 Calculation of Stresses

New section properties were calculated in this phase to account for the composite action in calculating the stresses at mid and quarter span.

The top and bottom stress before the introduction of creep are,

$$f_2 = -\frac{F_5}{A_C} - \frac{P_1}{A_C} + \frac{F_5 \times e_1 \times Y_t}{I_C} + \frac{P_1 \times e_2 \times Y_t}{I_C} - \frac{M_D \times Y_t}{I_C} - \frac{M_S \times Y_t}{I_C} \quad (3.18\text{ a})$$

$$f_1 = -\frac{F_5}{A_C} - \frac{P_1}{A_C} - \frac{F_5 \times e_1 \times Y_b}{I_C} - \frac{P_1 \times e_2 \times Y_b}{I_C} + \frac{M_D \times Y_b}{I_C} + \frac{M_S \times Y_b}{I_C} \quad (3.18\text{ b})$$

The effect of the remaining forty percent of post-tensioning force is then added to obtain the final stresses as shown in Figure 3-11.

$$f_4 = -\frac{P_2}{A_C} + \frac{P_2 \times e_2 \times Y_t'}{I_C} \quad (3.18\text{ c})$$

$$f_1 = -\frac{P_2}{A_C} - \frac{P_2 \times e_2 \times Y_b}{I_C} \quad (3.18\text{ d})$$

Reproduced with permission of the copyright owner. Further reproduction prohibited without permission.

The coefficient of creep is calculated using the ACI formula,

$$C_{t3} = \frac{t_3^{0.60}}{10 + t_3^{0.60}} \times C_u \times Q_{cr}, \qquad (3.19\ a)$$

Where,

t_3 = twenty seven days.

The increase in the creep strain is,

$$\varepsilon_{cr} = (C_{t3} - C_{t2}) \times \varepsilon_i \qquad (3.19\ b)$$

The increase in the strain in concrete is accompanied by a reduction in the stress in the pretensioning force, which is calculated by the formula,

$$f_{r3} = E_T \times \varepsilon_{cr} \qquad (3.19\ c)$$

where,

f_{r3} is the reduction in stress due to the creep in this phase.

The pretensioned force after the creep loss is,

$$F_6 = F_5 - f_{r3} \times A_T \qquad (3.19\ d)$$

Leading to F_6 = 4720 kN

The stresses at mid and quarter span are calculated after the losses in the pretensioned force due to the effect of creep, Figures 3-11 and 3-12 show the final stresses after the introduction of the creep effect.

Reproduced with permission of the copyright owner. Further reproduction prohibited without permission.

The top and bottom stresses after the introduction of the creep effect are,

$$f_2 = -\frac{F_6}{A_C} - \frac{P_1}{A_C} + \frac{F_6 \times e_1 \times Y_t}{I_C} + \frac{P_1 \times e_2 \times Y_t}{I_C} - \frac{M_D \times Y_t}{I_C} - \frac{M_S \times Y_t}{I_C} \quad (3.20\text{ a})$$

$$f_1 = -\frac{F_6}{A_C} - \frac{P_1}{A_C} - \frac{F_6 \times e_1 \times Y_b}{I_C} - \frac{P_1 \times e_2 \times Y_b}{I_C} + \frac{M_D \times Y_b}{I_C} + \frac{M_S \times Y_b}{I_C} \quad (3.20\text{ b})$$

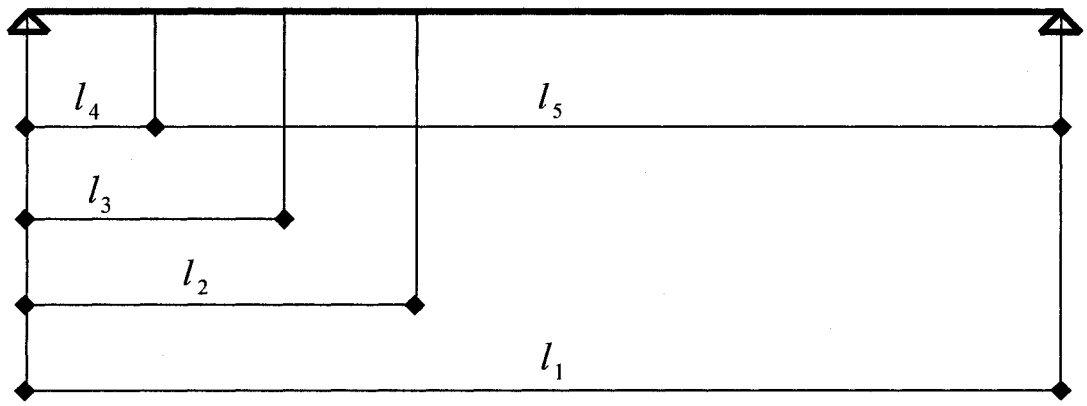

Where, l_1 = Span between external diaphragms (end supports).

l_2 = Distance from the end support to the point of application of the pre – tensioning force.

l_3 = Distance from the end support to the first deviator of the post – tensioning force.

l_4 = Distance from the end support to the quarter span.

$l_5 = l_1 - l_4$

Figure 3-10: Dimensions of The Beam in Phase D

Reproduced with permission of the copyright owner. Further reproduction prohibited without permission.

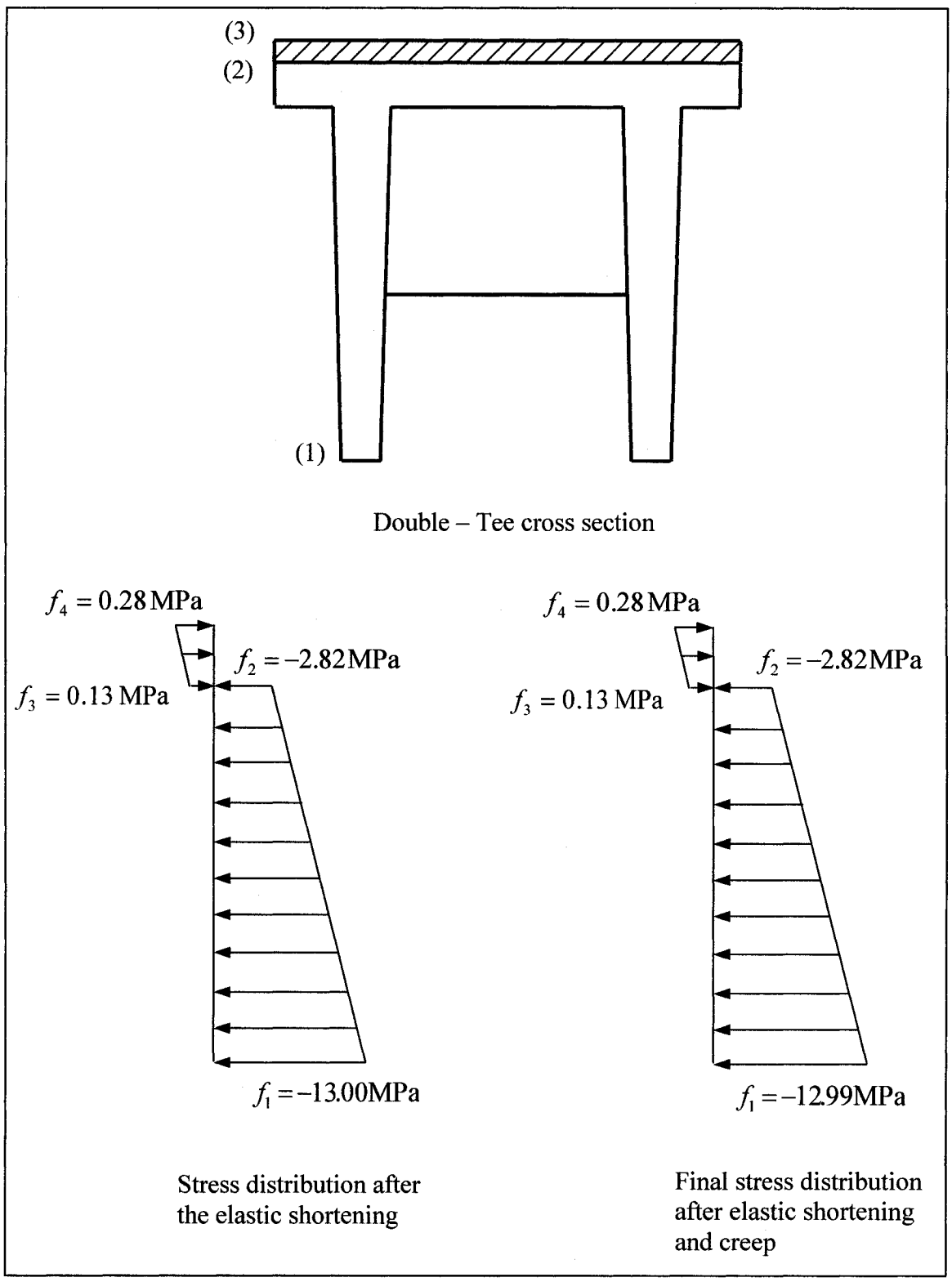

Figure 3-11: Distribution of Stresses at Mid Span for Phase D

Reproduced with permission of the copyright owner. Further reproduction prohibited without permission.

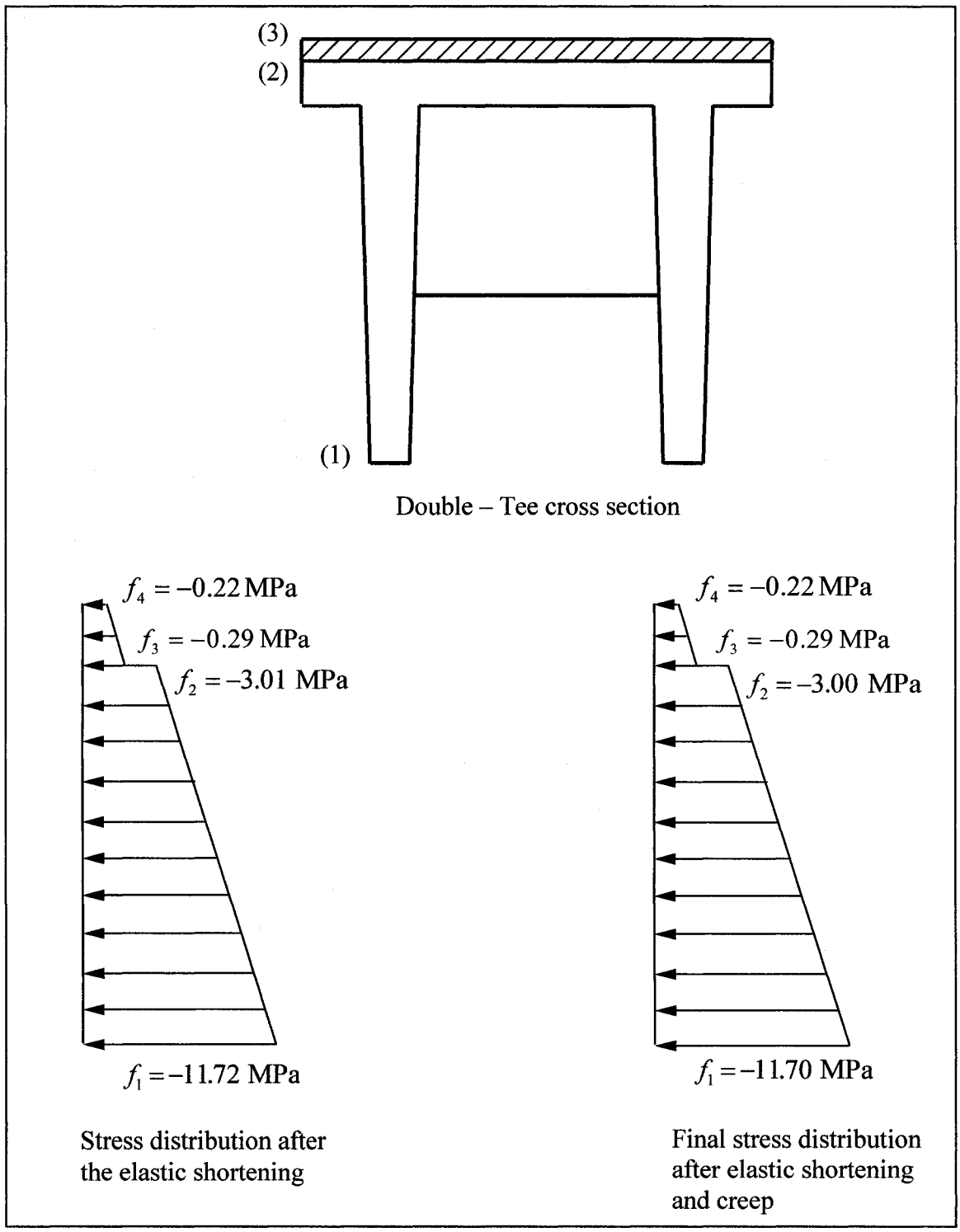

Figure 3-12: Distribution of Stresses at Quarter Span for Phase D

Reproduced with permission of the copyright owner. Further reproduction prohibited without permission.

Table 3-7: Stresses at Mid and Quarter Span for Phase D

Stresses (MPa)		Mid Span	Quarter Span
Stresses after elastic shortening	f_1 (MPa)	-13.00	-11.72
	f_2 (MPa)	-2.82	-3.00
	f_3 (MPa)	0.13	0.29
	f_4 (MPa)	0.28	0.22
Final stresses after elastic shortening and creep	f_1 (MPa)	-12.99	-11.70
	f_2 (MPa)	-2.82	-3.00
	f_3 (MPa	0.13	-0.29
	f_4 (MPa)	0.28	-0.22

3.6.3 Calculations for Deflection

3.6.3.1 Calculations for Deflection at Mid Span

Downward deflection due to own-weight, (Hibbeler 1999)

$$\delta_1 = \frac{5 \times W_D \times l_1^4}{384 \times E_C \times I_C} \qquad (3.21\ a)$$

Reproduced with permission of the copyright owner. Further reproduction prohibited without permission.

Deflection due to topping, (Hibbeler 1999)

$$\delta_2 = \frac{5 \times W_S \times l_1^4}{384 \times E_C \times I_C} \qquad (3.21\ b)$$

Upward deflection due to the pre-tensioning force, (CSCE, 2000)

$$\delta_3 = \frac{F_6 \times Sin\phi \times l_2}{24 \times E_C \times I_C}\left(3 \times l_1^2 - 4 \times l_2^2\right) \qquad (3.21\ c)$$

Deflection due to eccentricity of the tendons at the end, (Hibbeler 1999)

$$\delta_4 = \frac{M_T \times l_1^2}{8 \times E_C \times I_C} \qquad (3.21\ d)$$

Deflection due to external post-tensioning, (Hibbeler 1999)

$$\delta_5 = \frac{2 \times P_2 \times Sin\theta \times l_1^3}{48 \times E_C \times I_C} \qquad (3.21\ e)$$

$$\delta_6 = \frac{\left(P_2 \times Sin\theta_2 - P_2 \times Sin\theta_1\right) \times l_3}{24 \times E_C \times I_C}\left(3 \times l_1^2 - 4 \times l_3^2\right) \qquad \text{(CSCE, 2000)} \qquad (3.21\ f)$$

The total upward deflection,

$$\delta_f = -\delta_1 - \delta_2 + \delta_3 + \delta_4 + \delta_5 + \delta_6 \qquad (3.21\ g)$$

Reproduced with permission of the copyright owner. Further reproduction prohibited without permission.

3.6.3.2 Calculations for Deflection at Quarter Span

Downward deflection due to own-weight, (CSCE, 2000)

$$\delta_1 = \frac{W_D \times l_4}{24 \times E_C \times I_C}\left(l_1^{\,3} - 2 \times l_1 \times l_4^{\,2} + l_4^{\,3}\right) \qquad (3.22\text{ a})$$

Deflection due to topping, (CSCE, 2000)

$$\delta_2 = \frac{W_S \times l_4}{24 \times E_C \times I_C}\left(l_1^{\,3} - 2 \times l_1 \times l_4^{\,2} + l_4^{\,3}\right) \qquad (3.22\text{ b})$$

Upward deflection due to the pre-tensioning force, (CSCE, 2000)

$$\delta_3 = \frac{F_6 \times Sin\phi \times l_4}{6 \times E_C \times I_C}\left(3 \times l_1 \times l_2 - 3 \times l_2^{\,2} - l_4^{\,2}\right) \qquad (3.22\text{ c})$$

Deflection due to eccentricity of the tendons at the end, (Hibbeler 1999)

Left moment,

$$\delta_4 = \frac{M_T \times l_5}{6 \times E_C \times I_C \times l_1}\left(l_5^{\,2} - 3 \times l_1 \times l_5 + 2 \times l_1^{\,2}\right) \qquad (3.22\text{ d})$$

Right moment,

$$\delta_5 = \frac{M_T \times l_4}{6 \times E_C \times I_C \times l_1}\left(l_4^{\,2} - 3 l_1 \times l_4 + 2 \times l_1^{\,2}\right) \qquad (3.22\text{ e})$$

Deflection due to external post-tensioning, (CSCE, 2000)

$$\delta_6 = \frac{2 \times P_2 \times Sin\theta \times l_4}{48 \times E_C \times I_C}\left(3 \times l_1^{\,2} - 4 \times l_4^{\,2}\right) \qquad (3.22\text{ f})$$

Reproduced with permission of the copyright owner. Further reproduction prohibited without permission.

$$\delta_7 = \frac{(P_2 \times Sin\theta_2 - P_2 \times Sin\theta_1) \times l_4}{6 \times E_C \times I_C}\left(3 \times l_1 \times l_3 - 3 \times l_3^{\,2} - l_4^{\,2}\right) \qquad (3.22\text{ g})$$

The total upward deflection,

$$\delta_f = -\delta_1 - \delta_2 + \delta_3 + \delta_4 + \delta_5 + \delta_6 + \delta_7 \qquad (3.22\text{ h})$$

Table 3-8: Deflections at Mid and Quarter Span for Phase D

Deflection (mm)	Mid Span	Quarter Span	
Downward deflection due to the own-weight of the beam and topping (mm)	-10.64	-7.58	
Deflection due to the upward pressure of the pretensioning force (mm)	4.21	2.94	
Upward deflection due to the eccentricity of the pretensioned tendons at the end (mm)	12.95	Effect of the eccentricity of the tendons from the left end	4.04
		Effect of eccentricity of the tendons from the right end	5.65
Upward deflection due to external post - tensioning	9.15	6.40	
Total upward deflection (mm)	15.67	11.45	

Reproduced with permission of the copyright owner. Further reproduction prohibited without permission.

3.7 Calculating the Cracking Moment, Mcr.

The cracking moment is the moment producing first hair cracks in a prestressed concrete beam and is computed by assuming that cracking starts when the tensile stress in the extreme fiber of concrete reaches its modulus of rupture. The cracking moment has been estimated by calculating the moment needed to overcome the compression stresses from the final stage of loading and adding the moment to pick up the additional stresses to reach the modulus of rupture. The following equation is used for calculating the cracking moment,

$$M_{cr} = \frac{(f_{bot} + f_r) \times I_g}{Y_{bot}}, \tag{3.23}$$

Where; f_{bot} = bottom compression stress

f_r = modulus of rupture

I_g = gross moment of inertia

3.8 Effective Rigidity of The Double-Tee Beam

After the development of cracks, the deflection of the beam is calculated taking into consideration an effective moment of inertia, (Ie). Herein, two load deflection curves were constructed and compared to the actual load deflection curve from the structural test. The first load deflection curve uses the ACI equation (ACI 318) to estimate the effective moment of inertia,

Reproduced with permission of the copyright owner. Further reproduction prohibited without permission.

$$I_e = \left(\frac{M_{cr}}{M_a}\right)^3 \times \beta \times I_g + \left[1 - \left(\frac{M_{cr}}{M_a}\right)^3\right] \times I_{cr} \qquad (3.24\text{ a})$$

Where, β is a reduction Coefficient and is taken as,

$$\beta = \alpha\left[\frac{E_{CF}}{E_S} + 1\right] \qquad (3.24\text{ b})$$

α is a bond dependant coefficient and is taken as 0.50.

Equation (3.25 a) may overestimate the effective moment of inertia, in addition the lower modulus of elasticity and bond characteristics will also affect the deflection behaviour of the beam. Therefore the above equation are modified by the two variables β and α.

Salem Faza (presentation by Faza) proposed a second equation, based on the same equation for the effective moment of inertia used for steel reinforced concrete.

$$I_e = I_{cr} + (I_g - I_{cr}) \times \left(\frac{M_{cr}}{M_a}\right)^3 \qquad (3.25\text{ a})$$

Which is further modified for FRP,

$$I_m = \frac{23 \times I_{cr} \times I_e}{8 \times I_{cr} + 15 \times I_e} \qquad (3.25\text{ b})$$

where,

Im = modified moment of inertia.

Reproduced with permission of the copyright owner. Further reproduction prohibited without permission.

3.9 Calculating the Ultimate Moment

As the applied moment increases beyond the cracking moment, flexural tensile cracks develop in the bottom fibers of the beam and propagate gradually towards the neutral axis. Since the cracked portion of the concrete is ineffective in resisting the tensile stresses, the effective concrete section is reduced and the neutral axis shifts upwards.

One of the basic assumptions applied for a beam prestressed with bonded tendons is that the change in strain in the prestressing tendons is equal to the change in the strain in the surrounding concrete while the strain in the unbonded tendon is constant along the length of the tendon since the unbonded tendons slip with respect to concrete. Modification in the design procedure is suggested in which deflection is calculated at each load increment and as the beam deflects the length of the post-tensioned tendons changes. By knowing the initial length, the strain, the stress and hence the force in post-tensioned tendon can be calculated. A computer program has been developed, which takes into consideration this change in stresses and a new value for the post–tensioned force could be calculated at each load increment.

The behaviour and the ultimate moment of the beam are determined following the procedure described below:

a) The live load is increased gradually with 10 % increment until the first cracks in the beams developed.

b) The stresses due to the above loading are calculated and these stresses have to be modified to account for the cracked section of the beam.

Reproduced with permission of the copyright owner. Further reproduction prohibited without permission.

c) Based on the above stresses, the new position of the neutral axis is found by equating the compression and the tension forces.

d) The cracked moment of inertia, the cracked area and the effective moment of inertia are calculated.

e) The deflections and the elongation in the post – tensioned tendons are calculated.

f) The stresses are re-calculated with the new cracked moment of inertia, cracked section and the new force in the post – tensioned tendons.

g) The strains are compared with the ultimate strains for both concrete and tendons. Failure is identified when either concrete reach its maximum strain of 0.0035 or the strands (internal or external) reach their ultimate stress.

h) The above procedure is repeated with a 10 % increase in the live load every time until failure is reached either by crushing of concrete or rupture of the tendons.

As described above, this proposed procedure is iterative and therefore an interactive iterative program has been developed using the program "Matlab" to estimate the ultimate moment. Figure 3-13 shows a flow chart for the input and the output of the program. Table 3-1 summarizes the results from the program and show the different values for the post–tension force based on the deflection calculated using the ACI equation (equation 3.25 a) for the effective moment of inertia. Table 3-2 also summarizes the results from the program and shows the different values for the post – tensioning force based on the deflection calculated using Faza equation (equation 3.26 b).

Reproduced with permission of the copyright owner. Further reproduction prohibited without permission.

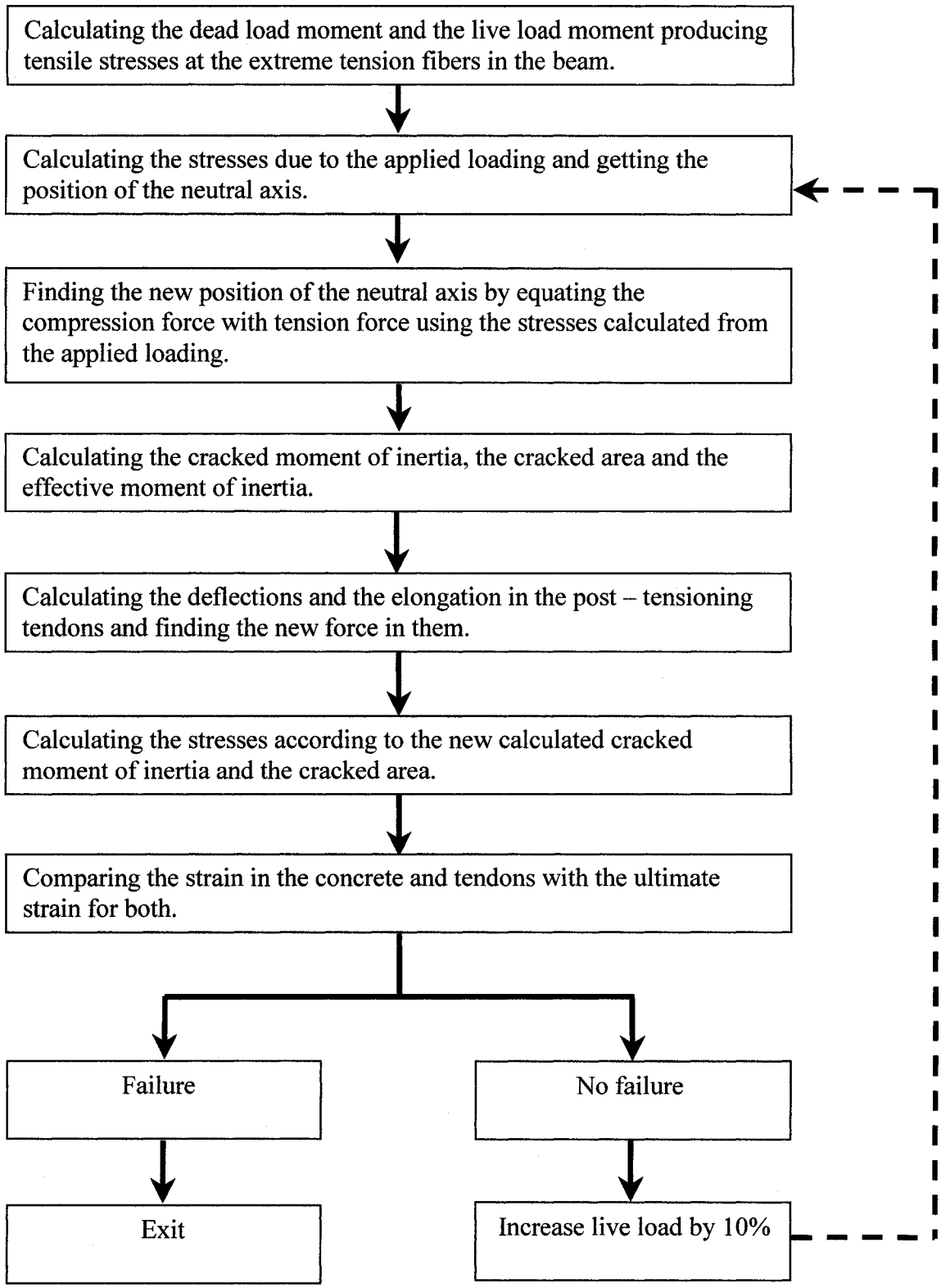

Figure 3-13: Flow Chart for the Computer Program

Reproduced with permission of the copyright owner. Further reproduction prohibited without permission.

Table 3-9: Summary of Results and the Ultimate Moment Based on the Deflection Calculated Using the ACI Equation

Live load Increment (%)	Post Tensioned Force (kN)	Top stress (MPa)	Bottom stress (MPa)			Distance from top of the beam to the N.A. (mm)	Icr (mm^4) 10E10	Ie (eq1) (mm^4) 10E10	
			Stress in Concrete (MPa)	Additional stress in pretensioned tendons (MPa)	Total stress in pretensioned tendons (MPa)				
0	1760	+0.28	- 12.986	---------	1412	----------	---------	Ig	
10	1800	-5.60	-7.679	23	1435	---------	---------	Ig	
20	1880	-7.680	-3.068	43	1458	---------	---------	Ig	
30	1960	-10.47	+1.542	63	1481	---------	---------	Ig	
40	2084	-17.68	--------	277	1758	180	4.1165	13.505	
50	2200	-21.44	--------	422	1903	162	4.0688	8.8936	
60	2360	-26.24	--------	542	2023	156	4.0473	6.8443	
70	2600	-30.16	--------	684	2165	152	4.0364	5.7993	
80	2840	-34.17	--------	804	2285	108	3.9084	5.1005	
90	3080	-36.11	--------	946	2427	105	3.9044	4.7419	
100	3360	-37.80	--------	1066	2547	100	3.9878	4.5087	
109	3560	-38.40	--------	1184	2596(Failure)	90	3.8967	4.3672	

Reproduced with permission of the copyright owner. Further reproduction prohibited without permission.

Table 3-10: Summary of results and the Ultimate Moment Based on the Deflection Calculated Using Faza Equation

Live load Increment (%)	Post Tensioned Force (kN)	Top stress (MPa)	Bottom stress (MPa)			Distance from top of the beam to the N.A. (mm)	Icr (mm^4) 10E10	Ie (eq2) (mm^4) 10E10
			Stress in Concrete (MPa)	Additional stress in pretensioned tendons (MPa)	Total stress in pretensioned tendons (MPa)			
0	1760	+0.28	- 12.986	--------	1412	----------	--------	Ig
10	1840	-4.879	-7.805	23	1435	---------	--------	Ig
20	1920	-7.775	-1.669	44	1458	---------	--------	Ig
30	2040	-10.435	+1.290	65	1477	---------	--------	Ig
40	2168	-17.60	--------	272	1684	181	4.1152	5.4728
50	2300	-21.12	--------	418	1830	163	4.0675	5.0137
60	2472	-25.89	--------	537	1949	156	4.0460	4.7166
70	2724	-29.44	--------	680	2092	153	4.0350	4.5122
80	2968	-33.60	--------	800	2212	108	3.9081	4.2539
90	3727	-35.76	--------	941	2353	106	3.9039	4.1590
100	3488	-37.44	--------	1061	2473	101	3.9875	4.0902
112	3896	-38.36	--------	1183	2595(Failure)	91	3.8973	4.0383

Reproduced with permission of the copyright owner. Further reproduction prohibited without permission.

CHAPTER FOUR

COMPARISON AND DISCUSSION

4.1 General

As stated in Chapter Two, the test data obtained by CTL became available to the author. Thirty strain gauges were placed in order to obtain data during the different phases of loading the DT-beam. Twenty-one gauges were installed in the pre-cast section while the remaining gauges were installed in the cast-in-place concrete topping. Data from each strain gauge were recorded to document the strain distribution over the cross section at the mid span and the quarter span during the fabrication sequence and throughout the structural test. Measurements were made from the beginning during the release of the force until the beam was loaded to failure.

A precision level and surveyor's rod including a high-resolution scale were used for recording early age deflection measurements. Prior to release, elevation measurements were recorded for each point and used as a zero reference for all subsequent measurements. After release, measured changes in elevation relative to the initial pre-release values were used to calculate beam deflections at the middle and quarter of the span. Also, during the loading test deflection was measured using two displacement transducers attached to the bottom of the beam stems. Figure 4-1 shows the measured deflection at the mid span obtained from the lab for the different prestressing phases.

Reproduced with permission of the copyright owner. Further reproduction prohibited without permission.

In the following sections a comparison and discussion are presented using analysis and lab measurements during the different stages of the beam fabrication and loading.

This leads to better understanding of behaviour of a combined system of pretensioning and post-tensioning for the DT-beam using carbon fibers.

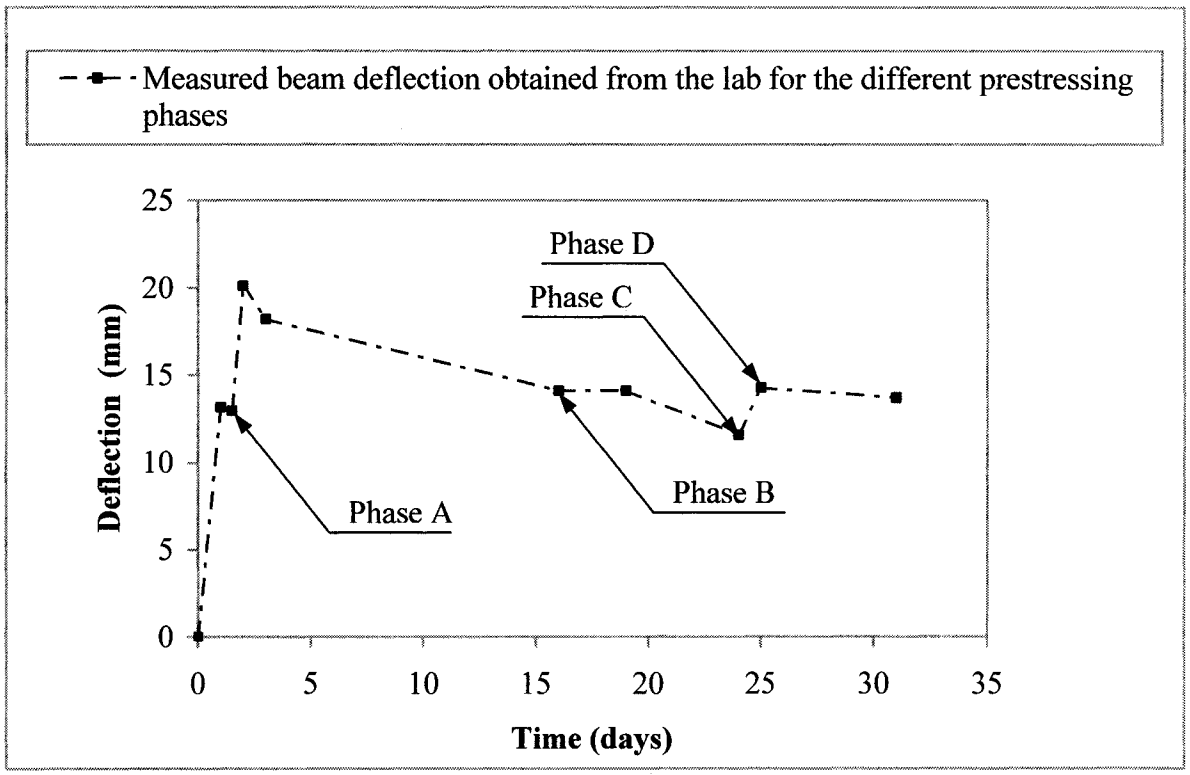

Figure 4-1: Deflections at Mid Span Obtained from the Lab for the Different Prestressing Phases

Reproduced with permission of the copyright owner. Further reproduction prohibited without permission.

4.2 Phase A: Application of Internal Prestressing

The sixty strands used for internal prestressing were arranged in ten rows and the force was released starting from the lowest row moving to the uppermost row. Hence, the lowest row of tendons suffered from the maximum effect of elastic shortening from the subsequent stressing of all other tendons. Due to this successive release of the force, the self-weight of the beam was not entirely acting until the forces in most strands are released. For simplicity, the elastic shortening is calculated for all strands at the same time assuming that an average value of stress equally affects them.

By applying equations (3.3 a, 3.3 b) and comparing the top and bottom stresses calculated from the analysis with those obtained from the strain measurement, Figure 4-2 and 4-3 show good agreement between the analysis and the test results for both mid and quarter span, respectively. Table 4-1 summarizes the comparison made between the stresses obtained from the analysis and those obtained from the strains.

Table 4-1: Stresses Obtained from the Analysis and the Stresses Obtained from Strain Measurement for Phase A

Stresses (MPa)		Stresses obtained from the analysis (MPa)	Stresses calculated from the strain measurement (MPa)
Mid Span	Top Stress (MPa)	-2.44	-1.98
	Bottom Stress (MPa)	-9.95	-10.21
Quarter Span	Top Stress (MPa)	-2.01	-1.89
	Bottom Stress (MPa)	-10.65	-9.69

Reproduced with permission of the copyright owner. Further reproduction prohibited without permission.

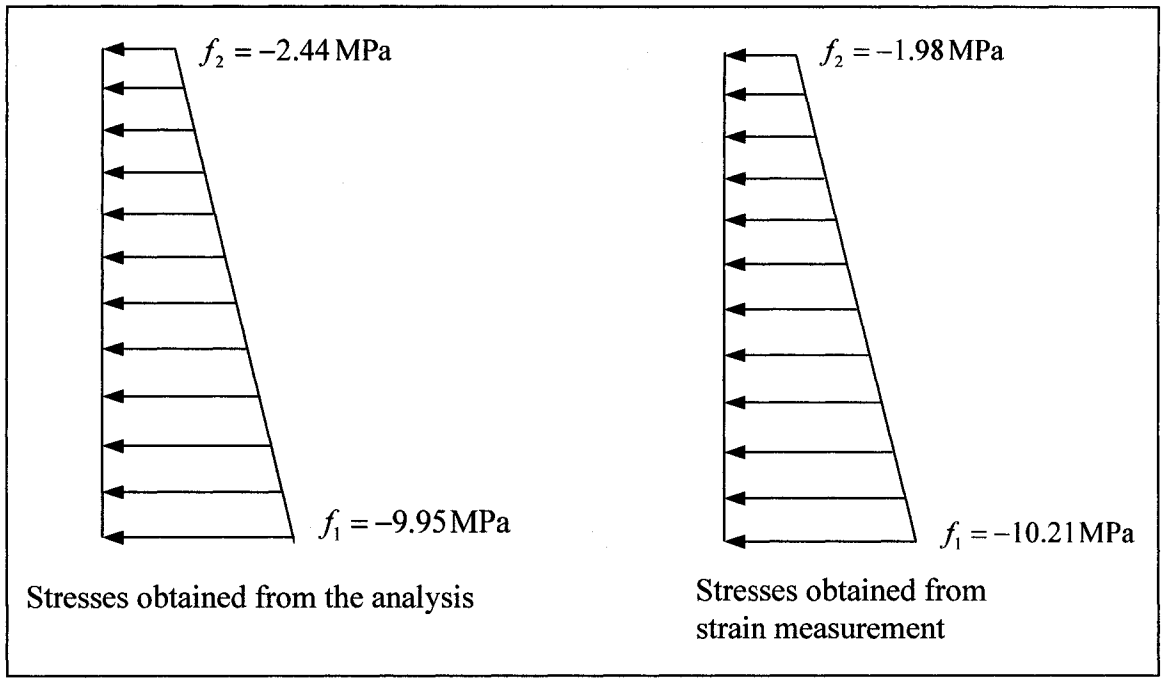

Figure 4-2: Stresses Obtained from the Analysis vs. Stresses Obtained from Strain Reading at Mid Span for Phase A

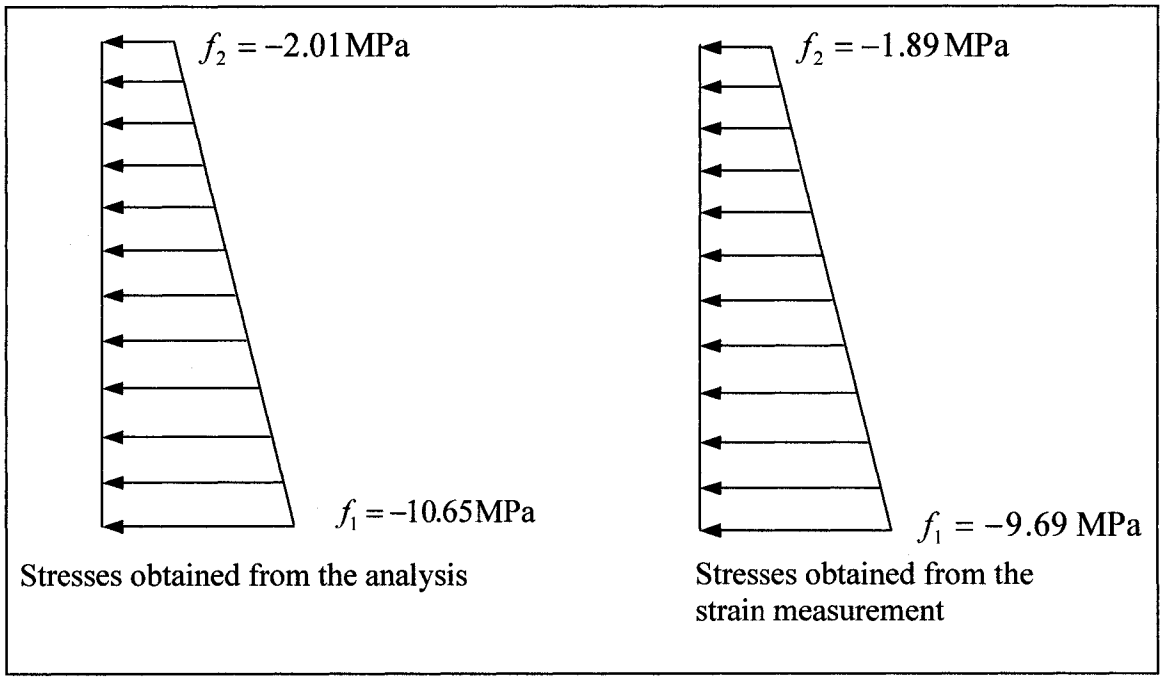

Figure 4-3: Stresses Obtained from the Analysis vs. Stresses obtained from the Strain Reading at Quarter Span for Phase A

Reproduced with permission of the copyright owner. Further reproduction prohibited without permission.

Deflections have been calculated using the fundamental principles of the mechanics of materials and the gross section. Deflections due to the different loads applied to the beam at each phase of loading are algebraically superimposed. In this manner the deflection of the beam under its own weight and prestressing are computed. Due to the effect of the internal prestressing, the beam experienced an upward deflection and it was resting on an effective support of length l_2. By estimating the length of effective support, the deflections were calculated at the mid span and the end of the beam allowing a comparison to those measured in the lab.

Considering creep calculations, it is noted that the time elapsed between casting the beam and the application of the pretensioning force was short. Therefore the effect of the creep should not be significant at this phase. Table 4-2 summarizes the comparison between the deflections obtained from the analysis and those obtained from the lab

Table 4-2: Deflections Obtained from the Analysis and from the Lab Measurement for Phase A

Deflection (mm)	Deflection obtained from the analysis (upward) (mm)	Deflection measured in lab (upward) (mm)
Mid Span	11.29	13.20
Quarter Span (average value for deflection for dead end and live end)	7.50	10.60

Reproduced with permission of the copyright owner. Further reproduction prohibited without permission.

4.3 Phase B: Sixty Percent of External Post-Tensioning

At this phase, the DT-beam was supported on its diaphragms D2 and D6 creating two cantilevers (Figure 3-4). Sixty percent of the total post-tensioning force was applied to the external cables leading to an increase in the compression stresses at the bottom fibers of the beam and a decrease in the compression stresses at the top fibers.

The increase in strain in concrete at this stage due to the effect of creep was 19 % and it must be noted that the concrete was five days mature at this stage. Figure 4-4 and Figure 4-5 show the effect of creep on the stresses and Appendix A shows detailed calculations for the creep.

Comparing the stresses after estimating the creep, it was found that stresses from the analysis are in reasonable agreement with those obtained from the strain reading of the test data. Table 4-3 shows a comparison between the stresses obtained from the analysis and the stresses obtained from the measured strains.

The test program included the determination of both the compressive strength and the modulus of elasticity of the concrete at the age of two days, twenty-eight days and thirty-three days, which correspond to the day of testing. Herein, the elastic modulus of concrete is also not a constant value for all stress levels and varies with the age of concrete.

It must be pointed out, that at this phase the computations of deflections in prestressed concrete flexural members has been made with the assumption that the concrete section is not cracked. This assumption is valid since the beam cross section is under compression. The DT-beam at this phase is subject to the highest value of camber,

Reproduced with permission of the copyright owner. Further reproduction prohibited without permission.

as in a fully prestressed concrete beam, the change in deflection is a function of two main factors, the time as well as the distribution of the stresses. Both factors determine the deflection due to creep. Herein, the case of prestressing and the own weight of the beam lead to more compression at the bottom than the top. Therefore the tendency for the creep is to increase the upward deflection. Table 4-4 shows summary for the deflection obtained from the analysis and the deflection measured in the lab.

Reproduced with permission of the copyright owner. Further reproduction prohibited without permission.

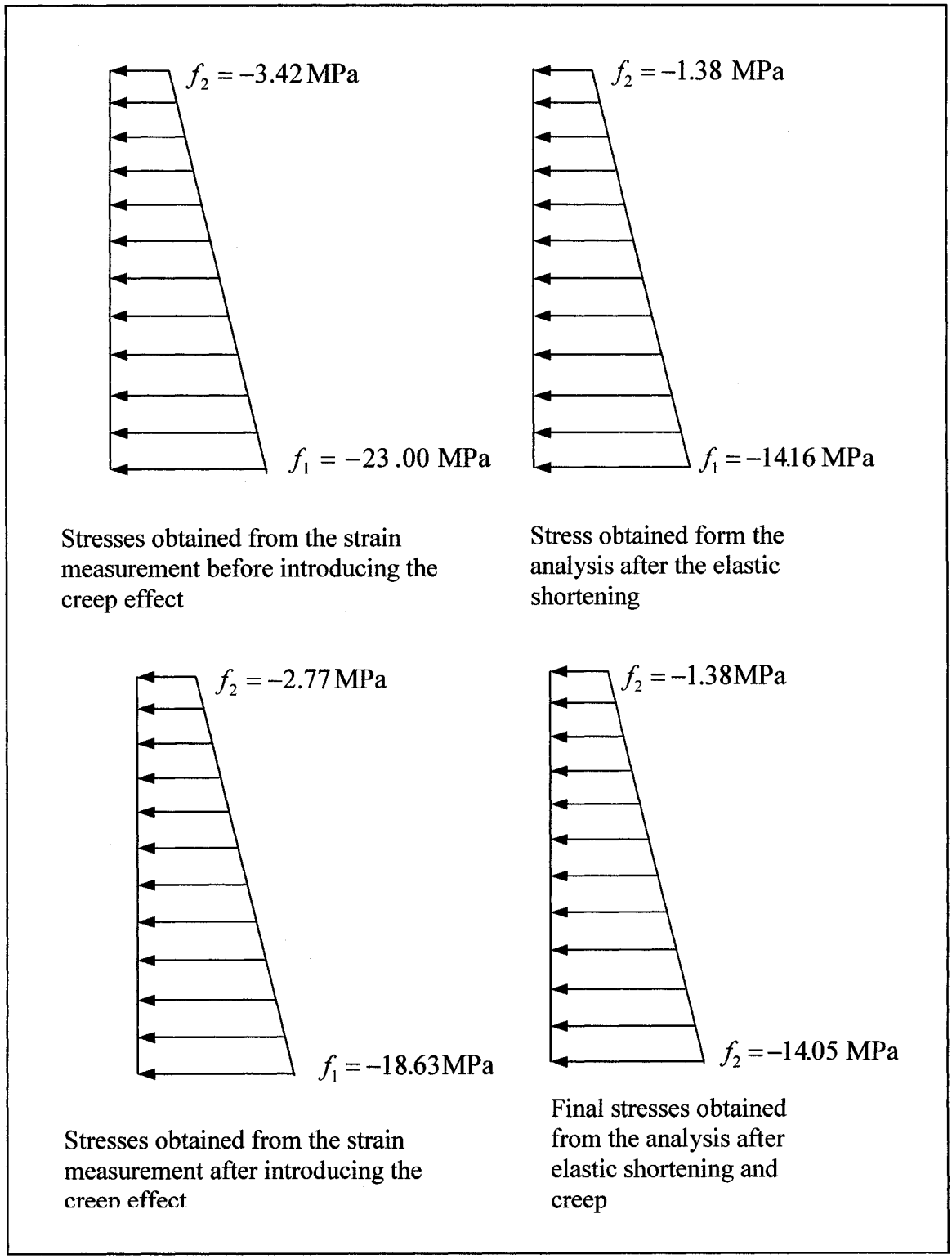

Figure 4-4: Effect of Creep on the Stresses at Mid Span for Phase B

Reproduced with permission of the copyright owner. Further reproduction prohibited without permission.

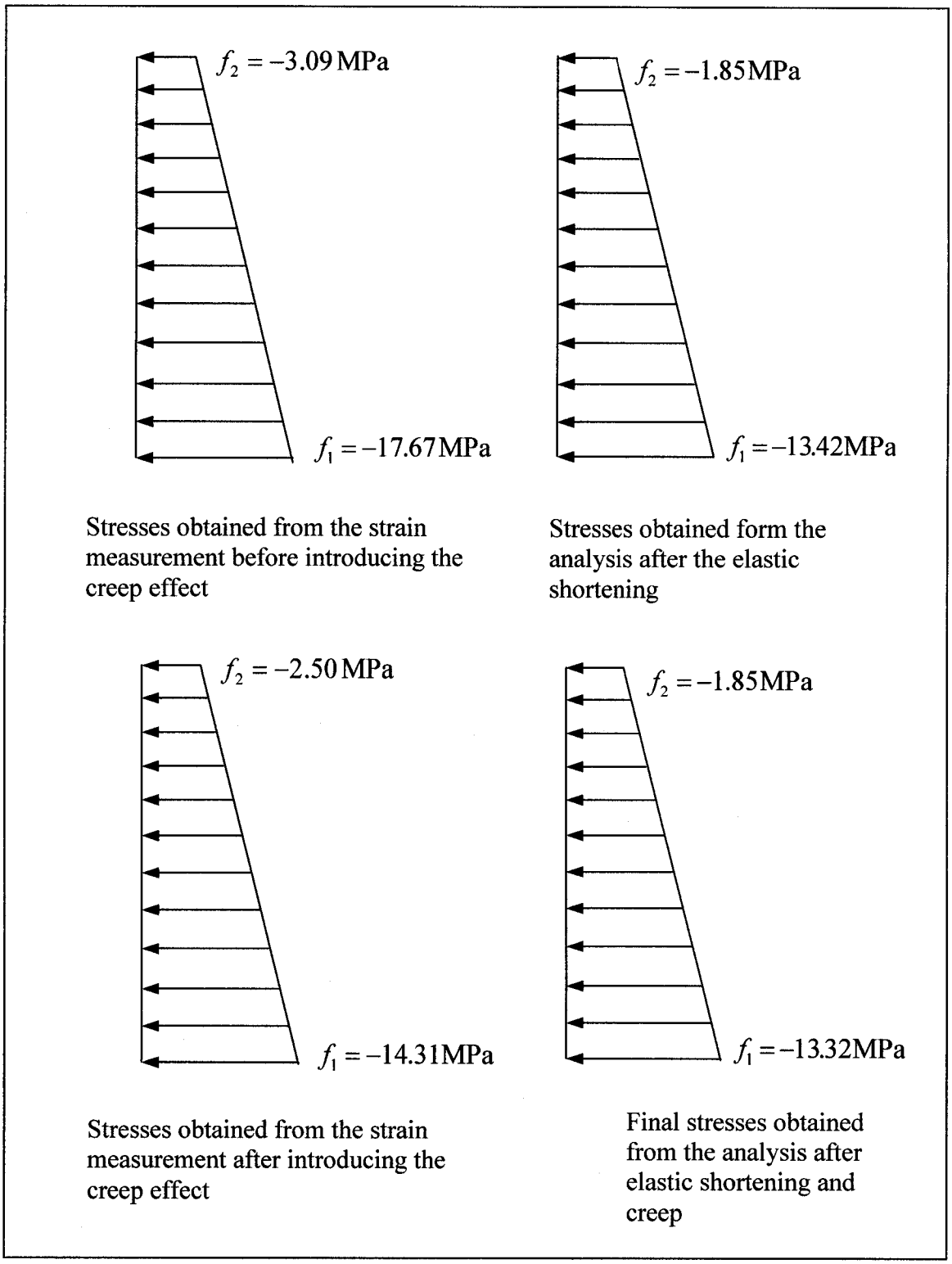

Figure 4-5: Effect of Creep on the Stresses at Quarter Span for Phase B

Reproduced with permission of the copyright owner. Further reproduction prohibited without permission.

Table 4-3: Stresses Obtained from the Analysis and the Stresses Obtained from Strain Measurement for Phase B

Stresses (MPa)		Stresses obtained from the analysis (MPa)	Stresses calculated from the strain measurement (MPa)
Mid Span	Top Stress (MPa)	-1.38	-2.77
	Bottom Stress (MPa)	-14.05	-18.63
Quarter Span	Top Stress (MPa)	-1.85	-2.50
	Bottom Stress (MPa)	-13.32	-14.31

Table 4-4: Deflections Obtained from the Analysis and from the Lab Measurement for Phase B

Deflection (mm)	Deflection obtained from the analysis (upward) (mm)	Deflection measured in lab (upward) (mm)
Mid Span	12.68	14.10
Quarter Span (average value for deflection for dead end and live end)	8.24	10.40

Reproduced with permission of the copyright owner. Further reproduction prohibited without permission.

4.4 Phase C: Casting Topping

The beam in this phase was transported to the testing facility. Thereafter, seventy-five millimeter topping slab was added to the DT-beam while the beam was supported on its two end diaphragms. The stresses were calculated on the assumption that the concrete was wet during this phase and no composite action was effective. Because of the topping and the new position of the supports the compression stresses in the top fibers increased and the compression stresses on the bottom fibers decreased. The coefficient of creep in this phase was estimated to be 31 %. Figure 4-6 and 4-7 show the effect of creep on the stresses and shows a comparison between the stresses before and after the introduction of creep. Tables 4-5 and 4-6 shows a comparison for the stresses and deflections obtained from the analysis and from the lab.

Reproduced with permission of the copyright owner. Further reproduction prohibited without permission.

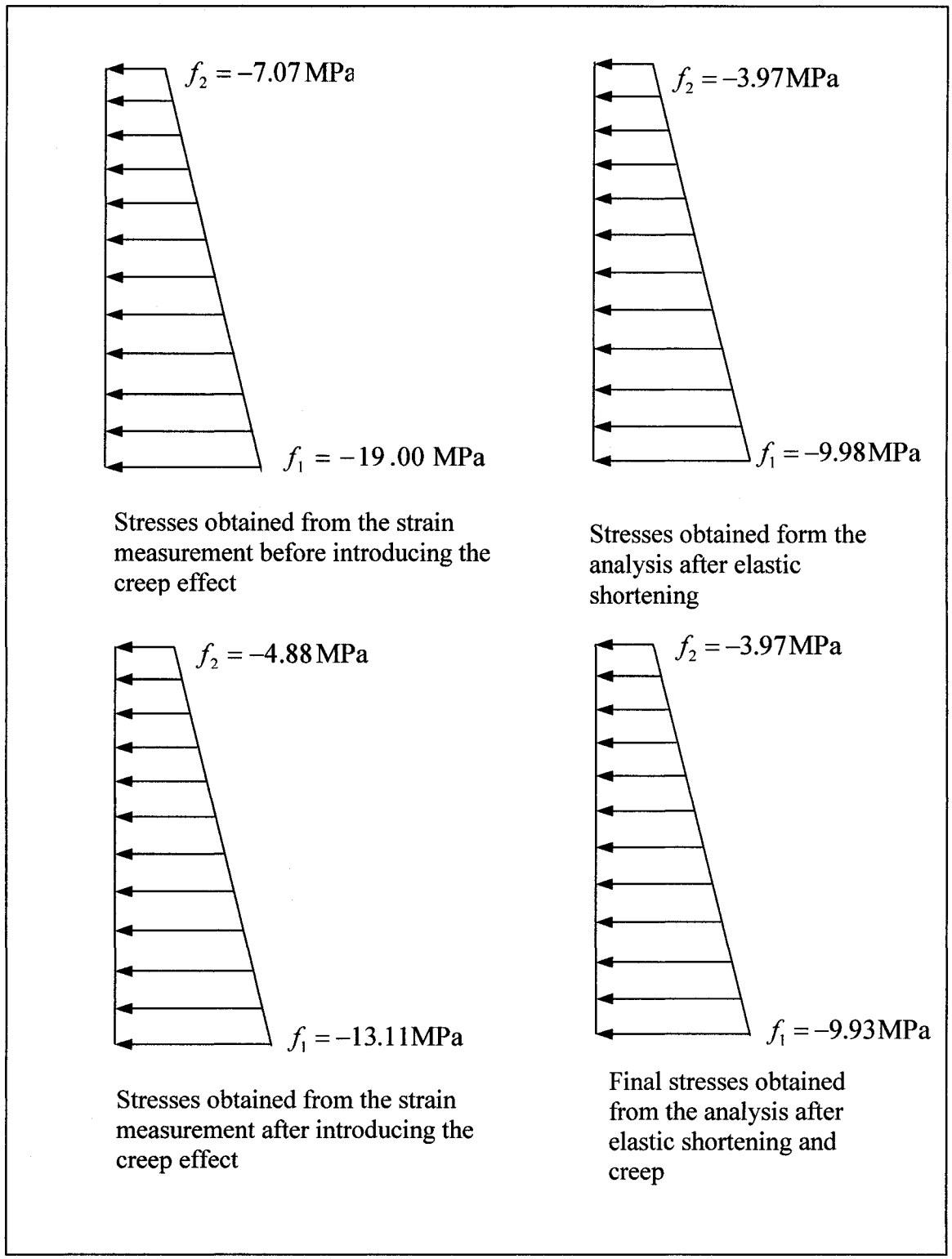

Figure 4-6: Effect of Creep on the Stresses at the Mid Span for Phase C

Reproduced with permission of the copyright owner. Further reproduction prohibited without permission.

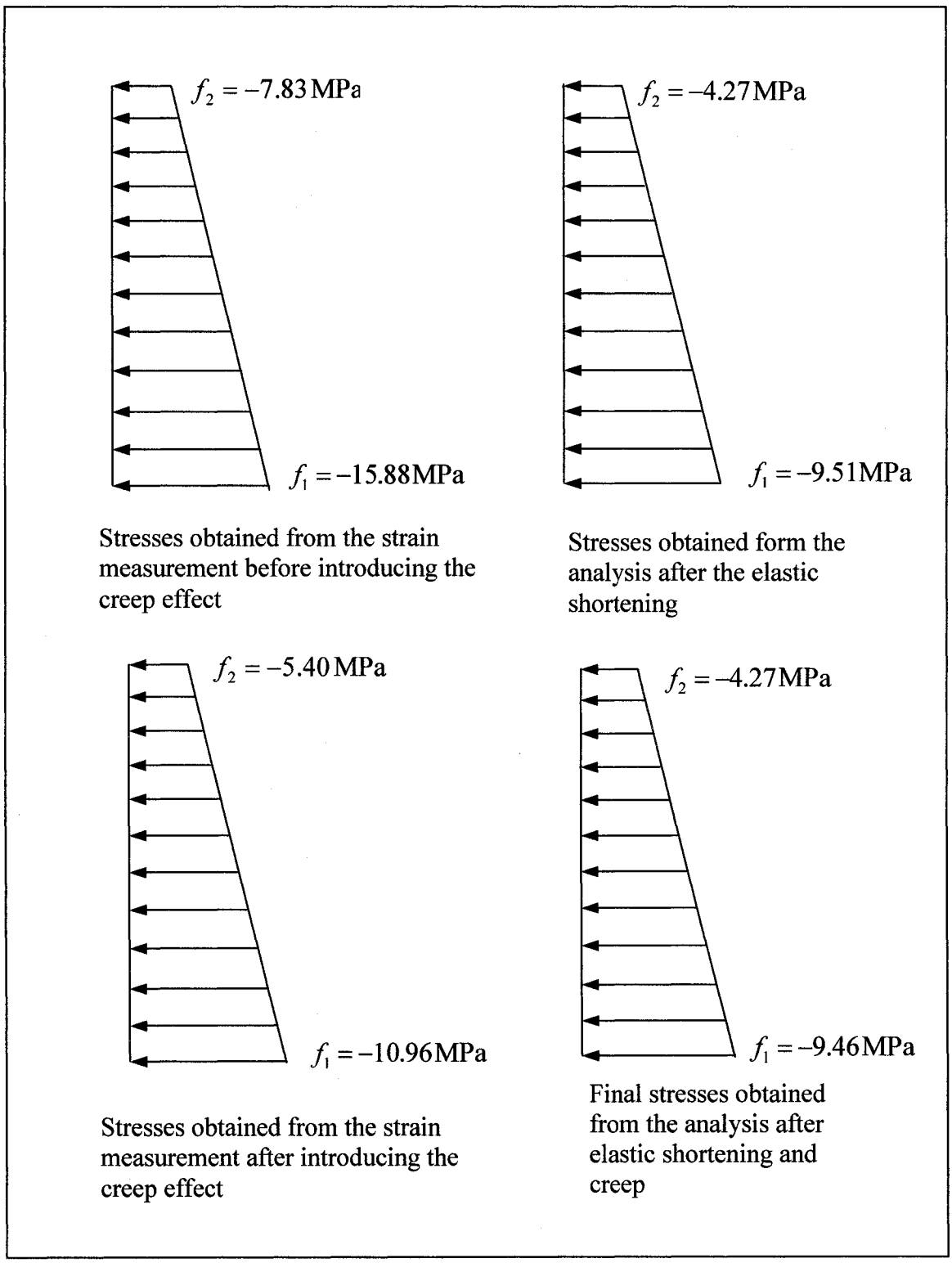

Figure 4-7: Effect of Creep on the Stresses at Quarter Span for Phase C

Reproduced with permission of the copyright owner. Further reproduction prohibited without permission.

Table 4-5: Stresses Obtained from the Analysis and the Stresses Obtained from Strain Measurement for Phase C

Stresses (MPa)		Stresses obtained from the analysis (MPa)	Stresses calculated from the strain measurement (MPa)
Mid Span	Top Stress (MPa)	-3.97	-3.97
	Bottom Stress (MPa)	-9.98	-9.93
Quarter Span	Top Stress (MPa)	-4.27	-4.27
	Bottom Stress (MPa)	-9.51	-9.46

Table 4-6: Deflections Obtained from the Analysis and from the Lab Measurement for Phase C

Deflection (mm)	Deflection obtained from the analysis (upward) (mm)	Deflection measured in lab (upward) (mm)
Mid Span	11.43	11.60
Quarter Span (average value for deflection for dead end and live end)	8.47	8.65

Reproduced with permission of the copyright owner. Further reproduction prohibited without permission.

4.5 Phase D: Full Post-Tensioning

At this phase the remaining post-tensioning force were applied to the DT- beam after the top composite slab was hardened and the beam became composite with the top slab. This phase ends the prestressing procedure and no additional losses due to elastic shortening will occur after this phase. The total loss due to elastic shortening was found to be 7.5 %. The coefficient of creep increased from 19 % in the phase of sixty percent of post-tensioning to 31 % at this phase of casting topping and continued to increase till 34 %. Figure 4-8 shows the rate of increase of the creep coefficient and it is observed that it started to slow down after the phase of casting topping. Figure 4-9 and 4-10 show the effect of creep on the stresses and illustrates a comparison between the stresses before and after the introduction of creep.

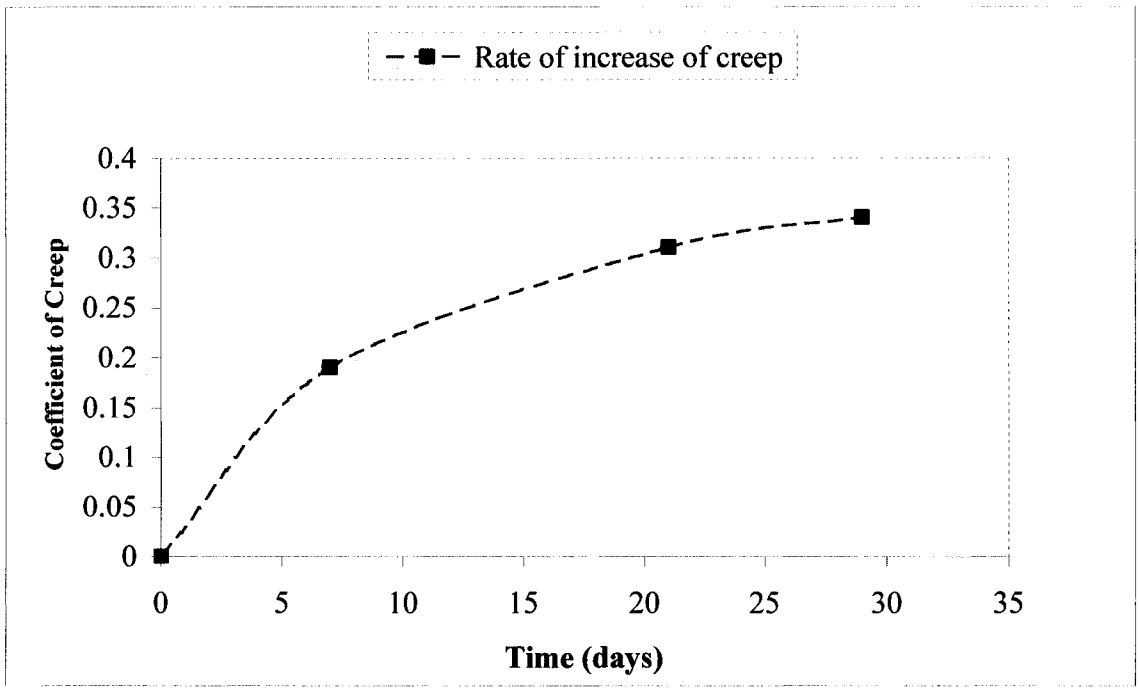

Figure 4-8: Increase of Coefficient of Creep vs. Time

Reproduced with permission of the copyright owner. Further reproduction prohibited without permission.

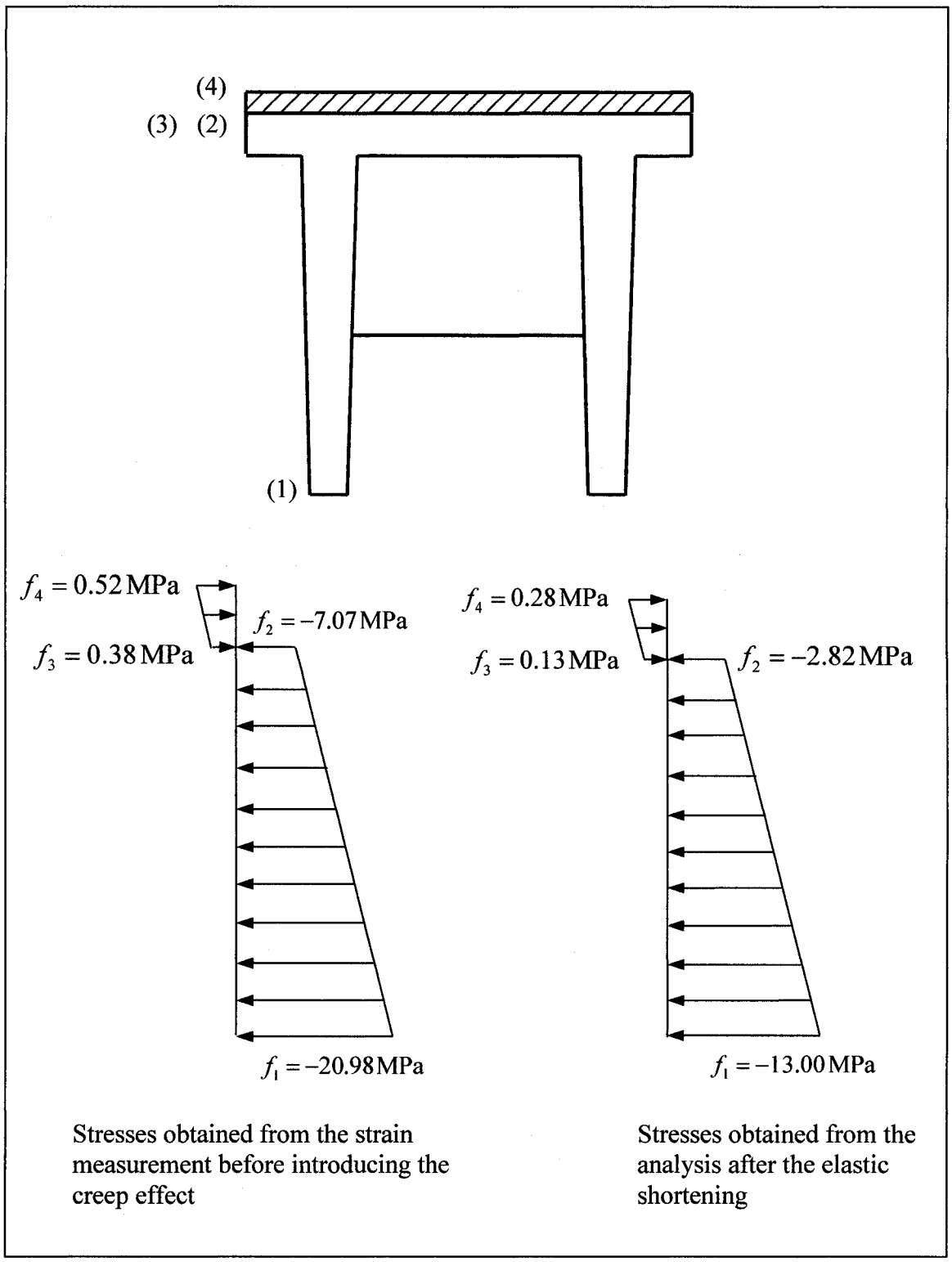

Figure 4-9: Stresses Obtained from the Analysis vs. Stresses obtained from the Strain Reading before Introducing the Creep Effect at Mid Span D

Reproduced with permission of the copyright owner. Further reproduction prohibited without permission.

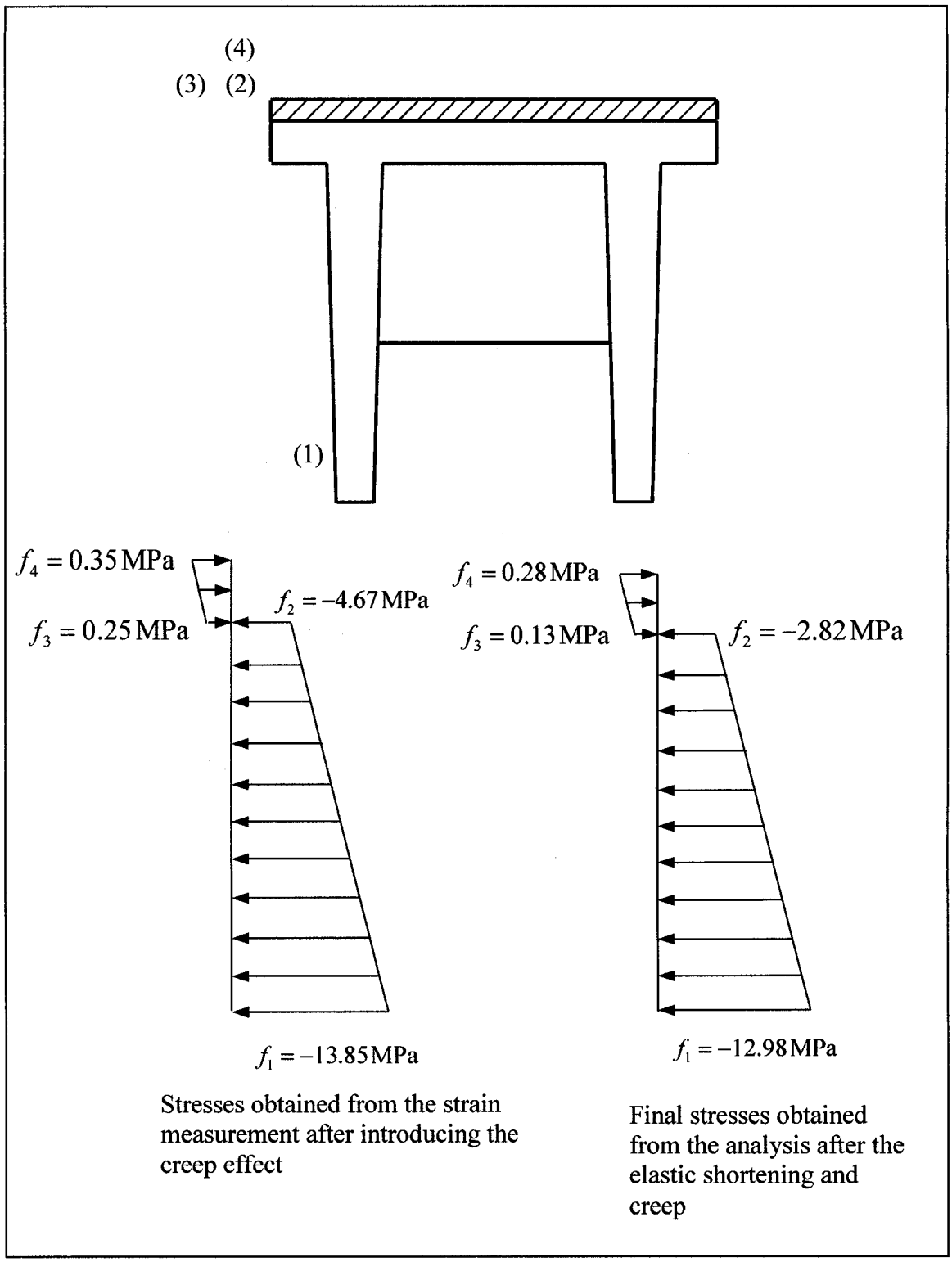

Figure 4-10: Stresses Obtained from the Analysis vs. Stresses Obtained from the Strain Reading after Introducing the Creep Effect at Mid Span D

Reproduced with permission of the copyright owner. Further reproduction prohibited without permission.

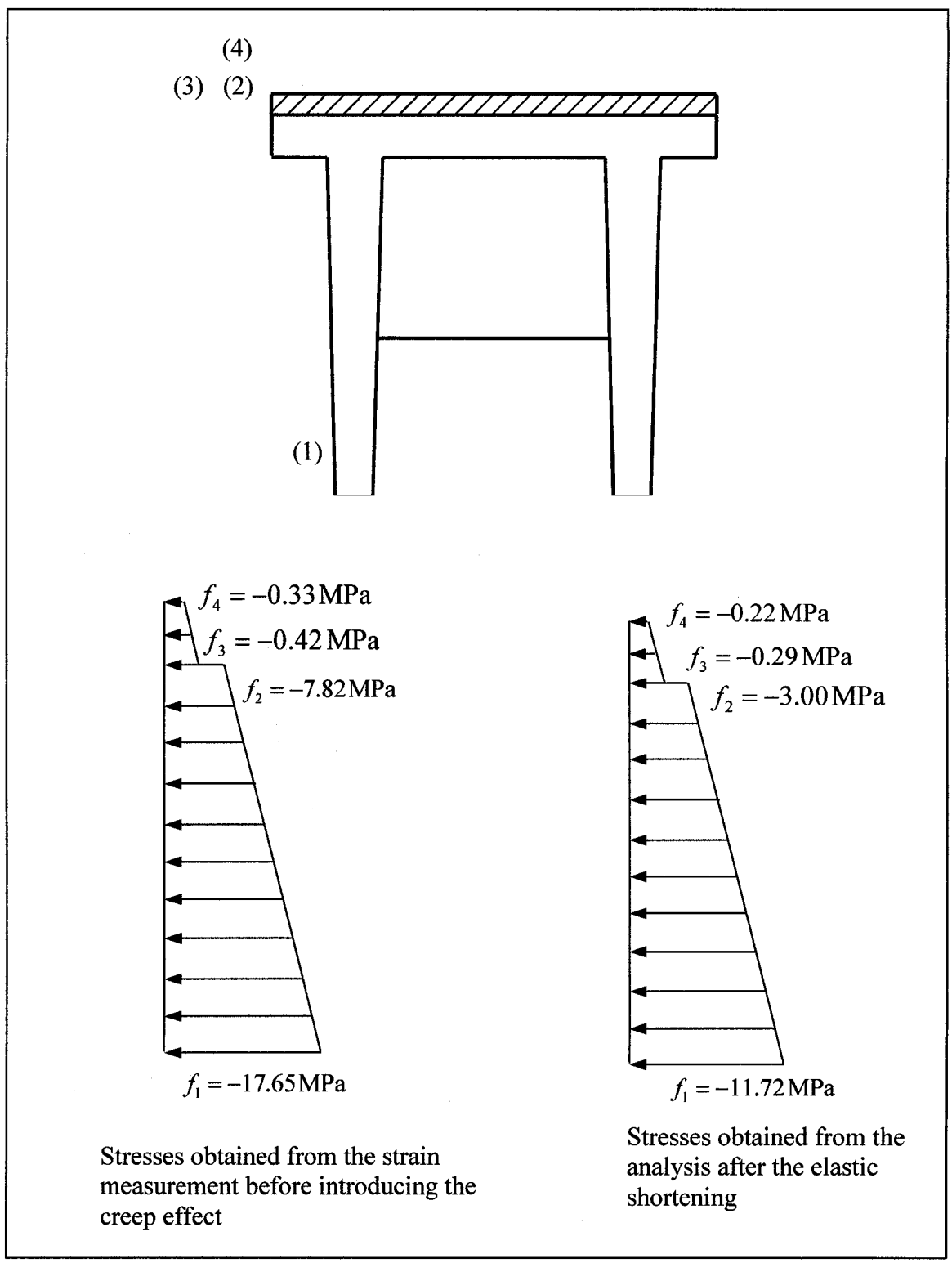

Figure 4-11: Stresses Obtained from the Analysis vs. Stresses Obtained from the Strain Reading before Introducing the Creep Effect at Quarter Span for Phase D

Reproduced with permission of the copyright owner. Further reproduction prohibited without permission.

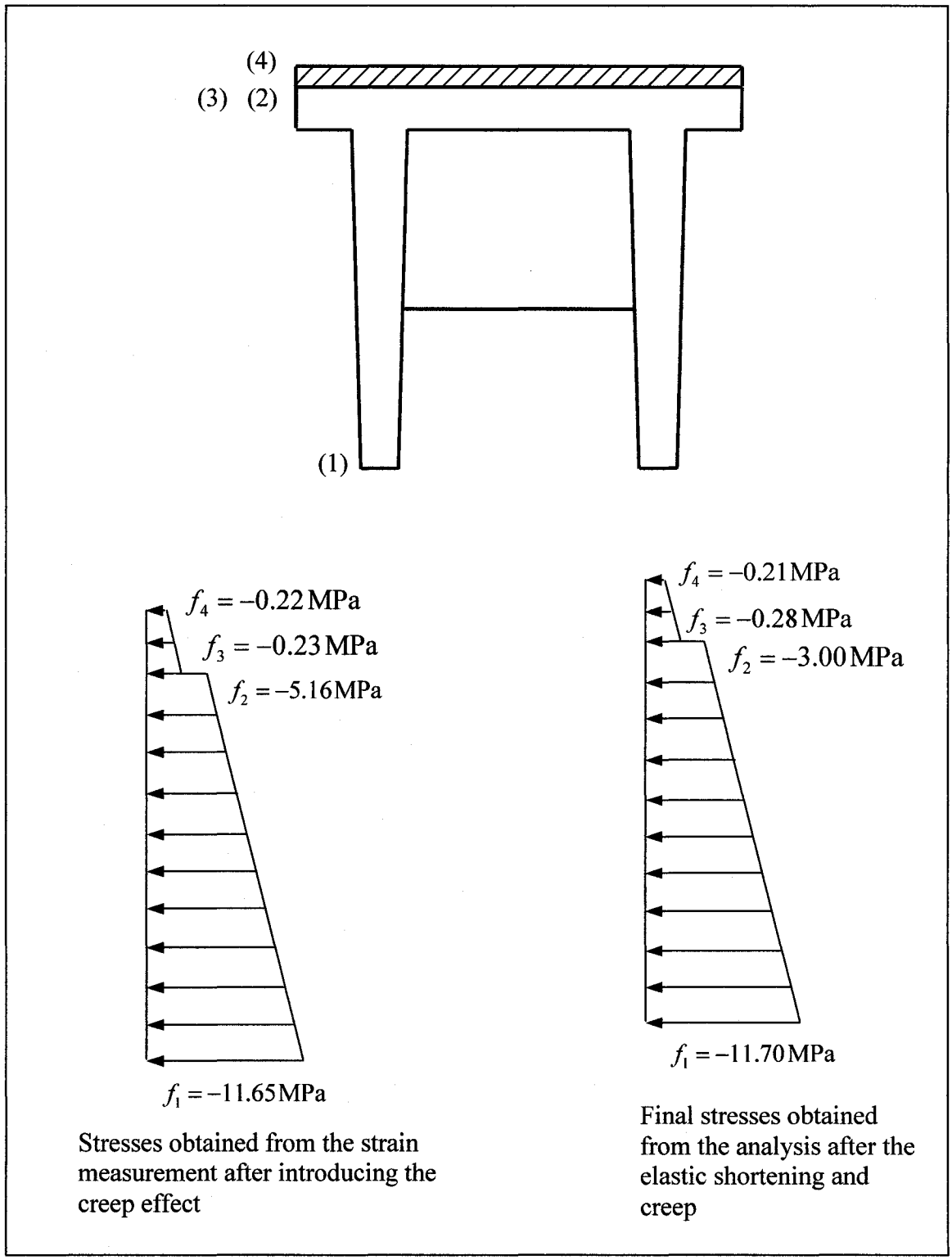

Figure 4-12: Stresses Obtained from the Analysis vs. Stresses Obtained from the Strain Reading after Introducing the Creep Effect at Quarter Span for Phase D

Reproduced with permission of the copyright owner. Further reproduction prohibited without permission.

Table 4-7: Stresses Obtained from the Analysis and the Stresses Obtained from Strain Measurement for Phase D

Stresses (MPa)		Stresses obtained from the analysis (MPa)	Stresses calculated from the strain measurement (MPa)
Mid Span	f_1 (MPa)	-12.98	-13.85
	f_2 (MPa)	-2.82	-4.67
	f_3 (MPa)	0.13	0.25
	f_4 (MPa)	0.28	0.35
Quarter Span	f_1 (MPa)	-11.70	-11.65
	f_2 (MPa)	-3.00	-5.16
	f_3 (MPa	-0.28	-0.23
	f_4 (MPa)	-0.21	-0.22

Table 4-8: Deflections Obtained from the Analysis and from the Lab Measurement for Phase D

Deflection (mm)	Deflection obtained from the analysis (upward) (mm)	Deflection measured in lab (upward) (mm)
Mid Span	15.67	14.30
Quarter Span (average value for deflection for dead end and live end)	11.45	10.35

Reproduced with permission of the copyright owner. Further reproduction prohibited without permission.

4.6 The Cracking Moment

The beam started cracking under the live load when the bending moment induced tensile stresses, which exceeded the compression pre-stress at the bottom of the beam. The difference between the cracking moment calculated from the analysis (3657 kN-m) and the one obtained from the lab based on the strain readings (3839 kN-m) is 4.8 %. Also a visual inspection has been conducted on the beam during the loading to record the first crack and corresponding load or cracking moment, the value observed was (3854 kN-m) which is close the cracking moment obtained from the strain reading.

4.7 The Ultimate Moment

The failure of the DT-beam was triggered in the lab by the crushing of concrete at a strain of 0.0025. Based on the lab report, the concrete reached a maximum compressive strain at failure of 0.0025, which is lower than the failure strain of concrete 0.0035. This could be attributed to the small thickness of the top slab causing it to separate from the DT-beam and failing prematurely in compression at a strain lower than the failure strain of concrete. However based on the analysis, the failure of the DT-beam was attained by the internal prestressing tendons reaching their ultimate strength of 2567 MPa.

The stresses in concrete has been calculated assuming a linear distribution of stresses over the cross section of the beam and for stress values lower than 0.5 fc, the strain is calculated assuming a linear relationship between stress and strain. In order to approximately account for the non-linear relation between stress and strain, equation (4-

Reproduced with permission of the copyright owner. Further reproduction prohibited without permission.

1) is used to calculate the strains when the stresses exceeded 0.5 *fc*. Tables 4-11 and 4-12 show the stresses and strains for the top concrete, pretensioned tendons and post-tensioned tendons based on the deflection calculated according to the ACI equation and Faza equation respectively.

$$f_C = f'_C\left[\frac{2\varepsilon}{\varepsilon_o} - \left(\frac{\varepsilon}{\varepsilon_o}\right)^2\right] \tag{4-1}$$

At failure load, the analysis indicated that the force in the external cables to be 3360 kN based on the deflection calculated using the ACI equation and 3440 kN based on the deflection calculated using Faza equation. The structural test data indicated that the force in the external cables at failure was 3240 kN which is 3.70 % lower than the force obtained for the first case and 6.17 % lower than the force obtained for the second case. This could be attributed to the underestimation of the rigidity of the beam, which leads to higher deflection and consequently more stress in the external cables.

This behaviour of the post-tensioning force affected the ultimate capacity of the DT-beam obtained from the analysis as Figure 4-14 shows the higher value for the ultimate moment obtained from the analysis compared to the ultimate moment obtained from the test data. If the load deflection curves obtained from the analysis are compared to each other, the ultimate moment based on deflection calculated from Faza equation shows a slightly higher value than the ultimate moment based on deflection calculated using the ACI equation, this is attributed to the higher values for deflection obtained by using Faza equation, which leads to more stress in the external cables. Tables 4-9 and 4-10 show the increase in the post-tensioning force for each live load increment and figure

Reproduced with permission of the copyright owner. Further reproduction prohibited without permission.

4-11 shows the increase in the post – tensioning force and compares it to the post tensioning force obtained from the test data.

In view of the above, care must be exercised during the calculation of the ultimate moment for internally and externally prestressed beams since the magnitude of the effective stress in the external cables is one of the most important variables that affects the ultimate capacity of the beam.

Another difficulty that stands in the way to arrive at a correct value for deflection is the value of the modulus of elasticity at failure as beyond the cracking load the concrete is under high stresses and therefore has a lower value of modulus of elasticity hence, the deflection will increase much faster and will be of a greater magnitude. The load deflection behaviour presented by the three curves is very close to a straight line up to the cracking load and has progressively increasing slope as the load is increased above the cracking load This progressive curvature is due to the plastic strains encountered by the concrete at higher load levels and since the carbon fibers are linearly elastic till failure the non-linearity is caused by the behaviour and the cracking of concrete only.

Reproduced with permission of the copyright owner. Further reproduction prohibited without permission.

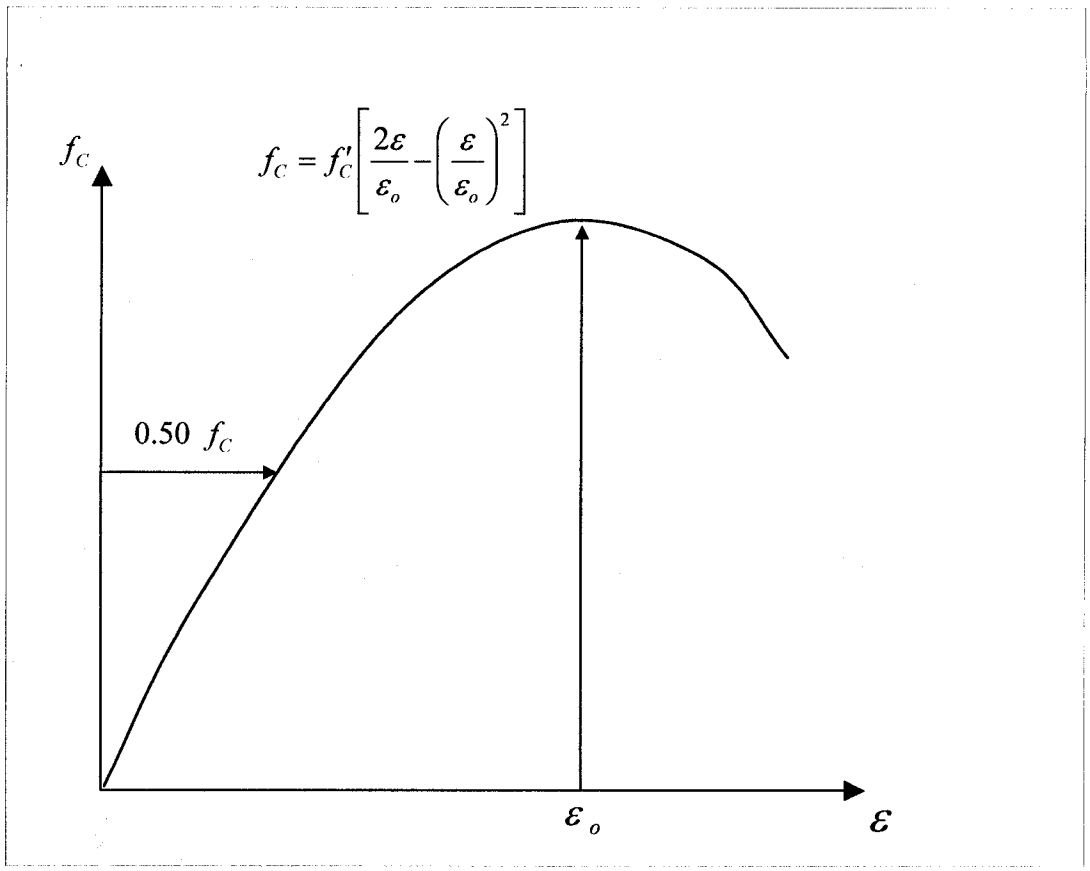

Figure 4-13: Stress- Strain curve of concrete.

Reproduced with permission of the copyright owner. Further reproduction prohibited without permission.

Table 4-9: Increase in the Post-Tensioning Force Based on the Deflection Calculated from the ACI Equation

Live load increment %	Total length of post -tensioned cables before elongation (mm)	Total length of post – tensioned cables after elongation (mm)	Strain (mm/mm) 10E-3	Initial stress (MPa)	Additional stress (Mpa)	Total Stress (Mpa)	Total force (kN)
10	16374	16442	4.151	565	12	577	1800
20	16374	16445	4.338	565	38	603	1880
30	16374	16448	4.525	565	64	629	1960
40	16374	16452	4.813	565	104	669	2084
50	16374	16457	5.079	565	141	706	2200
60	16374	16463	5.446	565	192	757	2360
70	16374	16472	6.000	565	269	834	2600
80	16374	16481	6.554	565	346	911	2840
90	16374	16490	7.108	565	423	988	3080
100	16374	16501	7.755	565	513	1078	3360
109.1	16374	16508	8.216	565	577	1142	3560

Reproduced with permission of the copyright owner. Further reproduction prohibited without permission.

Table 4-10: Increase in the Post-Tensioning Force Based on the Deflection Calculated from Faza Equation

Live load increment %	Total length of post – tensioned cables before elongation (mm)	Total length of post -tensioned cables after elongation (mm)	Strain (mm/mm) 10E-3	Initial stress (MPa)	Additional stress (Mpa)	Total Stress (Mpa)	Total force (kN)
10	16374	16444	4.252	565	26	591	1840
20	16374	16447	4.435	565	51	616	1920
30	16374	16451	4.712	565	90	655	2040
40	16374	16456	5.007	565	131	696	2168
50	16374	16461	5.309	565	173	738	2300
60	16374	16467	5.705	565	228	793	2472
70	16374	16477	6.288	565	309	874	2724
80	16374	16486	6.856	565	388	953	2968
90	16374	16498	7.554	565	485	1050	3272
100	16374	16506	8.050	565	554	1119	3488
112	16374	16521	8.992	565	685	1250	3896

Reproduced with permission of the copyright owner. Further reproduction prohibited without permission.

Table 4-11: Comparison between stresses and strains for the top concrete, pretensioned tendons and post-tensioned tendons based on the deflection calculated according to the ACI equation

Live load increment %	Top Concrete		Pretensioned Tendons		Post-tensioned Tendons	
	Stress (MPa)	Strain (millionth)	Stress (MPa)	Strain (mm/mm) 10E-3	Stress (MPa)	Strain (mm/mm) 10E-3
0	+0.28	+9.49	1412	10.158	577	4.151
10	-5.60	-190	1435	10.324	603	4.338
20	-7.680	-260	1458	10.489	629	4.525
30	-10.47	-354	1481	10.655	669	4.813
40	-17.68	-600	1758	12.647	706	5.079
50	-21.44	-822	1903	13.691	757	5.446
60	-26.24	-1070	2023	14.554	834	6.000
70	-30.16	-1310	2165	15.576	911	6.554
80	-34.17	-1620	2285	16.439	988	7.108
90	-36.11	-1820	2427	17.460	1078	7.755
100	-37.80	-2060	2547	18.324	1142	8.216
109	-38.40	-2190	2596(Failure)	18.676	577	4.151

Reproduced with permission of the copyright owner. Further reproduction prohibited without permission.

Table 4-12: Comparison between stresses and strains for the top concrete, pretensioned tendons and post-tensioned tendons based on the deflection calculated according to the Salem Faza equation

Live load increment %	Top Concrete		Pretensioned Tendons		Post-tensioned Tendons	
	Stress (MPa)	Strain (millionth)	Stress (MPa)	Strain (mm/mm) 10E-3	Stress (MPa)	Strain (mm/mm) 10E-3
0	+0.28	+9.49	1412	10.158	591	4.252
10	-4.879	-165	1435	10.323	616	4.435
20	-7.775	-263	1458	10.489	655	4.712
30	-10.435	-353	1477	10.626	696	5.007
40	-17.60	-596	1684	12.115	738	5.309
50	-21.12	-807	1830	13.165	793	5.705
60	-25.89	-1050	1949	14.022	874	6.288
70	-29.44	-1262	2092	15.050	953	6.856
80	-33.60	-1569	2212	15.914	1050	7.554
90	-35.76	-1780	2353	16.928	1119	8.050
100	-37.44	-2000	2473	17.791	1250	8.992
109	-38.36	-2180	2595(Failure)	18.669	591	4.252

Reproduced with permission of the copyright owner. Further reproduction prohibited without permission.

Reproduced with permission of the copyright owner. Further reproduction prohibited without permission.

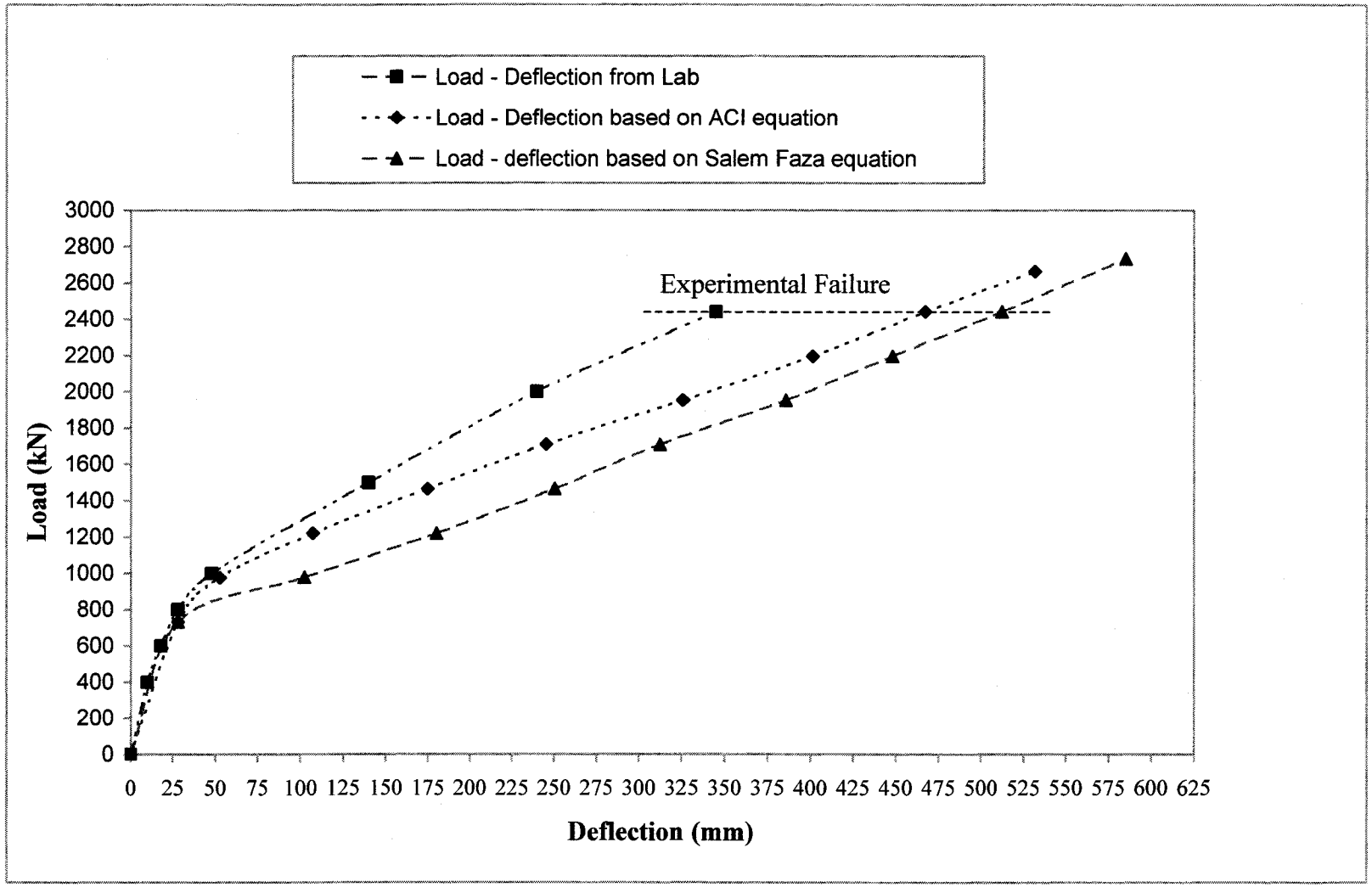

Figure 4-14: Comparison Between Load-Deflection Curve obtained from the Lab and Load Deflection Curves obtained from the Analysis

Reproduced with permission of the copyright owner. Further reproduction prohibited without permission.

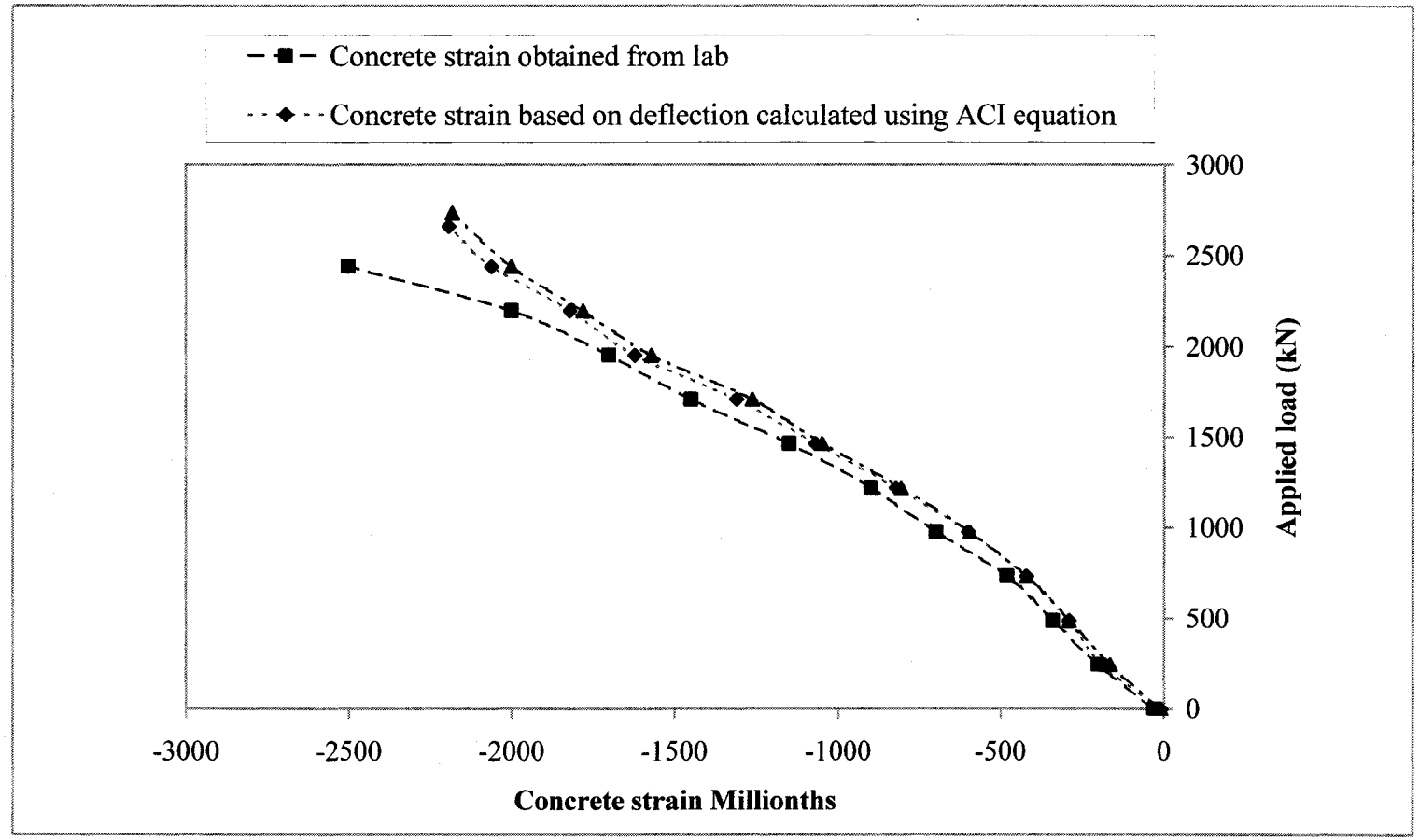

Figure 4 –15: Comparison Between the Top Concrete Strain obtained from the Lab and the Concrete Strain obtained from the Analysis

Reproduced with permission of the copyright owner. Further reproduction prohibited without permission.

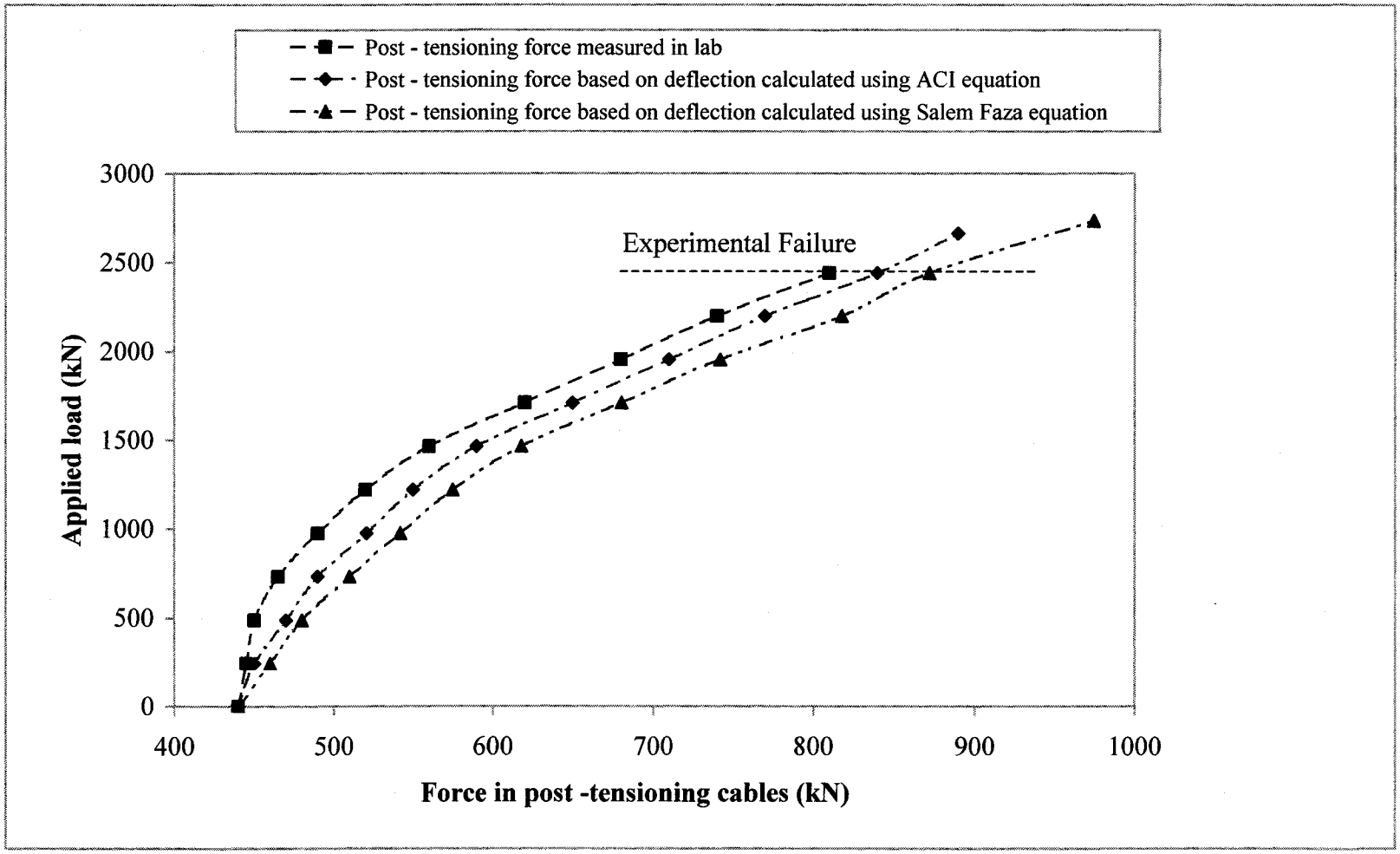

Figure 4-16: Post-Tensioning Force Measured from the Lab vs. Post-Tensioning Force Obtained From the Analysis

CHAPTER FIVE

CONCLUSIONS AND RECOMENDATION

5.1 Conclusions

The presented analysis and discussion show that the proposed precast/prestressd bridge system using carbon fibers is a promising structural system and the introduction of these new materials, new approaches and new design philosophies must be developed. The following conclusions can be drawn form the analysis of the prestressed double tee bridge system using carbon fibers:

1) The standard procedure of elastic analysis can be used to predict the behaviour of the combined system of pretensioned and post-tensioned beams. The loss of prestress due to elastic shortening and creep has to be calculated and herein, the stresses and deflections obtained from the analysis show good correlation to the test data.
2) A proposed procedure is presented for estimating the ultimate load carrying capacity of beams prestressed internally and externally with carbon fibers. This procedure takes into consideration the change in the strain of unbonded tendons relative to the concrete member as a result of their slippage.
3) The load deflection curve drawn using the modified effective moment of inertia suggested by ACI showed better relationship to the actual load deflection curve and could be used for calculating deflection for members prestressed with carbon fibers.

Reproduced with permission of the copyright owner. Further reproduction prohibited without permission.

5.2 Recommendation

A more accurate procedure of analysis could be conducted that takes into consideration the non-linear relationship between the stress and strain at higher stresses in concrete and near the ultimate load.

Reproduced with permission of the copyright owner. Further reproduction prohibited without permission.

APPENDIX A

ANALYSIS COMPUTATIONS

Reproduced with permission of the copyright owner. Further reproduction prohibited without permission.

APPENDIX A

ANALYSIS COMPUTATIONS

1. Phase A: Application of Internal Prestressing

1.1 Elastic Shortening for Pre-Tensioned Tendons

The stress of concrete at level of tendon is,

$$f_C = \frac{5220\times10^3}{942900} + \frac{5220\times10^3\times329^2}{1.367\times10^{11}} - \frac{823\times10^6\times329}{1.367\times10^{11}} = 7.69 \text{ MPa}$$

$$\text{Loss of stress} = \frac{139\times10^3}{22\times10^3}\times7.69 = 48.58 \text{ MPa}$$

The loss in the pre-tensioning force is,

$$\text{loss of force} = 48.58\times55.70\times60 = 163\,\text{kN}$$

Total pre-tensioned force after losses,

$$F = 5220000 - 162354 = 5057\,\text{kN}$$

Reproduced with permission of the copyright owner. Further reproduction prohibited without permission.

1.2 Calculation of Stresses

1.2.1 Calculation of Stresses at Mid Span

$$f_{top} = -\frac{5057646}{942900} + \frac{5057646 \times 329 \times 474}{1.367 \times 10^{11}} - \frac{823 \times 10^6 \times 474}{1.367 \times 10^{11}} = -2.44 \text{ MPa}$$

$$f_{bottom} = -\frac{5057646}{942900} - \frac{5057646 \times 329 \times 746}{1.367 \times 10^{11}} + \frac{823 \times 10^6 \times 746}{1.367 \times 10^{11}} = -9.95 \text{ MPa}$$

1.2.2 Calculation of Stresses at Quarter Span

$$f_{top} = -\frac{5057646}{942900} + \frac{5057646 \times 297 \times 474}{1.367 \times 10^{11}} - \frac{533 \times 10^6 \times 474}{1.367 \times 10^{11}} = -2.01 \text{ MPa}$$

$$f_{bottom} = -\frac{5057646}{942900} - \frac{5057646 \times 297 \times 746}{1.367 \times 10^{11}} + \frac{533 \times 10^6 \times 746}{1.367 \times 10^{11}} = -10.65 \text{ MPa}$$

1.3 Calculations for Deflection

1.3.1 Calculations for Deflection at Mid Span

Downward deflection due to own-weight,

$$\delta_1 = \frac{5 \times 22.30 \times 17180^4}{384 \times 22 \times 10^3 \times 1.367 \times 10^{11}} = 8.41 \text{ mm.}$$

Upward deflection the pre-tensioning force,

$$\delta_2 = \frac{80501 \times 5490}{24 \times 22 \times 10^3 \times 1.367 \times 10^{11}} \left(3 \times 17180^2 - 4 \times 5490^2\right) = 4.68 \text{ mm.}$$

Reproduced with permission of the copyright owner. Further reproduction prohibited without permission.

Deflection due to eccentricity of the tendons at the end,

$$\delta_3 = \frac{1224\times10^6\times17180^2}{8\times22\times10^3\times1.367\times10^{11}} = 15.02 \text{ mm.}$$

Therefore the total upward deflection,

$$\delta_f = -8.41 + 4.68 + 15.02 = 11.29 \text{ mm.}$$

1.3.2 Calculations for Deflection at Quarter Span

Downward deflection due to own-weight,

$$\delta_1 = \frac{22.30\times3490}{24\times22\times10^3\times1.367\times10^{11}}\left(3490^3 - 2\times17180\times3490^2 + 17180^3\right) = 5.02 \text{ mm.}$$

Upward deflection from the pre-tensioning force,

$$\delta_2 = \frac{80501\times3490}{6\times22\times10^3\times1.367\times10^{11}}\left(3\times17180\times5490 - 3\times5490^2 - 3490^2\right) = 2.81 \text{ mm.}$$

Deflection due to eccentricity of the tendons at the end,

Left moment,

$$\delta_3 = \frac{1224\times10^6\times13690}{6\times22\times10^3\times1.367\times10^{11}\times17440}\left(13690^2 - 3\times17180\times13690 + 2\times17180^2\right) = 3.89 \text{ mm}$$

Right moment,

$$\delta_4 = \frac{1224\times10^6\times3490}{6\times22\times10^3\times1.367\times10^{11}\times17180}\left(3490^2 - 3\times17180\times3490 + 2\times17180^2\right) = 5.82 \text{ mm}$$

Reproduced with permission of the copyright owner. Further reproduction prohibited without permission.

Therefore the total upward deflection,

$\delta_f = -5.02 + 2.81 + 3.89 + 5.82 = 7.50$ mm.

2 Phase B: Sixty Percent of External Post-Tensioning

2.1 Elastic Shortening of Pre-Tensioned Tendons due to Sixty Percent of External Post-Tensioning

The stress of concrete at level of tendon is,

$$f_C = \frac{5057646}{942900} + \frac{5057646 \times 329^2}{1.367 \times 10^{11}} + \frac{1072000}{942900} + \frac{1072000 \times 329^2}{1.367^{11}} - \frac{609 \times 10^6 \times 329}{1.367 \times 10^{11}} = 9.90 \text{ MPa}$$

$$\text{Loss of stress} = \frac{139 \times 10^3}{32 \times 10^3} \times 9.90 = 43 \text{ MPa}$$

The loss in the pre - tensioning force is,

$\text{loss of force} = 43 \times 55.70 \times 60 = 144 \text{ kN}$

Total pre – tensioned force after losses,

$F = 5057646 - 143706 = 4914$ kN

Reproduced with permission of the copyright owner. Further reproduction prohibited without permission.

2.2 Calculation of Stresses

2.2.1 Calculation of Stresses at Mid Span

Stresses after elastic shortening,

$$f_2 = -\frac{4913940}{942900} - \frac{1072000}{942900} + \frac{4913940 \times 329 \times 474}{1.367 \times 10^{11}} + \frac{1072000 \times 396 \times 474}{1.367 \times 10^{11}}$$
$$- \frac{609 \times 10^6 \times 474}{1.367 \times 10^{11}} = -1.38 \text{ MPa}$$

$$f_1 = -\frac{4913940}{942900} - \frac{1072000}{942900} - \frac{4913940 \times 329 \times 746}{1.367 \times 10^{11}} - \frac{1072000 \times 396 \times 746}{1.367 \times 10^{11}}$$
$$+ \frac{609 \times 10^6 \times 746}{1.367 \times 10^{11}} = -14.16 \text{ MPa}$$

Calculation of creep,

Coefficient of creep for five days,

$$C_t = \frac{5^{0.60}}{10 + 5^{0.60}} \times 2.35 \times 0.345 = 0.19$$

The creep strain is,

$$\varepsilon_{cr} = 0.19 \times 4.4625 \times 10 \text{ E - } 04 = 8.4098 \times 10 \text{ E - } 05$$

The increase in the strain in concrete is accompanied by a reduction in the stress in the pretensioning force, which is calculated by the formula,

$$f_r = 139 \times 10 \text{ E } 03 \times 8.409810 \text{ E - } 04 = 11.69 \text{ MPa}$$

The pretensioned force after the creep loss is,

$$F_3 = 4913940 - 11.689 \times 55.7 \times 60 = 4875 \text{ kN}$$

Reproduced with permission of the copyright owner. Further reproduction prohibited without permission.

Final tresses after the introduction of the creep effect,

$$f_2 = -\frac{4874919}{942900} - \frac{1072000}{942900} + \frac{4874919 \times 329 \times 474}{1.367 \times 10^{11}} + \frac{1072000 \times 396 \times 474}{1.367 \times 10^{11}}$$
$$- \frac{609 \times 10^6 \times 474}{1.367 \times 10^{11}} = -1.38 \text{ MPa}$$

$$f_1 = -\frac{4874919}{942900} - \frac{1072000}{942900} - \frac{4874919 \times 329 \times 746}{1.367 \times 10^{11}} - \frac{1072000 \times 396 \times 746}{1.367 \times 10^{11}}$$
$$+ \frac{609 \times 10^6 \times 746}{1.367 \times 10^{11}} = -14.05 \text{ MPa}$$

2.2.2 Calculation of Stresses at Quarter Span

Stresses after the elastic shortening,

$$f_2 = -\frac{4913940}{942900} - \frac{1072000}{942900} + \frac{4913940 \times 297 \times 474}{1.367 \times 10^{11}} + \frac{1072000 \times 145 \times 474}{1.367 \times 10^{11}}$$
$$- \frac{318 \times 10^6 \times 474}{1.367 \times 10^{11}} = -1.85 \text{ MPa}$$

$$f_1 = -\frac{4913940}{942900} - \frac{1072000}{942900} - \frac{4913940 \times 297 \times 746}{1.367 \times 10^{11}} - \frac{1072000 \times 145 \times 746}{1.367 \times 10^{11}}$$
$$+ \frac{318 \times 10^6 \times 746}{1.367 \times 10^{11}} = -13.42 \text{ MPa}$$

Reproduced with permission of the copyright owner. Further reproduction prohibited without permission.

Final stresses after the introduction of the creep effect,

$$f_2 = -\frac{4874919}{942900} - \frac{1072000}{942900} + \frac{4874919 \times 297 \times 474}{1.367 \times 10^{11}} + \frac{1072000 \times 145 \times 474}{1.367 \times 10^{11}}$$
$$- \frac{318 \times 10^6 \times 474}{1.367 \times 10^{11}} = -1.85 \text{ MPa}$$

$$f_1 = -\frac{4874919}{942900} - \frac{1072000}{942900} - \frac{4874919 \times 297 \times 746}{1.367 \times 10^{11}} - \frac{1072000 \times 145 \times 746}{1.367 \times 10^{11}}$$
$$+ \frac{318 \times 10^6 \times 746}{1.367 \times 10^{11}} = -13.36 \text{ MPa}$$

2.3 Calculations for Deflection

2.3.1 Calculations for Deflection at Mid Span

Downward deflection due to own-weight,

$$\delta_1 = \frac{5 \times 22.30 \times 15552^4}{384 \times 32 \times 10^3 \times 1.367 \times 10^{11}} = 3.88 \text{ mm.}$$

Upward deflection due to the effect of cantilevers,

$$\delta_2 = \frac{65.50 \times 10^6 \times 15552^2}{8 \times 32 \times 10^3 \times 1.367 \times 10^{11}} = 0.45 \text{ mm.}$$

Upward deflection from the pre – tensioning force,

$$\delta_3 = \frac{77593 \times 4676}{24 \times 32 \times 10^3 \times 1.367 \times 10^{11}} \left(3 \times 15552^2 - 4 \times 4676^2\right) = 2.17 \text{ mm.}$$

Reproduced with permission of the copyright owner. Further reproduction prohibited without permission.

Deflection due to eccentricity of the tendons at the end,

$$\delta_4 = \frac{1243\times10^6\times15552^2}{8\times32\times10^3\times1.367\times10^{11}} = 8.59 \text{ mm.}$$

Deflection due to external post-tensioning

$$\delta_5 = \frac{84\times10^3\times15552^3}{48\times32\times10^3\times1.367\times10^{11}} = 1.51 \text{ mm.}$$

$$\delta_6 = \frac{52\times10^3\times4184}{24\times32\times10^3\times1.367\times10^{11}}\left(3\times15552^2 - 4\times4184^2\right) = 1.36 \text{ mm.}$$

Therefore the total upward deflection,

$$\delta_f = -3.88 + 0.45 + 2.17 + 8.59 + 1.51 + 1.36 = 10.20 \text{ mm.}$$

The slope at the support is calculated due to the pretensioning force,

$$\alpha_1 = \frac{77593\times4676}{2\times32\times10^3\times1.367\times10^{11}}\left(15552 - 4676\right) = 4.51\times10^{-4}\text{rad}$$

The slope at the support is calculated due to the post-tensioning force

$$\alpha_2 = \frac{84\times10^3\times15552^2}{16\times32\times10^3\times1.367\times10^{11}} = 2.90\times10^{-4}\text{rad}$$

$$\alpha_3 = \frac{52\times10^3\times4184}{2\times32\times10^3\times1.367\times10^{11}}\left(15552 - 4184\right) = 2.82\times10^{-4}\text{rad}$$

The total slope at the support,

$$\alpha_T = 4.5104\times10^{-4} + 2.9028\times10^{-4} + 2.827\times10^{-4} = 10.24\times10^{-4}\text{rad}$$

Reproduced with permission of the copyright owner. Further reproduction prohibited without permission.

The downward deflection at the end of the cantilever

$\delta_C = 10.2402 \times 10^{-4} \times 2424 = 2.48$ mm

The relative deflection between the mid span and the end of the cantilever

$\delta_R = 10.20 + 2.48 = 12.68$ mm

2.3.2 Calculations for Deflection at Quarter Span

Downward deflection due to own-weight,

$$\delta_1 = \frac{22.30 \times 2676}{24 \times 32 \times 10^3 \times 1.367 \times 10^{11}} \left(15552^3 - 2 \times 15552 \times 2676^2 + 2676^3\right) = 2.02 \text{ mm.}$$

Upward deflection due to the effect of cantilevers

Left cantilever moment,

$$\delta_2 = \frac{65.50 \times 10^6 \times 12876}{6 \times 32 \times 10^3 \times 1.367 \times 10^{11} \times 15552} \left(12876^2 - 3 \times 15552 \times 12876 + 2 \times 15552^2\right) = 0.10 \text{ mm}$$

Right cantilever moment,

$$\delta_3 = \frac{65.50 \times 10^6 \times 2676}{6 \times 32 \times 10^3 \times 1.367 \times 10^{11} \times 15552} \left(2676^2 - 3 \times 15552 \times 2676 + 2 \times 15552^2\right) = 0.16 \text{ mm.}$$

Deflection from the upward pressure of the pre-tensioning force,

$$\delta_4 = \frac{77593 \times 2676}{6 \times 32 \times 10^3 \times 1.367 \times 10^{11}} \left(3 \times 15552 \times 4676 - 3 \times 4676^2 - 2676^2\right) = 1.15 \text{ mm.}$$

Reproduced with permission of the copyright owner. Further reproduction prohibited without permission.

Deflection due to eccentricity of the tendons at the end,

Left moment,

$$\delta_5 = \frac{1243\times10^6\times12876}{6\times32\times10^3\times1.367\times10^{11}\times15552}\left(12876^2-3\times15552\times12876+2\times15552^2\right)=1.91\,\text{mm}$$

Right moment,

$$\delta_6 = \frac{1243\times10^6\times2676}{6\times32\times10^3\times1.367\times10^{11}\times15552}\left(2676^2-3\times15552\times2676+2\times15552^2\right)=2.99\,\text{mm}$$

Deflection due to external post – tensioning

$$\delta_7 = \frac{84\times10^3\times5100}{48\times32\times10^3\times1.367\times10^{11}}\left(3\times15552^2-4\times5100^2\right)=1.26\ \text{mm.}$$

$$\delta_8 = \frac{52\times10^3\times2676}{6\times32\times10^3\times1.367\times10^{11}}\left(3\times15552\times4184-3\times4184^2-2676^2\right)=0.72\ \text{mm.}$$

Therefore the total upward deflection,

$$\delta_f = -2.02+0.10+0.16+1.15+1.91+2.99+0.75+0.72=5.76\,\text{mm.}$$

The slope at the support is calculated due to the pretensioning force,

$$\alpha_1 = \frac{77593\times4676}{2\times32\times10^3\times1.367\times10^{11}}\left(15552-4676\right)=4.51\times10^{-4}\,\text{rad}$$

The slope at the support is calculated due to the post-tensioning force

$$\alpha_2 = \frac{84\times10^3\times15552^2}{16\times32\times10^3\times1.367\times10^{11}}=2.90\times10^{-4}\,\text{rad}$$

Reproduced with permission of the copyright owner. Further reproduction prohibited without permission.

$$\alpha_3 = \frac{52\times10^3\times4184}{2\times32\times10^3\times1.367\times10^{11}}(15552-4184) = 2.82\times10^{-4}\,\text{rad}$$

The total slope at the support,

$$\alpha_T = 4.5104\times10^{-4} + 2.9028\times10^{-4} + 2.827\times10^{-4} = 10.24\times10^{-4}\,\text{rad}$$

The downward deflection at the end of the cantilever,

$$\delta_C = 10.2402\times10^{-4}\times2424 = 2.48\,\text{mm}$$

The relative deflection between the mid span and the end of the cantilever

$$\delta_R = 5.76 + 2.48 = 8.24\,\text{mm}$$

3. Stage of Casting Topping

3.1 Calculation of Stresses

3.1.1 Calculation of Stresses at Mid Span

Stresses before the introduction of the creep effect,

$$f_2 = -\frac{4874919}{942900} - \frac{1072000}{942900} + \frac{4874919\times329\times474}{1.367\times10^{11}} + \frac{1072000\times396\times474}{1.367\times10^{11}}$$
$$-\frac{1160\times10^6\times474}{1.367\times10^{11}} - \frac{195\times10^6\times474}{1.367\times10^{11}} = -3.97\,\text{MPa}$$

$$f_1 = -\frac{4874919}{942900} - \frac{1072000}{942900} - \frac{4874919\times329\times746}{1.367\times10^{11}} - \frac{1072000\times396\times746}{1.367\times10^{11}}$$
$$+\frac{1160\times10^6\times746}{1.367\times10^{11}} + \frac{195\times10^6\times746}{1.367\times10^{11}} = -9.98\,\text{MPa}$$

Calculation of creep,

Coefficient of creep for ninteen days,

$$C_t = \frac{19^{0.60}}{10+19^{0.60}}\times2.35\times0.345 = 0.31$$

Reproduced with permission of the copyright owner. Further reproduction prohibited without permission.

The creep strain is

$$\varepsilon_{cr} = (0.31-0.19)\times 3.1194\times 10\,\text{E-}04 = 3.74\times 10\,\text{E-}05$$

The increase in the strain in concrete is accompanied by a reduction in the stress in the pretensioning force, which is calculated by the formula

$$f_r = 139\times 10\,\text{E}\,03\times 3.7433\,\text{E-}05 = 5.20\,\text{MPa}$$

The pretensioned force after the creep loss is,

$$F_3 = 4874919 - 5.203\times 55.7\times 60 = 4857\,\text{kN}$$

Stresses after the introduction of the creep effect,

$$f_2 = -\frac{4857531}{942900} - \frac{1072000}{942900} + \frac{4857531\times 329\times 474}{1.367\times 10^{11}} + \frac{1072000\times 396\times 474}{1.367\times 10^{11}}$$
$$- \frac{1160\times 10^6\times 474}{1.367\times 10^{11}} - \frac{195\times 10^6\times 474}{1.367\times 10^{11}} = -3.97\,\text{MPa}$$

$$f_1 = -\frac{4857531}{942900} - \frac{1072000}{942900} - \frac{4857531\times 329\times 746}{1.367\times 10^{11}} - \frac{1072000\times 396\times 746}{1.367\times 10^{11}}$$
$$+ \frac{1160\times 10^6\times 746}{1.367\times 10^{11}} + \frac{195\times 10^6\times 746}{1.367\times 10^{11}} = -9.93\,\text{MPa}$$

3.1.2 Calculation of Stresses at Quarter Span

Stresses before the introduction of the creep effect,

$$f_2 = -\frac{4874919}{942900} - \frac{1072000}{942900} + \frac{4874919\times 297\times 474}{1.367\times 10^{11}} + \frac{1072000\times 145\times 474}{1.367\times 10^{11}}$$
$$- \frac{870\times 10^6\times 474}{1.367\times 10^{11}} - \frac{146\times 10^6\times 474}{1.367\times 10^{11}} = -4.27\,\text{MPa}$$

$$f_1 = -\frac{4874919}{942900} - \frac{1072000}{942900} - \frac{4874919\times 297\times 746}{1.367\times 10^{11}} - \frac{1072000\times 145\times 746}{1.367\times 10^{11}}$$
$$+ \frac{870\times 10^6\times 746}{1.367\times 10^{11}} + \frac{146\times 10^6\times 746}{1.367\times 10^{11}} = -9.98\,\text{MPa}$$

Reproduced with permission of the copyright owner. Further reproduction prohibited without permission.

Final stresses after the introduction of the effect of creep,

$$f_2 = -\frac{4857531}{942900} - \frac{1072000}{942900} + \frac{4857531\times 297\times 474}{1.367\times 10^{11}} + \frac{1072000\times 145\times 474}{1.367\times 10^{11}}$$
$$- \frac{870\times 10^6\times 474}{1.367\times 10^{11}} - \frac{146\times 10^6\times 474}{1.367\times 10^{11}} = -4.27 \text{ MPa}$$

$$f_1 = -\frac{4857531}{942900} - \frac{1072000}{942900} - \frac{4857531\times 297\times 746}{1.367\times 10^{11}} - \frac{1072000\times 145\times 746}{1.367\times 10^{11}}$$
$$+ \frac{870\times 10^6\times 746}{1.367\times 10^{11}} + \frac{146\times 10^6\times 746}{1.367\times 10^{11}} = -9.46 \text{ MPa}$$

3.2 Calculations for Deflection

3.2.1 Calculations for Deflection at Mid Span

Downward deflection due to own-weight,

$$\delta_1 = \frac{5\times 22.30\times 20400^4}{384\times 32\times 10^3\times 1.367\times 10^{11}} = 11.50 \text{ mm.}$$

Deflection due to topping

$$\delta_2 = \frac{5\times 3.75\times 20400^4}{384\times 32\times 10^3\times 1.367\times 10^{11}} = 1.93 \text{ mm.}$$

Deflection from the upward pressure of the pre – tensioning force,

$$\delta_3 = \frac{77316\times 7100}{24\times 32\times 10^3\times 1.367\times 10^{11}}\left(3\times 20400^2 - 4\times 7100^2\right) = 5.52 \text{ mm.}$$

Deflection due to eccentricity of the tendons at the end,

$$\delta_4 = \frac{1049\times 10^6\times 20400^2}{8\times 32\times 10^3\times 1.367\times 10^{11}} = 12.47 \text{ mm.}$$

Reproduced with permission of the copyright owner. Further reproduction prohibited without permission.

Deflection due to external post – tensioning

$$\delta_5 = \frac{84\times10^3\times20400^3}{48\times32\times10^3\times1.367\times10^{11}} = 3.39 \text{ mm.}$$

$$\delta_6 = \frac{52\times10^3\times6608}{24\times32\times10^3\times1.367\times10^{11}}\left(3\times20400^2 - 4\times6608^2\right) = 3.51 \text{ mm.}$$

Therefore the total upward deflection,

$$\delta_f = -11.50 - 1.93 + 5.52 + 12.47 + 3.39 + 3.51 = 11.44 \text{ mm.}$$

3.2.2 Calculations for Deflection at Quarter Span

Downward deflection due to own-weight,

$$\delta_1 = \frac{22.30\times5100}{24\times32\times10^3\times1.367\times10^{11}}\left(20400^3 - 2\times20400\times5100^2 + 5100^3\right) = 8.19 \text{ mm.}$$

Deflection due to topping

$$\delta_2 = \frac{3.75\times5100}{24\times32\times10^3\times1.367\times10^{11}}\left(20400^3 - 2\times20400\times5100^2 + 5100^3\right) = 1.38 \text{ mm.}$$

Deflection from the upward pressure of the pre – tensioning force,

$$\delta_3 = \frac{77316\times5100}{6\times32\times10^3\times1.367\times10^{11}}\left(3\times20400\times7100 - 3\times7100^2 - 5100^2\right) = 3.87 \text{ mm.}$$

Deflection due to eccentricity of the tendons at the end,

Left moment,

$$\delta_4 = \frac{1049\times10^6\times15300}{6\times32\times10^3\times1.367\times10^{11}\times20400}\left(15300^2 - 3\times20400\times15300 + 2\times20400^2\right) = 3.89\text{mm}$$

Reproduced with permission of the copyright owner. Further reproduction prohibited without permission.

Right moment,

$$\delta_5 = \frac{1049\times10^6\times5100}{6\times32\times10^3\times1.367\times10^{11}\times20400}\left(5100^2-3\times20400\times5100+2\times20400^2\right)=5.45 \text{ mm}$$

Deflection due to external post-tensioning

$$\delta_6 = \frac{84\times10^3\times5100}{48\times32\times10^3\times1.367\times10^{11}}\left(3\times20400^2-4\times5100^2\right)=2.33 \text{ mm.}$$

$$\delta_7 = \frac{52\times10^3\times5100}{6\times32\times10^3\times1.367\times10^{11}}\left(3\times20400\times6608-3\times6608^2-5100^2\right)=2.50 \text{ mm.}$$

Therefore the total upward deflection,

$$\delta_f = -8.19-1.38+3.87+3.89+5.45+2.33+2.50=8.47\,\text{mm.}$$

4 Phase D: Full Post-Tensioning

4.1 Elastic Shortening of Pre-Tensioned Tendons due to Full Post – Tensioning

The stress of concrete at level of tendon is,

$$f_C = \frac{487531}{1101900}+\frac{487531\times403^2}{1.724\times10^{11}}+\frac{1796000}{1101900}+\frac{1796000\times403^2}{1.724\times10^{11}}-\frac{1160\times10^6\times403}{1.724\times10^{11}}$$
$$-\frac{195\times10^6\times403}{1.724\times10^{11}}=9.14\,\text{MPa}$$

$$\text{Loss of stress}=\frac{139\times10^3}{32\times10^3}\times9.139=39.70 \text{ MPa}$$

The loss in the pre - tensioning force is,

$$\text{loss of force}=39.70\times55.70\times60=132 \text{ kN}$$

Total pre-tensioned force after losses,

$$F=4857531-132677=4724 \text{ kN}$$

Reproduced with permission of the copyright owner. Further reproduction prohibited without permission.

4.2 Calculation of Stresses

4.2.1 Calculation of Stresses at Mid Span

Stresses after the elastic shortening,

$$f_2 = -\frac{4724854}{1101900} - \frac{1072000}{1101900} + \frac{4724854 \times 403 \times 400}{1.724 \times 10^{11}} + \frac{1072000 \times 470 \times 400}{1.724 \times 10^{11}}$$
$$- \frac{1160 \times 10^6 \times 400}{1.724 \times 10^{11}} - \frac{195 \times 10^6 \times 400}{1.724 \times 10^{11}} = -2.82 \text{ MPa}$$

$$f_1 = -\frac{4724854}{1101900} - \frac{1072000}{1101900} - \frac{4724854 \times 403 \times 820}{1.724 \times 10^{11}} - \frac{1072000 \times 470 \times 820}{1.724 \times 10^{11}}$$
$$+ \frac{1160 \times 10^6 \times 820}{1.724 \times 10^{11}} + \frac{195 \times 10^6 \times 820}{1.724 \times 10^{11}} = -10.72 \text{ MPa}$$

Calculation of creep,

Coefficient of creep for twenty-seven days,

$$C_t = \frac{27^{0.60}}{10 + 27^{0.60}} \times 2.35 \times 0.345 = 0.34$$

The creep strain is,

$$\varepsilon_{cr} = (0.34 - 0.31) \times 3.3522 \times 10\,\text{E-}04 = 1.01 \times 10\,\text{E-}05$$

The increase in the strain in concrete is accompanied by a reduction in the stress in the pretensioning force, which is calculated by the formula,

$$f_r = 139 \times 10\,\text{E}\,03 \times 1.2190\,\text{E-}05 = 1.39 \text{ MPa}$$

The pretensioned force after the creep loss is,

$$F_3 = 4724854 - 1.3979 \times 55.7 \times 60 = 4720 \text{ kN}$$

Reproduced with permission of the copyright owner. Further reproduction prohibited without permission.

Stresses after the introduction of the creep effect,

$$f_2 = -\frac{4720182}{1101900} - \frac{1072000}{1101900} + \frac{4720182 \times 403 \times 400}{1.724 \times 10^{11}} + \frac{1072000 \times 470 \times 400}{1.724 \times 10^{11}}$$
$$- \frac{1160 \times 10^6 \times 400}{1.724 \times 10^{11}} - \frac{195 \times 10^6 \times 400}{1.724 \times 10^{11}} = -2.82 \text{ MPa}$$

$$f_1 = -\frac{4720182}{1101900} - \frac{1072000}{1101900} - \frac{4720182 \times 403 \times 820}{1.724 \times 10^{11}} - \frac{1072000 \times 470 \times 820}{1.724 \times 10^{11}}$$
$$+ \frac{1160 \times 10^6 \times 820}{1.724 \times 10^{11}} + \frac{195 \times 10^6 \times 820}{1.724 \times 10^{11}} = -10.71 \text{ MPa}$$

The effect of the remaining forty percent of post – tensioning force,

$$f_4 = -\frac{724000}{1101900} + \frac{724000 \times 470 \times 475}{1.724 \times 10^{11}} = +0.280 \text{ MPa}$$

$$f_1 = -\frac{724000}{1101900} - \frac{724000 \times 470 \times 475}{1.724 \times 10^{11}} = -2.28 \text{ MPa}$$

4.2.2 Calculation of Stresses at Quarter Span

Stresses after the elastic shortening,

$$f_2 = -\frac{4724854}{1101900} - \frac{1072000}{1101900} + \frac{4724854 \times 371 \times 400}{1.724 \times 10^{11}} + \frac{1072000 \times 219 \times 400}{1.724 \times 10^{11}}$$
$$- \frac{870 \times 10^6 \times 400}{1.724 \times 10^{11}} - \frac{146 \times 10^6 \times 400}{1.724 \times 10^{11}} = -3.00 \text{ MPa}$$

$$f_1 = -\frac{4724854}{1101900} - \frac{1072000}{1101900} - \frac{4724854 \times 371 \times 820}{1.724 \times 10^{11}} - \frac{1072000 \times 219 \times 820}{1.724 \times 10^{11}}$$
$$+ \frac{870 \times 10^6 \times 820}{1.724 \times 10^{11}} + \frac{146 \times 10^6 \times 820}{1.724 \times 10^{11}} = -10.30 \text{ MPa}$$

Reproduced with permission of the copyright owner. Further reproduction prohibited without permission.

Stresses after the introduction of the creep effect,

$$f_2 = -\frac{4720182}{1101900} - \frac{1072000}{1101900} + \frac{4720182 \times 371 \times 400}{1.724 \times 10^{11}} + \frac{1072000 \times 219 \times 400}{1.724 \times 10^{11}}$$
$$- \frac{870 \times 10^6 \times 400}{1.724 \times 10^{11}} - \frac{146 \times 10^6 \times 400}{1.724 \times 10^{11}} = -3.00 \text{ MPa}$$

$$f_1 = -\frac{4720182}{1101900} - \frac{1072000}{1101900} - \frac{4720182 \times 371 \times 820}{1.724 \times 10^{11}} - \frac{1072000 \times 219 \times 820}{1.724 \times 10^{11}}$$
$$+ \frac{870 \times 10^6 \times 820}{1.724 \times 10^{11}} + \frac{146 \times 10^6 \times 820}{1.724 \times 10^{11}} = -10.29 \text{ MPa}$$

The effect of the remaining forty percent of post – tensioning force,

$$f_4 = -\frac{724000}{1101900} + \frac{724000 \times 219 \times 475}{1.724 \times 10^{11}} = -0.22 \text{ MPa}$$

$$f_1 = -\frac{724000}{1101900} - \frac{724000 \times 219 \times 475}{1.724 \times 10^{11}} = -1.41 \text{ MPa}$$

4.3 Calculations for Deflection

4.3.1 Calculations for Deflection at Mid Span

Downward deflection due to self-weight,

$$\delta = \frac{5 \times 22.30 \times 20400^4}{384 \times 32 \times 10^3 \times 1.724 \times 10^{11}} = 9.11 \text{ mm.}$$

Deflection due to topping

$$\delta_1 = \frac{5 \times 3.75 \times 20400^4}{384 \times 32 \times 10^3 \times 1.724 \times 10^{11}} = 1.53 \text{ mm.}$$

Reproduced with permission of the copyright owner. Further reproduction prohibited without permission.

Upward deflection from the pre-tensioning force,

$$\delta_2 = \frac{75130 \times 7100}{24 \times 32 \times 10^3 \times 1.724 \times 10^{11}} \left(3 \times 20400^2 - 4 \times 7100^2\right) = 4.21 \text{ mm.}$$

Deflection due to eccentricity of the tendons at the end,

$$\delta_3 = \frac{1374 \times 10^6 \times 20400^2}{8 \times 32 \times 10^3 \times 1.724 \times 10^{11}} = 12.95 \text{ mm.}$$

Deflection due to external post – tensioning

$$\delta_4 = \frac{140 \times 10^3 \times 20400^3}{48 \times 32 \times 10^3 \times 1.724 \times 10^{11}} = 4.49 \text{ mm.}$$

$$\delta_5 = \frac{87 \times 10^3 \times 6608}{24 \times 32 \times 10^3 \times 1.724 \times 10^{11}} \left(3 \times 20400^2 - 4 \times 6608^2\right) = 4.66 \text{ mm.}$$

Therefore the total upward deflection,

$$\delta_f = -9.11 - 1.53 + 4.21 + 12.95 + 4.49 + 4.66 = 15.67 \text{ mm.}$$

4.3.2 Calculations for Deflection at Quarter Span

Downward deflection due to own-weight,

$$\delta_1 = \frac{22.30 \times 5100}{24 \times 32 \times 10^3 \times 1.724 \times 10^{11}} \left(20400^3 - 2 \times 20400 \times 5100^2 + 5100^3\right) = 6.49 \text{ mm.}$$

Deflection due to topping

$$\delta_2 = \frac{3.75 \times 5100}{24 \times 32 \times 10^3 \times 1.724 \times 10^{11}} \left(20400^3 - 2 \times 20400 \times 5100^2 + 5100^3\right) = 1.09 \text{ mm.}$$

Reproduced with permission of the copyright owner. Further reproduction prohibited without permission.

Upward deflection of the pre-tensioning force,

$$\delta_3 = \frac{75130\times 5100}{6\times 32\times 10^3\times 1.742\times 10^{11}}\left(3\times 20400\times 7100 - 3\times 7100^2 - 5100^2\right) = 2.94 \text{ mm.}$$

Deflection due to eccentricity of the tendons at the end,

Left moment,

$$\delta_4 = \frac{1374\times 10^6\times 15300}{6\times 32\times 10^3\times 1.724\times 10^{11}\times 20400}\left(15300^2 - 3\times 20400\times 15300 + 2\times 20400^2\right) = 4.04\,\text{mm}$$

Right moment,

$$\delta_5 = \frac{1374\times 10^6\times 5100}{6\times 32\times 10^3\times 1.724\times 10^{11}\times 20400}\left(5100^2 - 3\times 20400\times 5100 + 2\times 20400^2\right) = 5.65\,\text{mm}$$

Deflection due to external post-tensioning

$$\delta_6 = \frac{140\times 10^3\times 5100}{48\times 32\times 10^3\times 1.724\times 10^{11}}\left(3\times 20400^2 - 4\times 5100^2\right) = 3.08 \text{ mm.}$$

$$\delta_7 = \frac{87\times 10^3\times 5100}{6\times 32\times 10^3\times 1.724\times 10^{11}}\left(3\times 20400\times 6608 - 3\times 6608^2 - 5100^2\right) = 3.32 \text{ mm.}$$

Therefore the total upward deflection,

$$\delta_f = -6.49 - 1.09 + 2.94 + 4.04 + 5.65 + 3.08 + 3.32 = 11.45\,\text{mm.}$$

6. Estimation of the Cracking Moment

The cracking moment based on the analysis is calculated using the equation,

$$M_{cr} = \frac{(12.989 + 4.41)\times 1.724\times 10^{11}}{820} = 3657 \text{ kN-m}$$

Reproduced with permission of the copyright owner. Further reproduction prohibited without permission.

The cracking moment based on the strain readings,

$$M_{cr} = \frac{(13.85 + 4.41) \times 1.724 \times 10^{11}}{820} = 3839 \text{ kN-m}$$

7. Modification of the stresses obtained from the strains due to the effect of creep

7.1 Phase B: Sixty Percent of External Post-Tensioning

7.1.1 Mid Span

$f_1 = 23 - 23 \times 0.19 = 18.63$ MPa

$f_2 = 3.42 - 3.42 \times 0.19 = 2.77$ MPa

7.1.2 Quarter Span

$f_1 = 3.09 - 3.09 \times 0.19 = 2.50$ MPa

$f_2 = 17.67 - 17.67 \times 0.19 = 14.31$ MPa

7.2 Phase C: Casting Topping

7.2.1 Mid Span

$f_1 = 7.07 - 7.07 \times 0.31 = 4.88$ MPa

$f_2 = 19.00 - 19.00 \times 0.31 = 13.11$ MPa

7.2.2 Quarter Span

$f_1 = 7.83 - 7.83 \times 0.31 = 5.40$ MPa

$f_2 = 15.88 - 15.88 \times 0.31 = 10.96$ MPa

7.3 Phase D: Full Post – Tensioning

Reproduced with permission of the copyright owner. Further reproduction prohibited without permission.

7.3.1 Mid Span

$f_1 = 7.07 - 7.07 \times 0.34 = 4.67$ MPa

$f_2 = 20.984 - 20.984 \times 0.34 = 13.85$ MPa

7.3.2 Quarter Span

$f_1 = 17.648 - 17.648 \times 0.34 = 11.64$ MPa

$f_2 = 7.824 - 7.824 \times 0.34 = 5.16$ MPa

Reproduced with permission of the copyright owner. Further reproduction prohibited without permission.

APPENDIX B

THE ULTIMATE MOMENT COMPUTER PROGRAM

Reproduced with permission of the copyright owner. Further reproduction prohibited without permission.

APPENDIX B

THE ULTIMATE MOMENT COMPUTER PROGRAM

1. Program Code

```
clear;
a = input('Enter Top stress (absolute)(MPa) :');
b = input('Enter Bottom stress (absolute)(MPa) :');
Z1 = a*1295/(a+b);
x  = comp (a,b)
pause
Icr = icr (x)
Acr = acr (x)
pause
M = input('Enter Applied Moment (N.mm) : ');
F1 = input('Enter Pre - Tensionong Force (N) : ');
F2 = input('Enter Post Tensioning Force (N) : ');
e =  input('Enter Eccentricity (mm) : ');
Ftop = top (F1,F2,Acr,x,Icr,e,M)
Fbot = bot (F1,F2,Acr,x,Icr,e,M)
Z2 = -Ftop*1295/(-Ftop + Fbot);
dummy = 1;
pause
```


Reproduced with permission of the copyright owner. Further reproduction prohibited without permission.

```
while dummy ~= 0
  if abs (Z1-Z2)/Z1 <= 0.20
    disp('end');
    break
  else
    a = abs (Ftop) ;
    b = abs (Fbot);
    Z3 = a*1295/(a + b);
    x2 = comp2 (a,b,F2)
    pause
    Icr2 = icr2 (x2)
    Acr2 = acr2 (x2)
    pause
    F1 = F1;
    F2 = F2;
    e =  e;
    M = M;
    Ftopp = topp (F1,F2,Acr2,x2,Icr2,e,M)
    Fbott = bott (F1,F2,Acr2,x2,Icr2,e,M)
    pause
    Z4 = -Ftopp*1295/(-Ftopp + Fbott);
    abs (Z3-Z4)/Z3;
```


Reproduced with permission of the copyright owner. Further reproduction prohibited without permission.

```
while (Fbott < 1155 & Ftopp > -39) | (dummy == 1)
  if abs (Z3-Z4)/Z3 <= 0.20
    disp ('end');
  else
    M = input('Enter new Applied Moment (N.mm) : ');
    F = input('Enter new Post Tensioning Force (N) : ');
    Icr2 = icr2 (x2)
    Acr2 = acr2 (x2)
    pause
    Ftopp = topp (F1,F2,Acr2,x2,Icr2,e,M)
    Fbott = bott (F1,F2,Acr2,x2,Icr2,e,M)
    Z5 = -Ftopp*1295/(-Ftopp + Fbott);
    a = abs (Ftopp);
    b = abs (Fbott);
    pause
    x2 = comp2 (a,b,F2)
    pause
    Icr2 = icr2 (x2)
    Acr2 = acr2 (x2)
    pause
    Ftopp = topp (F1,F2,Acr2,x2,Icr2,e,M)
    Fbott = bott (F1,F2,Acr2,x2,Icr2,e,M)
```


Reproduced with permission of the copyright owner. Further reproduction prohibited without permission.

```
            if Fbott >= 1155
               disp ('Ultimate Moment (N.mm):  ');
               disp (M);
               dummy=0;
            elseif   Ftopp <= -39
               disp ('Ultimate Moment (N.mm):  ');
               disp (M);
               dummy=0;
            end
         end
      end
   end
end
```


Reproduced with permission of the copyright owner. Further reproduction prohibited without permission.

APPENDIX C

OUTPUT DATA FROM THE COMPUTER PROGRAM

Reproduced with permission of the copyright owner. Further reproduction prohibited without permission.

APPENDIX C

OUTPUT DATA FROM THE COMPUTER PROGRAM

1. Estimating The Ultimate Moment For Post-Tensioning Force Based on Deflection

Calculated According to The ACI Equation

Enter Top stress (absolute)(MPa) :13.32
Enter Bottom stress (absolute)(MPa) :6.02

x =

65

Icr =

4.2588e+010

Acr =

9.6379e+005

Enter Applied Moment (N.mm) : 4089e6
Enter Pre - Tensionong Force (N) : 4720e3
Enter Post Tensioning Force (N) : 2084e3
Enter Eccentricity (mm) : 470

Ftop =

-10.97

Fbot =

290.75

Reproduced with permission of the copyright owner. Further reproduction prohibited without permission.

x2 =

180

Icr2 =

4.1165e+010

Acr2 =

7.2004e+005

Ftopp =

-17.68

Fbott =

277

Enter new Applied Moment (N.mm) : 5111e6
Enter new Post Tensioning Force (N) : 2200e3

Icr2 =

3.8967e+010

Acr2 =

7.2004e+005

Ftopp =

-26.01

Fbott =

404.41

Reproduced with permission of the copyright owner. Further reproduction prohibited without permission.

x2 =

162

Icr2 =

4.0688e+010

Acr2 =

7.5846e+005

Ftopp =

-21.44

Fbott =

422.89

Enter new Applied Moment (N.mm) : 6133e6
Enter new Post Tensioning Force (N) : 2360e3

Icr2 =

4.1164e+010

Acr2 =

9.0908e+005

Ftopp =

-17.66

Fbott =

552.74

Reproduced with permission of the copyright owner. Further reproduction prohibited without permission.

x2 =

156

Icr2 =

4.0473e+010

Acr2 =

7.7118e+005

Ftopp =

-26.24

Fbott =

542.20

Enter new Applied Moment (N.mm) : 7155e6
Enter new Post Tensioning Force (N) : 2600e3

Icr2 =

3.8978e+010

Acr2 =

7.5695e+005

Ftopp =

-32.48

Fbott =

671.16

Reproduced with permission of the copyright owner. Further reproduction prohibited without permission.

x2 =

152

Icr2 =

4.0364e+010

Acr2 =

7.7960e+005

Ftopp =

-30.16

Fbott =

684.18

Enter new Applied Moment (N.mm) : 8177e6
Enter new Post Tensioning Force (N) : 2840e3

Icr2 =

4.0688e+010

Acr2 =

8.8791e+005

Ftopp =

-24.16

Fbott =

814.46

Reproduced with permission of the copyright owner. Further reproduction prohibited without permission.

x2 =

108

Icr2 =

3.9084e+010

Acr2 =

8.7294e+005

Ftopp =

-34.17

Fbott =

804.39

Enter new Applied Moment (N.mm) : 9199e6
Enter new Post Tensioning Force (N) : 3080e3

Icr2 =

3.9044e+010

Acr2 =

7.7118e+005

Ftopp =

-39.47

Fbott =

Reproduced with permission of the copyright owner. Further reproduction prohibited without permission.

933.90

x2 =

105

Icr2 =

3.9044e+010

Acr2 =

8.7930e+005

Ftopp =

-36.11

Fbott =

946.53

Enter new Applied Moment (N.mm) : 10222e6
Enter new Post Tensioning Force (N) : 3360e3

Icr2 =

4.0473e+010

Acr2 =

8.7755e+005

Ftopp =

-30.48

Reproduced with permission of the copyright owner. Further reproduction prohibited without permission.

Fbott =

1.0761e+003

x2 =

100

Icr2 =

3.9878e+010

Acr2 =

8.8990e+005

Ftopp =

-37.80

Fbott =

1.0656e+003

Enter new Applied Moment (N.mm) : 11142e6
Enter new Post Tensioning Force (N) : 3560e3

Icr2 =

3.9084e+010

Acr2 =

7.7759e+005

Ftopp =

-36.38

Reproduced with permission of the copyright owner. Further reproduction prohibited without permission.

Fbott =

1.1824e+003

x2 =

90

Icr2 =

3.8967e+010

Acr2 =

9.1110e+005

Ftopp =

-38.40

Fbott =

1.1840e+003

Ultimate Moment (N.mm):
1.1142e+010

>>

Reproduced with permission of the copyright owner. Further reproduction prohibited without permission.

2. Estimating The Ultimate Moment For Post-Tensioning Force Based on Deflection

Calculated According to Salem Faza Equation

Enter Top stress (absolute)(MPa) :13.32
Enter Bottom stress (absolute)(MPa) :6.02

x =

65.14

Icr =

4.2588e+010

Acr =

9.6379e+005

Enter Applied Moment (N.mm) : 4089e6
Enter Pre - Tensionong Force (N) : 4720e3
Enter Post Tensioning Force (N) : 2168e3
Enter Eccentricity (mm) : 470

Ftop =

-11.00

Fbot =

285.41

x2 =

181

Reproduced with permission of the copyright owner. Further reproduction prohibited without permission.

Icr2 =

4.1152e+010

Acr2 =

7.18180e+005

Ftopp =

-17.60

Fbott =

272.29

Enter new Applied Moment (N.mm) : 5111e6
Enter new Post Tensioning Force (N) : 2300e3

Icr2 =

3.8977e+010

Acr2 =

7.1685e+005

Ftopp =

-26.12

Fbott =

398.10

x2 =

163

Reproduced with permission of the copyright owner. Further reproduction prohibited without permission.

Icr2 =

4.0675e+010

Acr2 =

7.5634e+005

Ftopp =

-21.12

Fbott =

418.50

Enter new Applied Moment (N.mm) : 6133e6
Enter new Post Tensioning Force (N) : 2472e3

Icr2 =

4.1149e+010

Acr2 =

9.0842e+005

Ftopp =

-17.71

Fbott =

547.37

x2 =

156

Reproduced with permission of the copyright owner. Further reproduction prohibited without permission.

Icr2 =

4.0460e+010

Acr2 =

7.7118e+005

Ftopp =

-25.89

Fbott =

537.35

Enter new Applied Moment (N.mm) : 7155e6
Enter new Post Tensioning Force (N) : 2724e3

Icr2 =

3.8973e+010

Acr2 =

7.5536e+005

Ftopp =

-32.56

Fbott =

665.24

Reproduced with permission of the copyright owner. Further reproduction prohibited without permission.

x2 =

153

Icr2 =

4.0350e+010

Acr2 =

7.7754e+005

Ftopp =

-29.44

Fbott =

679.78

Enter new Applied Moment (N.mm) : 8177e6
Enter new Post Tensioning Force (N) : 2968e3

Icr2 =

4.0672e+010

Acr2 =

8.8714e+005

Ftopp =

-24.22

Fbott =

809.07

Reproduced with permission of the copyright owner. Further reproduction prohibited without permission.

x2 =

108

Icr2 =

3.9081e+010

Acr2 =

8.7294e+005

Ftopp =

-33.60

Fbott =

799.66

Enter new Applied Moment (N.mm) : 9199e6
Enter new Post Tensioning Force (N) : 3727e3

Icr2 =

3.9039e+010

Acr2 =

7.7026e+005

Ftopp =

-39.52

Fbott =

928.13

Reproduced with permission of the copyright owner. Further reproduction prohibited without permission.

x2 =

106

Icr2 =

3.9039e+010

Acr2 =

8.7718e+005

Ftopp =

-35.76

Fbott =

941.13

Enter new Applied Moment (N.mm) : 10222e6
Enter new Post Tensioning Force (N) : 3488e3

Icr2 =

4.0457e+010

Acr2 =

8.7677e+005

Ftopp =

-30.57

Reproduced with permission of the copyright owner. Further reproduction prohibited without permission.

Fbott =

1.0707e+003

x2 =

101

Icr2 =

3.9875e+010

Acr2 =

8.8778e+005

Ftopp =

-37.44

Fbott =

1.0610e+003

Enter new Applied Moment (N.mm) : 11449e6
Enter new Post Tensioning Force (N) : 3896e3

Icr2 =

3.9080e+010

Acr2 =

7.7704e+005

Ftopp =

-47.61

Reproduced with permission of the copyright owner. Further reproduction prohibited without permission.

```
Fbott =

  1.2157e+003

x2 =

  91

Icr2 =

  3.8973e+010

Acr2 =

  9.0890e+005

Ftopp =

  -38.36

Fbott =

  1.183e+003

Ultimate Moment (N.mm):
  1.1449e+010

>>
```


Reproduced with permission of the copyright owner. Further reproduction prohibited without permission.

REFERENCES

Abdelrahman, A. A., Tadros, G. and Rizkalla, S. H., " Test Model for the First Canadian Smart Highway Gridge", ACI Structural Journal, V. 92, No 4, July-August (1995)

ACI (1995) "Building Code Requirements for Reinforced Concrete", (ACI 318-95/ACI 318 R-95), American Concrete Institute, Detroit, MI.

ACI Committee 440 (1999), "Provisional Design Recommendations for Concrete Reinforced with FRP bars", American Concrete Institute, Detroit, MI.

ACI Committee 209, Report No. ACI 209R-82, American Concrete Institute, Special Publication SP-76, 1982.

Bakis, C. E., Bhat, B. B., Giernacky, R.G. and Boothby T.E., " Investigation of Concrete Beams Post-Tensioned with Unbonded CFRP Tendons", Report submitted to the Federal Highway Administration by Composites Technology Center, Pennsylvania State University.

Construction Technology Laboratories," Instrumentation and Structural Testing of Full-Scale Double-Tee Beam, Bridge Street Bridge, City of Southfield, Michigan", Final Report Submitted to City of Southfield Michigan, 2001.

Reproduced with permission of the copyright owner. Further reproduction prohibited without permission.

Dolan, C. W. and Burke, C. R., " Flexural Strength and Design of FRP Beams", Canadian Society for Civil Engineering, Montreal, Quebec 1996.

Edwards, H. H.," The Taylor Bridge, Headingly, Manitoba, Canada.", PCI Journal, Vol. 43, No. 5, September-October 1998.

Grace, N. F. and Sayed, G. A., " Double Tee and CFRP / GFRP Bridge System", Concrete International February 1996.

Grace, N. F. and Sayed, G. A.," Ductility of Prestressed Bridges Using CFRP Strands", Concrete International June 1998.

Grace, N. F. and Sayed, G. A., " Behavior of Externally Draped CFRP Tendons in Prestressed Concrete Bridges", PCI Journal October 1998.

Grace, N. F. and Sayed, G. A., " Behavior of CFRP / GFRP Bridge System", Canadian Society for Civil Engineers, Montreal, Quebec 1996.

Hibbeler, R. C., " Mechanics of Materials", Prentice Hall, New Jersey, U.S.A., 3rd edition 1999.

Reproduced with permission of the copyright owner. Further reproduction prohibited without permission.

Jerret, C. V., and Ahmad, S.H., " Behavior of Prestressed Concrete beams Strengthened by External FRP Post-Tensioned Tendons", Canadian Society for Civil Engineering, Montreal, Quebec, 1996.

Lin, T.Y., and Burns, N.H. 1981. " Design of Prestressed Concrete Structures", John Wiley & Sons, Inc., New York, 3rd edition.

Naaman, A. E., " Ductility Implications for Prestressed and Partially Prestressed Concrete Structures Using Fiber Reinforced Plastic Reinforcements", FIP Symposium 1993 Kyoto, Japan.

Rao, P. S. and Mathew, G., " Behavior of Externally Concrete Beams with Multiple Deviators", ACI Structural Journal August 1996.

Tommaso, A. D., Focacci, F. and Foraboschi P., " Driven Failure Mechanisms in Fiber Reinforced Plastic Prestressed Concrete Beams for Ductility Requirements", Canadian Society of Civil Engineering, Montreal, Quebec, 1996.

Reproduced with permission of the copyright owner. Further reproduction prohibited without permission.

VITA AUCTORIS

1975 Born in Egypt

1998 Obtained B.Sc. degree from Civil Engineering Department, Ain Shams University, Egypt

2001 Enrolled in the Faculty of Graduate Studies and Research, University of Windsor, Windsor, Ontario, Canada, in a program leading to the degree of M.Sc. Also joined the Department of Civil and Environmental Engineering as a Teaching and Research Assistant.

Reproduced with permission of the copyright owner. Further reproduction prohibited without permission.